Summer 1961

Threshold improvement in F-M detection by use of feedback

Alan Robert Hamilton
University of Iowa

Follow this and additional works at: https://ir.uiowa.edu/etd
Part of the Electrical and Computer Engineering Commons

83

THRESHOLD IMPROVEMENT IN F-M DETECTION BY USE OF FEEDBACK

by

Alan Robert Hamilton

A thesis submitted in partial fulfillment
of the requirements for the degree of
Master of Science, in the Department
of Electrical Engineering in the
Graduate College of the State
University of Iowa

August 1961

Chairman: Professor Darrel E. Newell

ACKNOWLEDGMENTS

The author wishes to express his sincere appreciation to Mr. Robert H. Pool of Collins Radio Company for his invaluable assistance during all phases of the project. Of particular help were his ideas and suggestions resulting from frequent discussions, and his assistance in circuitry design and laboratory testing.

The author would also like to acknowledge the assistance rendered by the Collins Radio Company whose support made this investigation possible.

TABLE OF CONTENTS

Chapter		Page
I.	Historical Information.......................	1
II.	Purpose..................................	3
III.	Analysis.................................	6
IV.	System Design............................	28
V.	Circuit Design...........................	50
VI.	Experimental Results.....................	54
VII.	Conclusions..............................	89
	Appendix A...............................	92
	Appendix B...............................	93
	Appendix C...............................	94
	Appendix D...............................	112
	Bibliography.............................	113

LIST OF ILLUSTRATIONS

Figure Number	Title	Page
1.	Open-Loop Detector Block Diagram	6
2.	$(S/N)_{out}$ vs $(S/N)_{in}$ for an Ideal Symmetrical Bandpass Limiter	7
3.	Linearized Open-Loop Detector Block Diagram .	9
4.	Closed-Loop Detector Block Diagram	12
5.	Linearized Closed-Loop Detector Block Diagram	13
6.	Local Oscillator Noise Spectral Density	25
7.	Input-to-Discriminator Transfer Function for Open-Loop Detector	31
8.	First-Order Loop Transfer Function	37
9.	Input-to-Discriminator Transfer Function for Second-Order Loop-1	39
10.	Loop Transfer Function for Second-Order Loop-1	40
11.	Input-to-Discriminator Transfer Function for Second-Order Loop-2	42
12.	Loop Transfer Function for Second-Order Loop-2	43
13.	Input-to-Discriminator Transfer Function for Second-Order Loop-3	45
14.	Loop Transfer Function for Second-Order Loop-3	46
15.	Input-to-Discriminator Transfer Function for Second-Order Loop-4	47

LIST OF ILLUSTRATIONS

(continued)

Figure Number	Title	Page
16.	Loop Transfer Function for Second-Order Loop-4	48
17.	Block Diagram of Experimental Equipment	51
18.	Output S/N Curve, First-Order Loop and Open-Loop	60
19.	Output S/N Curve, Second-Order Loop-1 and Open-Loop	61
20.	Output S/N Curve, Second-Order Loop-2 and Open-Loop	62
21.	Output S/N Curve, Second-Order Loop-3 and Open-Loop	63
22.	Output S/N Curve, Second-Order Loop-4 and Open-Loop	64
23.	Output S/N Curve, Second-Order Loops 5 and 6	68
24.	Comparison of Detected Signals with Noise	70
25.	Comparison of Detected Signals with Noise	71
26.	Comparison of Detected Signals with Noise	72
27.	Comparison of Output S/N Curves for Two Measurement Techniques, Second-Order Loop-2	76
28.	Comparison of Output S/N Curves for Two Measurement Techniques, Second-Order Loop-4	77
29.	Output S/N Curves for 30-KC Deviation, Second-Order Loop-2 and Open-Loop	79
30.	Output S/N Curves for 22.5-KC Deviation, Second-Order Loop-2 and Open-Loop	80

LIST OF ILLUSTRATIONS
(continued)

Figure Number	Title	Page
31.	Output S/N Curves for 15-KC Deviation, Second-Order Loop-2 and Open-Loop............	81
32.	Output S/N Curves for 7.5-KC Deviation, Second-Order Loop-2 and Open-Loop............	82
C-1	60-MC Voltage-Controlled Oscillator Schematic	96
C-2	62-MC Voltage-Controlled Oscillator Schematic	97
C-3	60-MC Mixer Schematic.......................	98
C-4	2-MC IF, Limiter, and Discriminator Schematic	99
C-5	5-KC Audio Filter and Cathode Follower Schematic..................................	100
C-6	2-MC Bandpass Filter Schematics.............	101
C-7	5-KC Rejection Filter Schematic.............	102
C-8	Phase-Lag Networks..........................	103
C-9	60-MC Voltage-Controlled Oscillator, Output Frequency vs Input Voltage...........	104
C-10	62-MC Voltage-Controlled Oscillator, Output Frequency vs Input Voltage...........	105
C-11	2-MC Discriminator Curve....................	106
C-12	2-MC Limiter Characteristic.................	107
C-13	Wide-Band Loop Response Curve...............	108
C-14	Narrow-Band Filter Response Curve...........	109
C-15	Wide-Band Filter Response Curve.............	110
C-16	5-KC Rejection Filter Response Curve.........	111

LIST OF TABLES

Table Number	Title	Page
1.	Closed-Loop Detection Circuit Parameters.....	34
2.	Calculated S/N Improvement..................	35
3.	Calculated Phase Deviation Reduction Factor for Closed-Loop Detection............	36
4.	Closed-Loop S/N Improvement Referenced to Open-Loop Results.......................	59
5.	Additional Second-Order Loop Constants.......	67
6.	Loop Threshold Characteristics for Unmodulated Carrier.......................	73
7.	Harmonic Distortion.........................	84
8.	Intermodulation Distortion..................	87

CHAPTER I

HISTORICAL INFORMATION

The first articles describing a closed-loop feedback system for f-m detection appeared in 1939[1,2] in the Bell System Technical Journal. However, the main interest of the authors was improved linearity in detection, and the possibility of improved threshold characteristics was not discussed.

From 1939 until the middle 1950's it appears that little was done with f-m feedback for detection. At this time the increased use of scatter transmission caused the f-m threshold effect to be a major factor in system design. Scatter systems using many repeater stations required extremely good signal-to-noise ratios which directed the use of large deviation ratios to obtain the maximum f-m improvement. However, because of the large transmission losses and fading characteristics in scatter systems it became difficult to maintain a sufficient margin above threshold.

To overcome the threshold effect, the idea of f-m feedback to reduce the deviation before detection was presented by several writers. The first appears to have been made by M. Morita and S. Ito of Japan. In a paper by them published in the United States in 1960[3] they refer to previous publications presented in Japan on threshold improvement dating back to 1955. They appear to have had the first operating system, but unfortunately do not describe their work in sufficient detail to make it possible to repeat any specific results.

A few other articles appeared describing f-m feedback systems[4,5] but not with sufficient detail to allow the design of a system. It is very likely additional work has been done under government contract, but is not readily available.

The recent advent of space communications has again increased interest in f-m feedback detection. The limited power available and extremely large propagation losses has made it important to overcome the threshold effect. Since the start of work on this study, two papers have been presented describing the application of f-m feedback to space communications. The first,[6] of which only a summary is available, describes a working system used by Bell Telephone Laboratories in the Project Echo work, and the second[7] describes a system Hughes Aircraft is committed to build for transmission of television from the moon to earth in Project Surveyor. The Hughes report is a superficial analysis with no experimental work.

Because of its increasing importance, a study of the use of feedback in f-m detection was undertaken at Collins Radio Company. The following report is based upon this work.

CHAPTER II

PURPOSE

The use of angle modulation, both frequency and phase, in the transmission of intelligence makes possible the attainment of an improvement in signal-to-noise ratio over linear amplitude-modulation systems such as single-sideband and double-sideband suppressed carrier. This improvement for frequency modulation over amplitude-modulated systems is proportional to the square of the peak deviation. Thus, the wider the bandwidth occupied by the signal during transmission, the greater the signal-to-noise improvement possible. However, as with most nonlinear detection methods[8], f-m detection has a threshold effect due to small signal suppression. As is common in detection systems, the threshold will be defined as that point at which the signal-to-noise ratio in the output begins to decrease more rapidly than the signal-to-noise ratio at the input to the detector.

In the past the most common method of detection of f-m has been the frequency discriminator where the discriminator has been as wideband as the transmitted signal spectrum. The discriminator threshold has been shown, both analytically and experimentally, to be at the level where the signal-to-noise ratio at the detector input is approximately 10 db. Thus, while signal-to-noise improvement can be obtained by increasing the deviation, the threshold of the normal discriminator detector is deteriorated by this means.

The purpose of the study is to investigate a different method of f-m detection whereby the threshold is determined only by the transmitted intelligence bandwidth while the signal-to-noise improvement is determined, as before, by the transmitted deviation ratio. In the proposed detection method, a portion of the detected intelligence signal is fed back to modulate a voltage-controlled local oscillator in a superhetrodyne receiver. By this method of modulating the oscillator, the signal deviation at the output of the mixer can be reduced from the transmitted value. Proper feedback gain will allow the modulation index in the receiver i-f amplifier to be reduced to values as low as unity or less for the highest modulation frequency. This will allow the i-f bandwidth to be reduced to a value dependent upon the intelligence bandwidth rather than the transmitted bandwidth. A discriminator used to demodulate the i-f signal will then have a threshold dependent upon only the i-f, or intelligence bandwidth, thus accomplishing the desired result.

The study consists of analytical and experimental results. In the analytical portion the equations describing open-loop detectors and several closed-loop detectors are developed. In the experimental portion several detection circuits are designed and built in accordance with the analytical results. These detectors are then tested and the predicted analytical results compared with

with experimental measurements to verify the analysis.

CHAPTER III

ANALYSIS

A. Open-Loop Conditions

The f-m improvement factor attainable with a normal limiter-discriminator detector will be determined analytically first. This will be used as a reference against which the feedback loop detector can be compared both analytically and experimentally. The circuitry will be linearized for purposes of analysis. Thus, the analysis is applicable only above threshold, and other methods are required to determine threshold.

A block diagram of the receiver configuration is shown in figure 1.

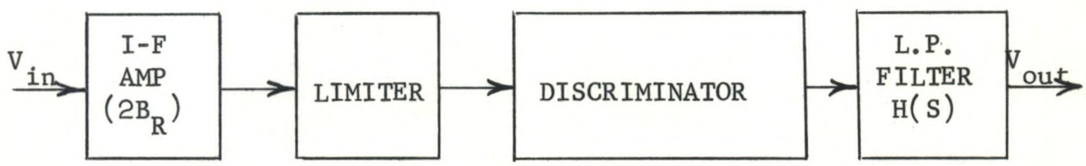

Figure 1. Open-Loop Detector Block Diagram

The input signal is of the form:

$$V_{in} = \sqrt{2}\, S \sin\left[\omega_c t + \frac{\Delta f}{f_s} \sin 2\pi f_s t\right] + N(t) \qquad (1)$$

where:

Δf = peak deviation, cps

f_s = modulation frequency, cps

S = rms signal amplitude, volts

N(t) = input noise voltage

The i-f amplifier will be considered as being designed as narrow as possible while still capable of passing the signal within the desired distortion limitation. This will produce the best detector threshold. The noise bandwidth of the amplifier is $2B_R$ cycles per second. With a double-tuned circuit this is 1.11 times the 3 db bandwidth (see Appendix A), and for more stages approaches the 3 db bandwidth more closely.

It has been shown by Davenport[9] that the ideal limiter will affect the signal-to-noise ratio as shown in figure 2. From this it can be seen that for large S/N ratios, the output S/N ratio is exactly twice the input S/N ratio. For this reason the limiter will not be included in the linear analysis; since only large S/N ratios are being considered, an additional 3-db improvement will be added at the end of the calculation to account for the limiter action.

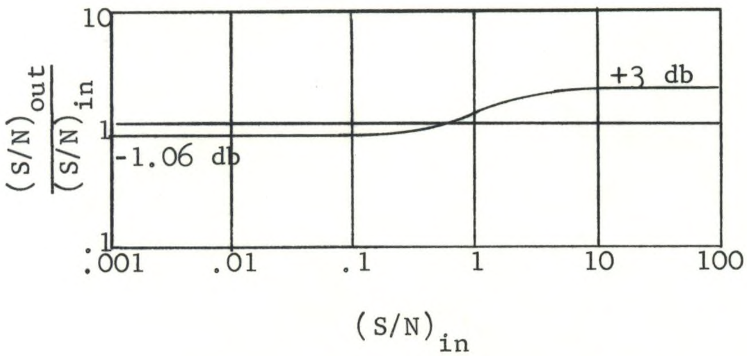

Figure 2. $(S/N)_{out}$ vs $(S/N)_{in}$ For an Ideal Symmetrical Bandpass Limiter

The action of the discriminator is to take the derivative of the phase of the input signal. Thus, if the analysis is made on a phase basis rather than voltage, the discriminator will have a transfer function of $K_1 S$ volts per radian, where S is the normal La Place operator.

The output low-pass filter is designed to pass the signal while removing the high-frequency noise which passes the discriminator. It will be considered as a second-order filter with damping factor of 0.707. It has been shown[10] that this is the optimum realizable filter for the detection of a frequency step function for the conditions of minimum output noise and a specified transient error. The transfer function of this filter is:

$$H(S) = \frac{B_o^2}{S^2 + \sqrt{2}\, B_o S + B_o^2} \tag{2}$$

where $2B_o$ equals the 3-db bandwidth in radians per second.

Assuming a double-tuned i-f filter, figure 1 can now be redrawn using linear transfer functions by considering the input to be a phase and the output a voltage. This is shown in figure 3.

The phase noise spectral density, Φ_N, is considered as uniform over the i-f bandwidth of $2B_R$. The total input phase noise when normalized to the signal power is[3]:

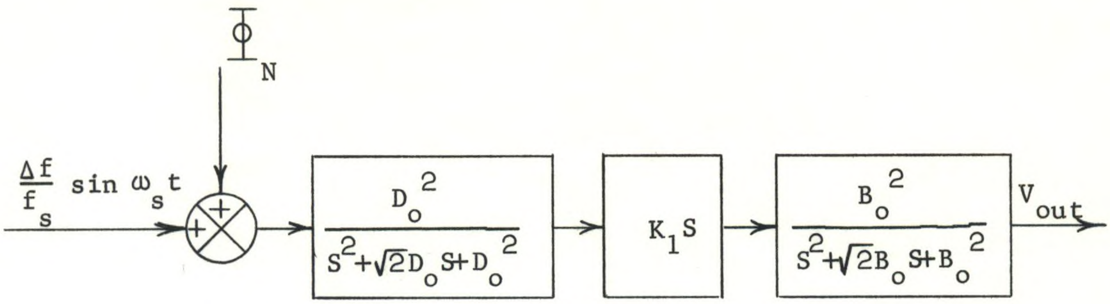

Figure 3. Linearized Open-Loop Detector Block Diagram

$$\Phi_N \, 2B_R = \left(\frac{N}{S}\right)^2_{in}$$

or

$$\Phi_N = \left(\frac{N}{S}\right)^2_{in} \frac{1}{2B_R} \quad \frac{(\text{radians})^2}{\text{cps}}$$

where $\left(\frac{N}{S}\right)_{in}$ = noise-to-signal voltage ratio at the discriminator input.

The signal voltage out of the discriminator can be determined by La Place transforms as follows:

$$V(S)_{out} = \frac{\Delta f}{f_s} \left[\frac{2\pi f_s}{S^2 + (2\pi f_s)^2}\right] (K_1 S) \left[\frac{D_o^2}{(S + \frac{\sqrt{2}\, D_o}{2})^2 + \frac{D_o^2}{2}}\right] \qquad (3)$$

From Gardner and Barnes, "Transients in Linear Systems", equation 1.359, the steady state output voltage is:

$$V(t)_{out} = \frac{2\pi\Delta f \; K_1 D_o^2}{\left[D_o^4 + (2\pi f_s)^4\right]^{1/2}} \sin(2\pi f_s t + \psi) \qquad (4)$$

where $$\psi = \frac{\pi}{2} - \tan^{-1}\left[\frac{2\sqrt{2}\,\pi\, D_o f_s}{D_o^2 - (2\pi f_s)^2}\right]$$

In transmission through the audio filter the signal voltage will be attenuated by a factor which is equal to the absolute value of the transfer function of the filter. This factor is:

$$\frac{B_o^2}{\left[B_o^4 + (2\pi f_s)^4\right]^{1/2}}$$

Thus, the signal power in the output will be:

$$S_{out}^2 = \frac{\left[2\pi\Delta f\, K_1 B_o^2 D_o^2\right]^2}{2\left[B_o^4 + (2\pi f_s)^4\right]\left[D_o^4 + (2\pi f_s)^4\right]} \tag{5}$$

The noise power at the output can be determined by integrating the product of the input noise spectrum and the absolute magnitude of the system transfer function[8]. Thus:

$$N_{out}^2 = \int_{-\infty}^{\infty} \Phi_N \left|H(j\omega)\right|^2 \frac{d\omega}{2\pi} \tag{6}$$

The system transfer function is:

$$H(S) = \frac{D_o^2 K_1 B_o^2 S}{\left[S^2 + \sqrt{2}\, D_o S + D_o^2\right]\left[S^2 + \sqrt{2}\, B_o S + B_o^2\right]} \tag{7}$$

Since the noise spectral density at the input to the detector system can be considered constant, the noise at the output can be evaluated from:

$$N_{out}^{2} = \frac{\Phi_N}{2\pi} \int_{-\infty}^{\infty} \left|H(j\omega)\right| \times \left|H(-j\omega)\right| \, d\omega \tag{8}$$

This integral is evaluated in the book by Newton, Gould, and Kaiser, "Analytical Design of Linear Feedback Controls", Appendix E.2:

$$N_{out}^{2} = \frac{\Phi_N K_1^{2} \sqrt{2}\, D_o^{3} B_o^{3}}{4(B_o + D_o)(D_o^{2} + B_o^{2})} \tag{9}$$

Making the substitutions:

$$\Phi_N = \left(\frac{N}{S}\right)_{in}^{2} \times \frac{1}{2B_R}$$

$$B_o = 2\pi b_o$$

$$D_o = 2\pi d_o$$

the signal-to-noise ratio at the output is given by:

$$\left(\frac{S}{N}\right)_{out}^{2} = \left(\frac{S}{N}\right)_{in}^{2} \frac{\sqrt{2}\, B_R \, (\Delta f)^{2} b_o d_o (b_o + d_o)(b_o^{2} + d_o^{2})}{\pi(b_o^{4} + f_s^{4})(d_o^{4} + f_s^{4})} \tag{10}$$

Adding 3-db improvement obtained by the limiter gives a final result of:

$$\left(\frac{S}{N}\right)^2_{out} = \left(\frac{S}{N}\right)^2_{in} \frac{2\sqrt{2}\, B_R\, (\Delta f)^2 b_o d_o (b_o + d_o)(b_o^{\,2} + d_o^{\,2})}{\pi(b_o^{\,4} + f_s^{\,4})(d_o^{\,4} + f_s^{\,4})} \tag{11}$$

B. First-Order Loop

The proposed feedback detection system to be analyzed is shown in figure 4. The input signal, either i-f or r-f, consists of the frequency modulated signal of full transmitted deviation plus the receiver noise. The signal is hetrodyned with the local oscillator signal in the first mixer. The local oscillator is frequency modulated sufficiently to reduce the i-f signal deviation to the desired amount. The i-f bandwidth is that necessary to pass the signal with the reduced deviation. This signal is then detected in the limiter-discriminator and the output signal filtered with a low-pass filter as before. The discriminator output is also fed back to the VCO local oscillator through a stabilization filter.

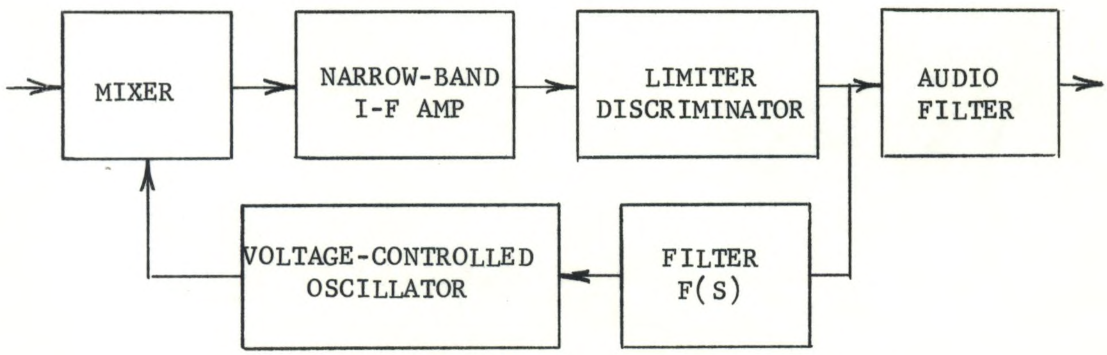

Figure 4. Closed-Loop Detector Block Diagram

The feedback loop can be linearized for analysis to the configuration shown in figure 5. The mixer is a product device which produces the sum and difference of the input phases. Using phase as the variable as before, the mixer can then be represented as a differencing circuit. The noise is added linearly as before.

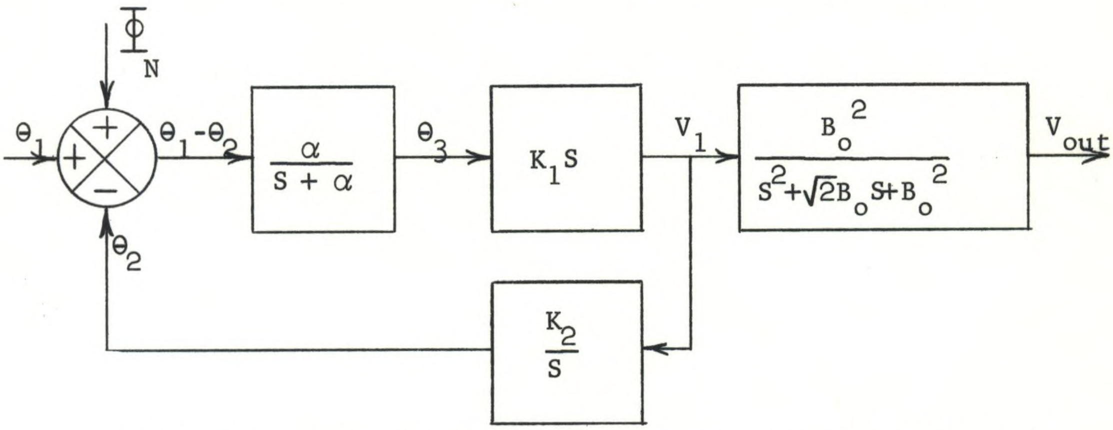

Figure 5. Linearized Closed-Loop Detector Block Diagram

Since each tuned circuit in the i-f produces phase shift that affects the loop stability, only one narrow-band single-tuned circuit will be used to obtain the band narrowing in the i-f. The discriminator and audio filter are represented as before. The filter in the feedback loop has been neglected in this first approach to the loop analysis. It can be seen that for the first-order loop the open-loop function rolls off at 6 db per octave which by Bode's criterion indicates that the first-order loop will be stable.

The voltage-controlled oscillator can be represented as an integrator as shown. This can be seen by the fact that an input voltage change causes a change in output frequency. Thus:

$$\Delta V_{in} = \frac{\Delta\omega}{K_2} = \frac{1}{K_2}\frac{d\phi}{dt}$$

and

$$K_2 \int \Delta V_{in} dt = \phi$$

$$\frac{K_2}{S} = \frac{\phi_{out}}{\Delta V_{in}}$$

where K_2 = cycles per second per volt.

Representation of the loop as shown in figure 5 has assumed that any other tuned circuits in the loop are wide enough so that phase shift in them is negligible over the range of interest. A minimum of circuits commonly present would be a double-tuned circuit in the discriminator, one tuned circuit in the VCO and one tuned circuit in the limiter. This assumption is of primary importance in the actual equipment design.

Referring to figure 5, the open loop transfer function can be determined to be:

$$\frac{\theta_2}{\theta_1 - \theta_2} = \frac{K_1K_2\alpha}{S + \alpha} \tag{12}$$

The closed-loop transfer function is:

$$\frac{\theta_2}{\theta_1} = H(S) = \frac{K_1K_2\alpha}{S + \alpha(1 + K_1K_2)} \tag{13}$$

The transfer function to the input of the audio filter is:

$$\frac{V_1}{\theta_1} = \frac{K_1 \alpha S}{S + \alpha(1 + K_1 K_2)} \tag{14}$$

and the transfer function from input to the audio filter output is:

$$\frac{V_{out}}{\theta_1} = \frac{K_1 \alpha S}{S + \alpha(1 + K_1 K_2)} \cdot \frac{B_o^2}{S^2 + \sqrt{2}\, B_o S + B_o^2} \tag{15}$$

From these equations the signal-to-noise ratio at the output can be calculated as before. The steady-state signal out of the discriminator for an input of:

$$\theta_1 = \frac{\Delta f}{f_s} \sin 2\pi f_s t$$

is:

$$V_1(t) = \mathcal{L}^{-1}\left[\frac{\Delta f}{f_s} \cdot \frac{2\pi f_s}{S^2 + (2\pi f_s)^2} \cdot \frac{\alpha K_1 S}{S + \alpha(1 + K_1 K_2)}\right] \tag{16}$$

Evaluating the steady-state output from the tables given in Gardner and Barnes gives:

$$V_1(t) = \frac{2\pi \alpha K_1 \Delta f}{\left[\alpha^2(1 + K_1 K_2)^2 + (2\pi f_s)^2\right]^{1/2}} \sin(2\pi f_s t + \psi) \tag{17}$$

The steady-state output of the audio filter is:

$$V_{out} = \frac{2\pi \alpha K_1 \Delta f}{\left[\alpha^2(1 + K_1 K_2)^2 + (2\pi f_s)^2\right]^{1/2}} \mathcal{L}^{-1}\left[\frac{2\pi f_s}{S^2 + (2\pi f_s)^2} \cdot \frac{B_o^2}{S^2 + \sqrt{2}\, B_o S + B_o^2}\right]$$

$$V_{out} = \frac{2\pi\alpha K_1 \Delta f\ B_o^{\,2}\ \sin(2\pi f_s t + \theta)}{\left[\alpha^2(1 + K_1K_2)^2 + (2\pi f_s)^2\right]^{1/2}\left[B_o^{\,4} + (2\pi f_s)^4\right]^{1/2}} \tag{18}$$

The output signal power is:

$$S_{out}^{\;2} = \frac{\left[2\pi\alpha K_1 \Delta f\ B_o^{\,2}\right]^2}{2\left[\alpha^2(1 + K_1K_2)^2 + (2\pi f_s)^2\right]\left[B_o^{\,4} + (2\pi f_s)^4\right]} \tag{19}$$

The noise power in the output is:

$$N_{out}^{\;2} = \frac{1}{2\pi}\int_{-\infty}^{\infty} \Phi_N \left| \frac{K_1\alpha S}{S + \alpha(1 + K_1K_2)} \cdot \frac{B_o^{\,2}}{S^2 + \sqrt{2}\,B_o S + B_o^{\,2}} \right|^2 dS \tag{20}$$

Evaluating this from Newton, Gould and Kaiser as before for the condition of uniform noise spectral density gives:

$$N_{out}^{\;2} = \frac{\Phi_N K_1^{\,2}\alpha^2 B_o^{\,3}}{2\sqrt{2}\left[B_o^{\,2} + \sqrt{2}\,B_o\alpha(1 + K_1K_2) + \alpha^2(1 + K_1K_2)^2\right]} \tag{21}$$

The signal-to-noise ratio can be evaluated after making the substitutions:

$$\Phi_N = \left(\frac{N}{S}\right)_{in}^2 \times \frac{1}{2B_R}$$

$$B_o = 2\pi b_o$$

$$\left(\frac{S}{N}\right)^2_{out} = \left(\frac{S}{N}\right)^2 \frac{\sqrt{2}\,(\Delta f)^2 b_o B_R}{\pi\left[b_o^{\;4} + f_s^{\;4}\right]} \times$$

$$\frac{B_o^{\;2} + \sqrt{2}\,B_o\alpha(1 + K_1K_2) + \alpha^2(1 + K_1K_2)^2}{\alpha^2(1 + K_1K_2)^2 + (2\pi f_s)^2} \tag{22}$$

Adding 3-db improvement due to the limiter gives the final result:

$$\left(\frac{S}{N}\right)^2_{out} = \left(\frac{S}{N}\right)^2_{in} \frac{2\sqrt{2}\,(\Delta f)^2 b_o B_R}{\pi\left[b_o^{\;4} + f_s^{\;4}\right]} \times$$

$$\frac{B_o^{\;2} + \sqrt{2}\,B_o\alpha(1 + K_1K_2) + \alpha^2(1 + K_1K_2)^2}{\alpha^2(1 + K_1K_2)^2 + (2\pi f_s)^2} \tag{23}$$

From a preliminary comparison of equations 11 and 23, it is not obvious that the improvement factor with feedback is approximately equivalent to the open-loop detector. However, a substitution of design values into the equations will show this, as is done in Chapter IV.

The noise bandwidth of the circuit is:

$$2B_N = \frac{1}{2\pi} \int_{-\infty}^{\infty} \frac{\left|H\,(j\omega)\right|^2}{\left|H\,(j\omega)\right|^2_{max}}\, d\omega \tag{24}$$

$$2B_N = \left[\frac{1 + K_1K_2}{K_1K_2}\right]^2 \frac{1}{2\pi} \int_{-\infty}^{\infty} \left| \frac{K_1K_2\alpha}{j\omega + \alpha(1 + K_1K_2)} \right|^2 d\omega$$

$$2B_N = \frac{\alpha(1 + K_1K_2)}{2} \quad \text{cps} \tag{25}$$

The signal deviation in the narrow-band i-f amplifier will next be calculated to ensure that the deviation has been reduced. The signal at the mixer output is:

$$\theta_1(S)-\theta_2(S) = \theta_1\left[1-H(S)\right] = \frac{\Delta f}{f_s}\left[\frac{2\pi f_s}{S^2+(2\pi f_s)^2}\right]\left[\frac{S + \alpha}{S + \alpha(1+K_1K_2)}\right]$$

$$\theta_1(t)-\theta_2(t) = \frac{\Delta f}{f_s}\left[\frac{\alpha^2 + (2\pi f_s)^2}{\alpha^2(1+K_1K_2)^2+(2\pi f_s)^2}\right]^{1/2} \sin(2\pi f_s t+\psi) \tag{26}$$

From this it can be seen that the reduction in signal deviation will be the factor:

$$\left[\frac{\alpha^2 + (2\pi f_s)^2}{\alpha^2(1 + K_1K_2)^2 + (2\pi f_s)^2}\right]^{1/2}$$

C. Second-Order Loop

From experimental evidence during the project, it became apparent that a first-order loop was not satisfactory because of the wide loop noise bandwidth. A second-order loop can be designed which will have a narrower bandwidth and will be stable.

An analysis will therefore be presented at this time.

The network added to the feedback loop will be a phase lag compensation network, shown in figure C-8, with the transfer function:

$$F(S) = \frac{\beta}{\gamma}\,\frac{S+\gamma}{S+\beta} \tag{27}$$

The analysis will be developed in the same manner as for the first-order loop. The open-loop transfer function is:

$$\frac{\theta_2}{\theta_1 - \theta_2} = \frac{K_1K_2\alpha\beta(S+\gamma)}{\gamma(S+\alpha)(S+\beta)} \tag{28}$$

The closed-loop transfer function is:

$$\frac{\theta_2}{\theta_1} = H_2(S) = \frac{\frac{K_1K_2\alpha\beta}{\gamma}(S+\gamma)}{S^2 + \left[\alpha + \beta + \frac{K_1K_2\alpha\beta}{\gamma}\right]S + \alpha\beta(1 + K_1K_2)} \tag{29}$$

An examination of equation 29 shows that the second-order loop is stable for realizable circuit values. The transfer function from input to the discriminator output is:

$$\frac{V_1(S)}{\theta_1(S)} = \frac{K_1\alpha S(S+\beta)}{S^2 + \left[\alpha + \beta + \frac{K_1K_2\alpha\beta}{\gamma}\right]S + \alpha\beta(1 + K_1K_2)} \tag{30}$$

To determine the signal-to-noise ratio as before, assume an input signal of:

$$\theta_1 = \frac{\Delta f}{f_s}\sin 2\pi f_s t$$

The discriminator steady-state output is:

$$V_1(t) = 2\pi\Delta f K_1\alpha \quad x$$

$$\frac{\left[(2\pi f_s)^2 + \beta^2\right]^{1/2} \operatorname{Sin}(2\pi f_s t + \psi)}{\left[\left[\alpha\beta(1 + K_1K_2) - (2\pi f_s)^2\right]^2 + (2\pi f_s)^2\left(\alpha + \beta + \frac{K_1K_2\alpha\beta}{\gamma}\right)^2\right]^{1/2}} \tag{31}$$

The signal passing through the output filter will be attenuated by the factor:

$$\frac{B_o^{\,2}}{\left[B_o^{\,4} + (2\pi f_s)^4\right]^{1/2}}$$

so that the signal power output is:

$$S_{out}^{\,2} = \frac{(2\pi\Delta f K_1\alpha B_o^{\,2})^2 \left[(2\pi f_s)^2 + \beta^2\right]}{2\left[\left[\alpha\beta(1 + K_1K_2) - (2\pi f_s)^2\right]^2 + (2\pi f_s)^2\left(\alpha + \beta + \frac{K_1K_2\alpha\beta}{\gamma}\right)^2\right]} \quad x$$

$$\frac{1}{B_o^{\,4} + (2\pi f_s)^4} \tag{32}$$

From a comparison of this equation with the corresponding one for the first-order loop (equation 19) it is not readily apparent that they are equivalent. However, at least for low modulating frequencies, i.e., f_s approaches zero, they both approach the same value. A more detailed comparison will be presented after specific parameters are chosen.

The noise power in the output is:

$$N_{out}^2 = \frac{1}{2\pi}\int_{-\infty}^{\infty} \Phi_N \left| \frac{K_1 \alpha S(S+\beta)}{S^2 + \left(\alpha + \beta + \frac{K_1 K_2 \alpha\beta}{\gamma}\right) S + \alpha\beta(1 + K_1 K_2)} \cdot \frac{B_o^2}{S^2 + \sqrt{2}\, B_o S + B_o^2} \right|^2 dS \tag{33}$$

Evaluating again from Newton, Gould and Kaiser gives

$$N_{out}^2 = \frac{\Phi_N B_o^3 K_1^2 \alpha^2 \left[B_o^2 + \sqrt{2}\, B_o \left(\frac{D + \beta^2}{A}\right) + \beta^2\right]}{2\sqrt{2}\left[B_o^4 + \sqrt{2}\, AB_o^3 + A^2 B_o^2 + \sqrt{2}\, ADB_o + D^2\right]} \tag{34}$$

where $A = \alpha + \beta + \dfrac{K_1 K_2 \alpha\beta}{\gamma}$

$D = \alpha\beta(1 + K_1 K_2)$

Making the substitutions of:

$$\Phi_N = \left(\frac{N}{S}\right)_{in}^2 \frac{1}{2B_R}$$

$$B_o = 2\pi b_o$$

and adding 3 db for limiter improvement gives a signal-to-noise ratio of:

$$\left(\frac{S}{N}\right)_{out}^2 = \left(\frac{S}{N}\right)_{in}^2 \frac{2\sqrt{2}\, b_o B_R (\Delta f)^2 \left[B_o^4 + \sqrt{2}\, AB_o^3 + A^2 B_o^2 + \sqrt{2}\, B_o AD + D^2\right]\left[(2\pi f_s)^2 + \beta^2\right]}{\pi\left[b_o^4 + f_s^4\right]\left[B_o^2 + \sqrt{2}\, B_o\left(\frac{D + \beta^2}{A}\right) + \beta^2\right]\left[D^2 + (2\pi f_s)^2 (A^2 - 2D) + (2\pi f_s)^4\right]} \tag{35}$$

While this equation is similar to equation 23, which is the corresponding equation for the first-order loop, it is difficult to compare them for any general case. Thus, the comparison will be left until later and evaluated at that time for a specific case.

The noise bandwidth of the loop can be evaluated by equations 24 and 29. Thus:

$$2B_N = \left[\frac{1 + K_1K_2}{K_1K_2}\right]^2 \frac{1}{2\pi} \int_{-\infty}^{\infty} \left| \frac{\frac{K_1K_2\alpha\beta}{\gamma}(j\omega + \gamma)}{-\omega^2 + jA\omega + D} \right|^2 d\omega \quad (36)$$

$$2B_N = \frac{(1 + K_1K_2)(\alpha\beta)\left[\alpha\beta(1 + K_1K_2) + \gamma^2\right]}{2\left[(\alpha + \beta)\gamma^2 + K_1K_2\ \alpha\beta\gamma\right]} \quad (37)$$

The signal deviation at that input to the narrow-band i-f circuit for a sine wave input is:

$$\theta_1(S) - \theta_2(S) = \theta_1\left[1 - H_2(S)\right]$$

$$= \frac{\Delta f}{f_s} \cdot \frac{2\pi f_s}{S^2 + (2\pi f_s)^2} \cdot \frac{(S + \alpha)(S + \beta)}{S^2 + AS + D} \quad (38)$$

By use of Gardner and Barnes the steady-state portion of this can be evaluated to be:

$$\theta_1(t) - \theta_2(t) = \frac{\Delta f}{f_s}\left[\frac{\left[\alpha^2+(2\pi f_s)^2\right]\left[\beta^2+(2\pi f_s)^2\right]}{D^2+(2\pi f_s)^2(A^2-2D)+(2\pi f_s)^4}\right]^{1/2} \times$$

$$\sin(2\pi f_s t + \psi) \quad (39)$$

A comparison of this equation with equation 26, which is the corresponding one for a first-order loop, shows they both approach the same value as the modulation frequency, f_s, approaches zero.

Also of interest for experimental measurements is the deviation at the discriminator input. This is the value of deviation measured by observing the discriminator output voltage, and it is important to know its relationship to the deviation before the narrow-band filter. Thus, applying equation 39 to the narrow-band filter gives:

$$\theta_{Disc} = \frac{\Delta f}{f_s}\left[\frac{\left[\alpha^2+(2\pi f_s)^2\right]\left[\beta^2+(2\pi f_s)^2\right]}{D^2+(2\pi f_s)^2(A^2-2D)+(2\pi f_s)^4}\right]^{1/2}\left[\frac{2\pi f_s}{S^2+(2\pi f_s)^2}\cdot\frac{\alpha}{S+\alpha}\right] \quad (40)$$

$$\theta_{Disc}(t) = \frac{\Delta f}{f_s}\frac{\alpha\left[\beta^2+(2\pi f_s)^2\right]^{1/2}\sin(2\pi f_s t+\psi)}{\left[D^2+(2\pi f_s)^2(A^2-2D)+(2\pi f_s)^4\right]^{1/2}} \quad (41)$$

Equation 37 gives an expression for noise bandwidth in terms of α, β, γ and loop gain. Since α, β and loop gain are determined by the reduction in deviation desired in the loop, only γ is somewhat free to be varied. One criterion for determining γ would be to minimize the loop bandwidth and thus, reduce the noise feedback to the mixer. Thus, differentiating equation 37 with respect to γ, setting this equal to zero, and solving for γ gives:

$$\gamma = \frac{(\alpha + \beta)(1 + K_1K_2)}{K_1K_2} + \sqrt{\frac{(\alpha + \beta)^2(1 + K_1K_2)^2}{K_1K_2} + \alpha\beta(1+K_1K_2)} \qquad (42)$$

D. Noise Bandwidth Considerations

Past experience with phase-lock loops used for signal detection has shown that these loops exhibit a threshold characteristic; i.e., below a given signal-to-noise ratio the loop can no longer adequately follow the signal and the detected signal deteriorates rapidly below this point. It would be expected that the f-m feedback loop would also have a threshold completely independent of the discriminator threshold point. A physical interpretation of threshold is as follows. At all signal levels the noise detected by the discriminator is fed back to the VCO. This appears as phase jitter on the local oscillator signal. As the signal level decreases the noise fed back increases, increasing the VCO phase jitter. A point is eventually reached where the VCO jitter will cause the difference signal-frequency in the narrow-band i-f to be pushed out of the passband an appreciable portion of the time decreasing the signal level even more. This point can be considered as the loop threshold. It is the purpose of this section to develop an analytical description of this process. Figure 6a shows a flat noise spectrum which can be considered as applied

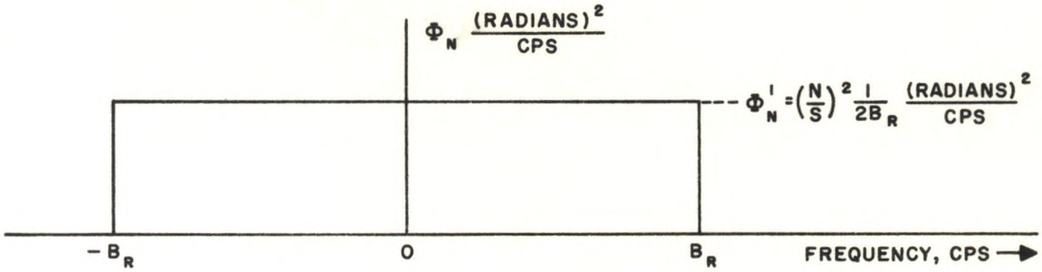

(A) INPUT PHASE NOISE SPECTRAL DENSITY

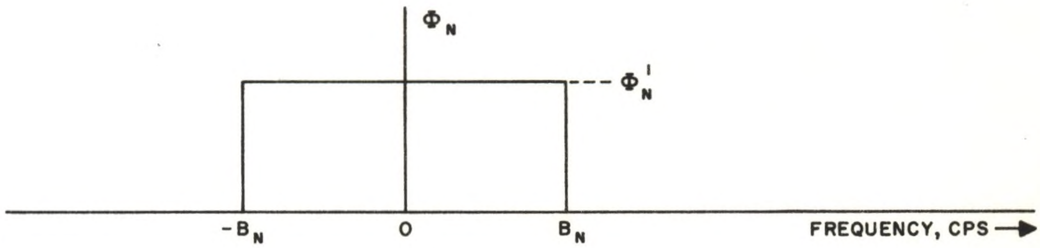

(B) VCO PHASE NOISE SPECTRAL DENSITY

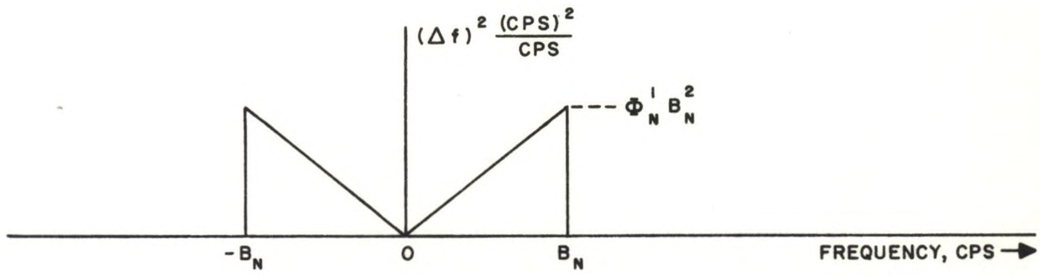

(C) VCO FREQUENCY NOISE SPECTRAL DENSITY

FIGURE 6. LOCAL OSCILLATOR NOISE SPECTRAL DENSITY

to the detection loop. The noise spectral density can be expressed as a function of signal level as shown. Assuming the loop bandwidth, $2B_N$, can be represented as a rectangular function, the noise spectrum on the VCO is shown in figure 6b. The spectral density is the same as the input but the bandwidth has been limited.

The desired parameter in this case is the frequency jitter, rather than phase jitter, to allow determination of the percentage of the time the signal is out of the i-f passband. The relationship between the two is:

$$\phi \text{ (radians)} = \frac{\Delta f}{f} \quad \text{(cps/cps)}$$

$$(\Delta f)^2 = (\phi \times f)^2$$

$$(\Delta f)^2/\text{cps} = \Phi_N \times f^2 \quad (\text{cps})^2/\text{cps}$$

Thus, the noise spectral density in terms of frequency jitter is as shown in figure 6c. The mean-square value of the noise jitter is equal to the area under the spectral density curve. Thus:

$$\sigma_{\Delta f}^{\,2} = \Phi_N \, B_N^{\,3} \quad (\text{cps})^2 \tag{43}$$

or:

$$\sigma_{\Delta f} = B_N^{\,3/2}\sqrt{\Phi_N} \quad \text{cps} \tag{44}$$

This equation states that for a given input noise spectral density, the frequency jitter on the VCO will increase as the 3/2 power of the noise bandwidth. This, it would seem, indicates the need in the design for obtaining as narrow a loop noise bandwidth as possible.

CHAPTER IV

SYSTEM DESIGN

A. Open-Loop Detector

To perform an experimental verification of the analysis, and to measure the relative thresholds, three types of detection systems will now be designed for a specific set of transmission parameters. The three types will be (1) open-loop, or normal discriminator detector, (2) first-order closed-loop detector, and (3) second-order closed-loop detector. The transmission parameters for which the detector systems will be designed were chosen as being adequate to investigate the technique of feedback detection, while not requiring extremely complex laboratory equipment.

The system parameters chosen were:

Modulation Frequency	$0 \leq f_s \leq 5$ kc
Peak Frequency Deviation	30 kc
Carrier Frequency	60 mc

To determine the i-f bandwidth necessary for transmission of the signal requires that a choice be made as to how many of the sidebands are significant. In actual practice this choice depends upon the particular application and quality of transmission desired. Good quality transmission can be obtained by making the 3-db bandwidth equal to $3\Delta f$, or 90 kc for this amplication. This will pass all sidebands that are

2% or greater of the unmodulated carrier amplitude. If a double-tuned i-f circuit is used, Appendix A shows that the noise bandwidth is 1.11 times the 3-db bandwidth. Thus:

$$2B_R = (1.11)(3)(30 \text{ kc}) = 99.9 \text{ kc}$$

The audio filter will be designed so that the highest modulation frequency, 5 kc, is the 3-db transmission point. Again, this is somewhat arbitrary, but does have precedent in past experience. Thus:

$$b_o = 5 \text{ kc}$$

From equation 11, the signal-to-noise improvement ratio is:

$$\frac{(S/N)^2_{out}}{(S/N)^2_{in}} = \frac{361}{1 + \left(\frac{f_s}{5000}\right)^4}$$

This is equal to 25.55-db improvement for low frequencies and drops 3 db to 22.55 db at 5 kc.

The threshold for an f-m detector as determined by other authors[11] occurs at approximately 10-db signal-to-noise ratio at the discriminator. Since this is in a 99.9-kc noise bandwidth, it is of interest to determine the improvement referred to twice the intelligence bandwidth, or 10 kc. On this basis the threshold is at 20-db signal-to-noise ratio in 10 kc. The signal-to-noise ratio in the output at threshold is 32.55 db for 5 kc and 35.55 db for low frequencies. A comparison to linear amplitude detection would then show an improvement of from

20 to 35.55 db (15.55 db) for signals at threshold, and an equal improvement for signals above threshold.

Also of importance is the transfer function from the detector input to the discriminator. This is the transfer function of the double-tuned filter since all other circuits can be considered as extremely wide as compared to the filter. Thus:

$$\frac{\theta_3}{\theta_1}(s) = \frac{D_o^2}{D_o^2 + \sqrt{2}\, D_o S + D_o^2} \tag{45}$$

The curve of the transfer function is presented in figure 7 for the condition of d_o equal to 45 kc.

B. First-Order Loop

In designing a feedback loop to be compared with the open-loop detection system the problem arises as to what closed-loop system constitutes an equivalent detection system. The first possible criterion that might be suggested would be the reduction of the deviation in the narrow-band i-f to unity. However, this does not necessarily ensure equivalent detection quality, and might put an unnecessary qualification on the closed-loop system. A second criterion became apparent during the study program, and was the one finally used in determining equivalence of design. This one was based upon making the transfer function from input to output of the closed-loop system at least as wide as the open-loop system. The open-loop system as determined in Chapter IV-A

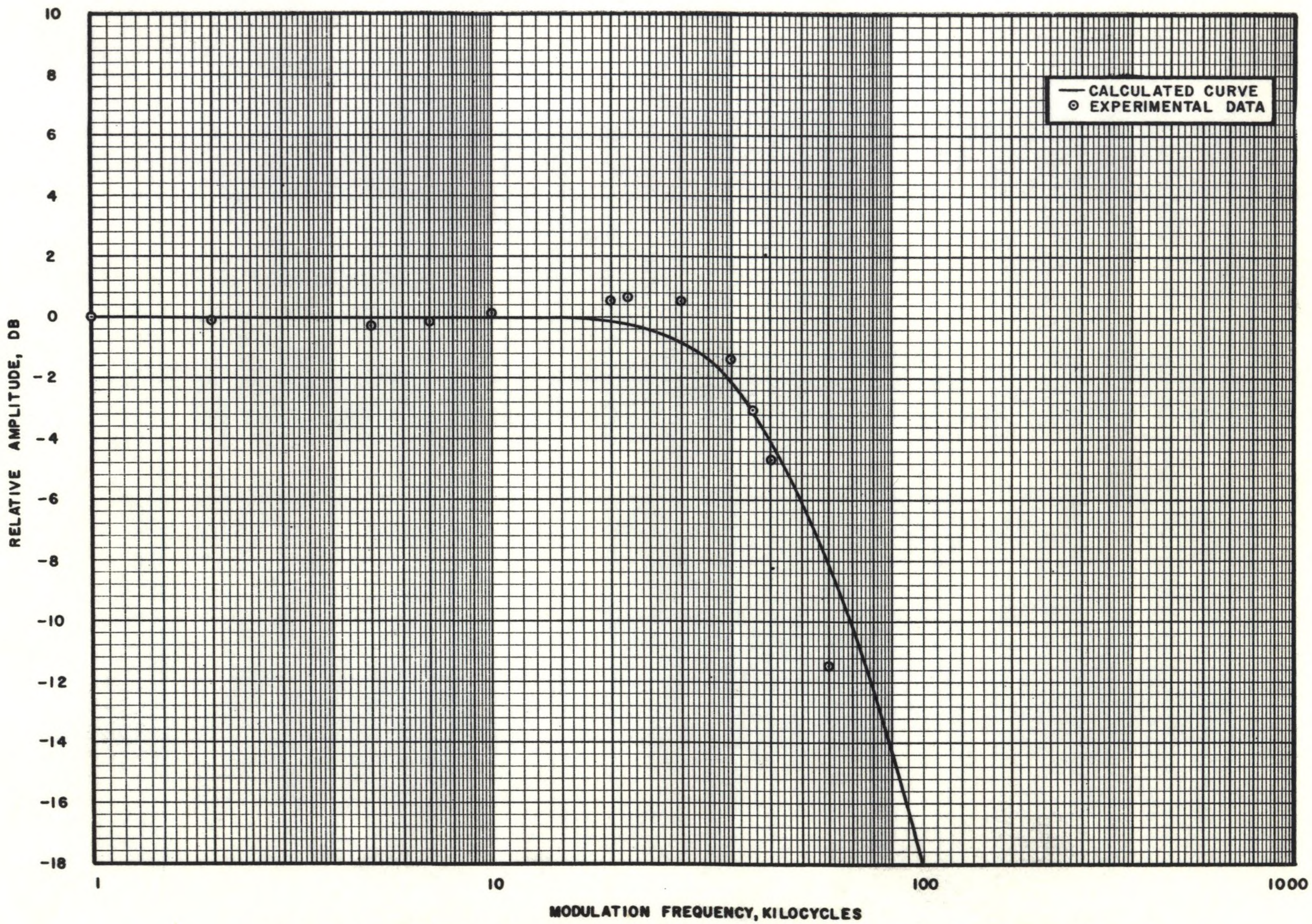

FIGURE 7 INPUT TO DISCRIMINATOR TRANSFER FUNCTION FOR OPEN LOOP DETECTOR

passed the signal through a double-tuned circuit with 3-db points at $\pm$ 45 kc. Thus, the closed-loop transfer functions, equations 14 and 30, should provide at least 45 kc of bandwidth at the 3-db points before entering the discriminator.

The first-order loop can now be designed on this basis. By referring to equation 14, a new equation can be written for the transfer function to the discriminator. This is:

$$\frac{\theta_3}{\theta_1} = \frac{\alpha}{S + \alpha(1 + K_1K_2)} \tag{46}$$

For the 3-db point to be at 45 kc requires that:

$$\alpha(1 + K_1K_2) = 2\pi(45 \text{ kc})$$

A second desire in designing a closed-loop system would be to minimize the loop bandwidth, as discussed previously. Referring to equation 25 it can be seen that for the first-order loop choosing the product $\alpha(1 + K_1K_2)$ determines the bandwidth. This leaves the choice of either α or gain rather arbitrary. For this case, α was chosen so that the narrow-band i-f 3-db points were three times the intelligence bandwidth of 5 kc, or:

$$\alpha = 2\pi \times 7.5 \text{ kc}$$

This then requires a gain of:

$$K_1K_2 = 5$$

Having chosen these values, it remains to substitute these in equations 25, 23, 26, 46, and 13 to obtain respectively noise bandwidth, S/N improvement, phase deviation reduction factor, input-to-discriminator transfer function, and loop transfer function. This information is presented in tables 1, 2, and 3 and figure 8. For a first-order loop the two transfer functions are identical when normalized and are presented together.

The ratio of the open-loop filter noise bandwidth of 99.9 kc to the first-order loop filter noise bandwidth of 15 kc x 1.571 (see Appendix B) is 6.27 db. Thus, the discriminator threshold improvement should be 6.27 for the first-order loop.

C. Second-Order Loop

The design of a second-order loop to the requirement of at least a bandwidth equal to the open-loop transfer function is not as straightforward as the first-order loop design because of the four parameters that must be chosen. This can be seen by referring to equation 30, the transfer function, and equation 37, the loop noise bandwidth. For this reason four second-order loops will be designed and compared to cover a range of values.

First it is desirable to modify equation 30 so that it expresses the transfer function from detector input to the discriminator input rather than discriminator output. Thus:

$$\frac{\theta_3}{\theta_1} = \frac{\alpha(s + \beta)}{s^2 + \left[\alpha + \beta + \frac{K_1 K_2 \alpha\beta}{\gamma}\right] s + \alpha\beta(1 + K_1 K_2)} \qquad (47)$$

	First-Order Loop	Second-Order Loop-1	Second-Order Loop-2	Second-Order Loop-3	Second-Order Loop-4
$\alpha/2\pi$	7.5 kc	7.5 kc	7.5 kc	7.5 kc	7.5 kc
$\beta/2\pi$		20 kc	7.5 kc	28.3 kc	7.5 kc
$\gamma/2\pi$		80 kc	45 kc	100 kc	45 kc
K_1K_2	5	3.5	3.5	5.35	6.5
$2B_N$	141 kc	68.75 kc	46.1 kc	102 kc	69.3 kc

Table 1. Closed-Loop Detection Circuit Parameters

	Modulation Frequency		
	1 kc	3 kc	5 kc
Open Loop (over Input)	25.55 db	25.03 db	22.55 db
First-Order Loop (Referred to Open Loop)	+0.17 db	+0.15 db	+0.12 db
Second-Order Loop-1 (Referred to Open Loop)	-1.03 db	-0.91 db	-0.72 db
Second-Order Loop-2 (Referred to Open Loop)	-5.14 db	-4.52 db	-3.48 db
Second-Order Loop-3 (Referred to Open Loop)	-0.98 db	-0.93 db	-0.82 db
Second-Order Loop-4 (Referred to Open Loop)	-4.74 db	-4.11 db	-3.05 db

Table 2. Calculated Signal-to-Noise Improvement

Circuit Configuration	Modulation Frequency		
	1 kc	3 kc	5 kc
First-Order Loop	0.168	0.1795	0.199
Second-Order Loop-1	0.224	0.242	0.276
Second-Order Loop-2	0.227	0.260	0.327
Second-Order Loop-3	0.158	0.171	0.192
Second-Order Loop-4	0.136	0.156	0.196

Table 3. Calculated Phase Deviation Reduction Factor for Closed-Loop Detection

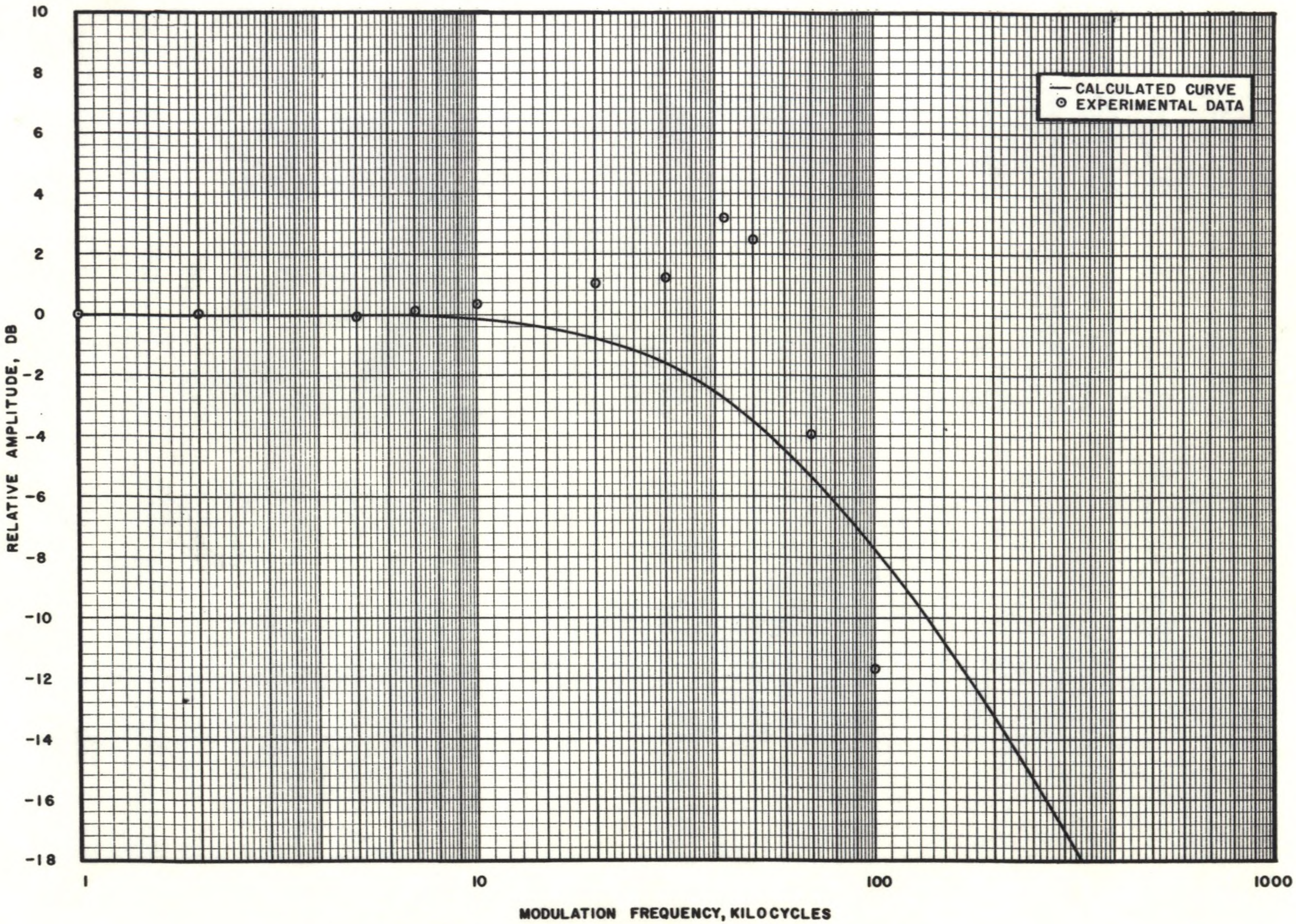

FIGURE 8 FIRST ORDER LOOP TRANSFER FUNCTION

The first design was intended to match the open-loop transfer function rather closely. The i-f bandwidth was again chosen to be $\pm$ 7.5 kc at the 3-db points. The other three parameters were then varied in a systematic manner to find a flat response with a 3-db point at approximately 45 kc. This resulted in:

$$\alpha = 2\pi\ 7{,}500$$

$$\beta = 2\pi\ 20{,}000$$

$$\gamma = 2\pi\ 80{,}000$$

$$K_1K_2 = 3.5$$

These values were then substituted into equations 37, 35, 39 47, and 29 to give respectively noise bandwidth, signal-to-noise improvement, phase deviation reduction factor, input-to-discriminator transfer function, and loop transfer function. This information is presented in tables 1, 2, and 3, and figures 9 and 10.

A second second-order loop can be designed with the same loop gain as before, but a narrower loop noise bandwidth. With α and K_1K_2 the same as before, the value of β can be reduced to narrow the noise bandwidth. Intuitively, β can be reduced to approximately 2π x 7.5 kc without increasing the signal deviation in the i-f greatly. Reducing β much beyond this value will begin to greatly reduce the feedback at the higher modulation frequencies (5 kc) and thus appreciably increase the i-f deviation. Having thus chosen 3 values, γ can be determined from equation 42 to minimize noise

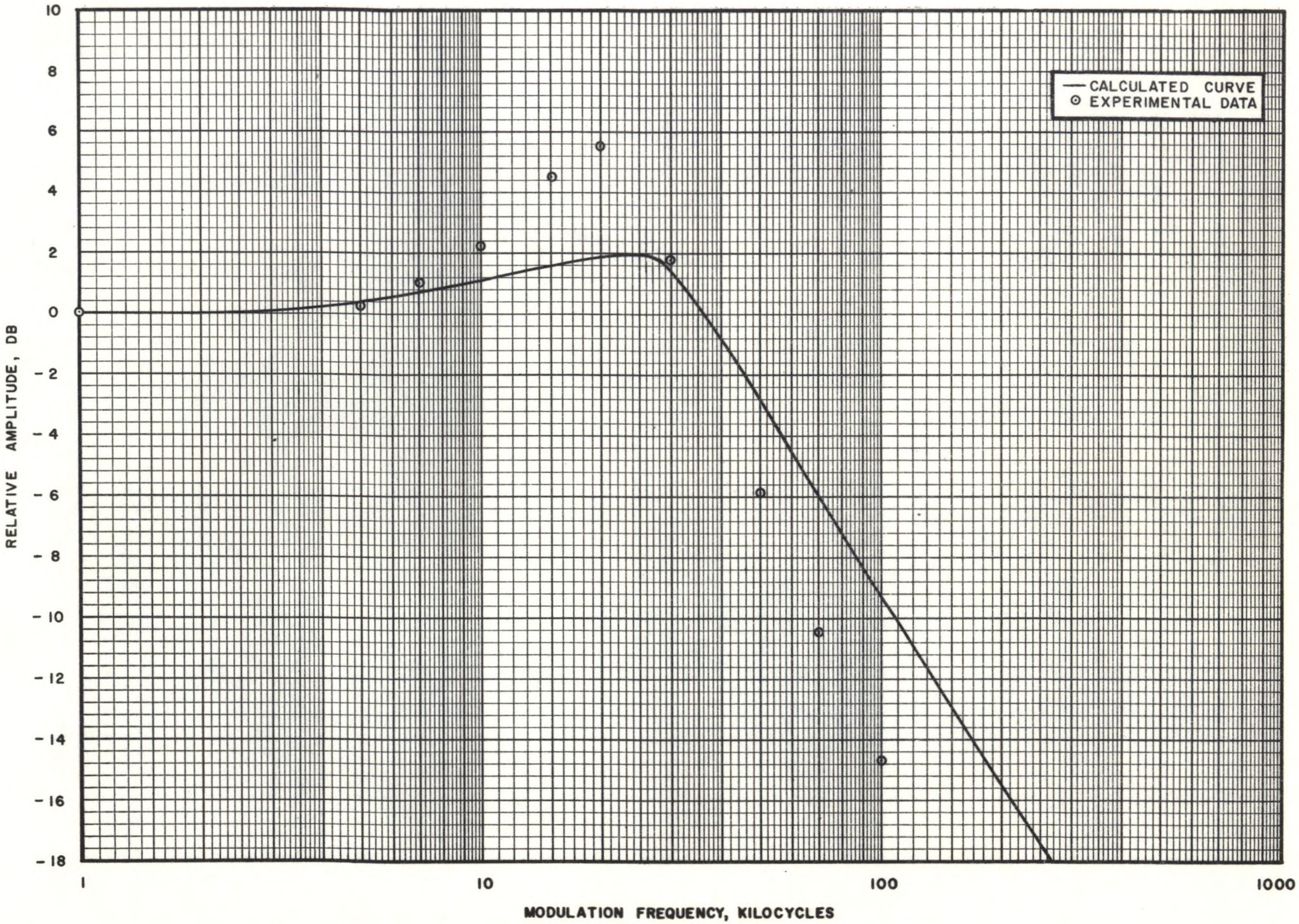

FIGURE 9 INPUT TO DISCRIMINATOR TRANSFER FUNCTION FOR SECOND ORDER LOOP NO. I

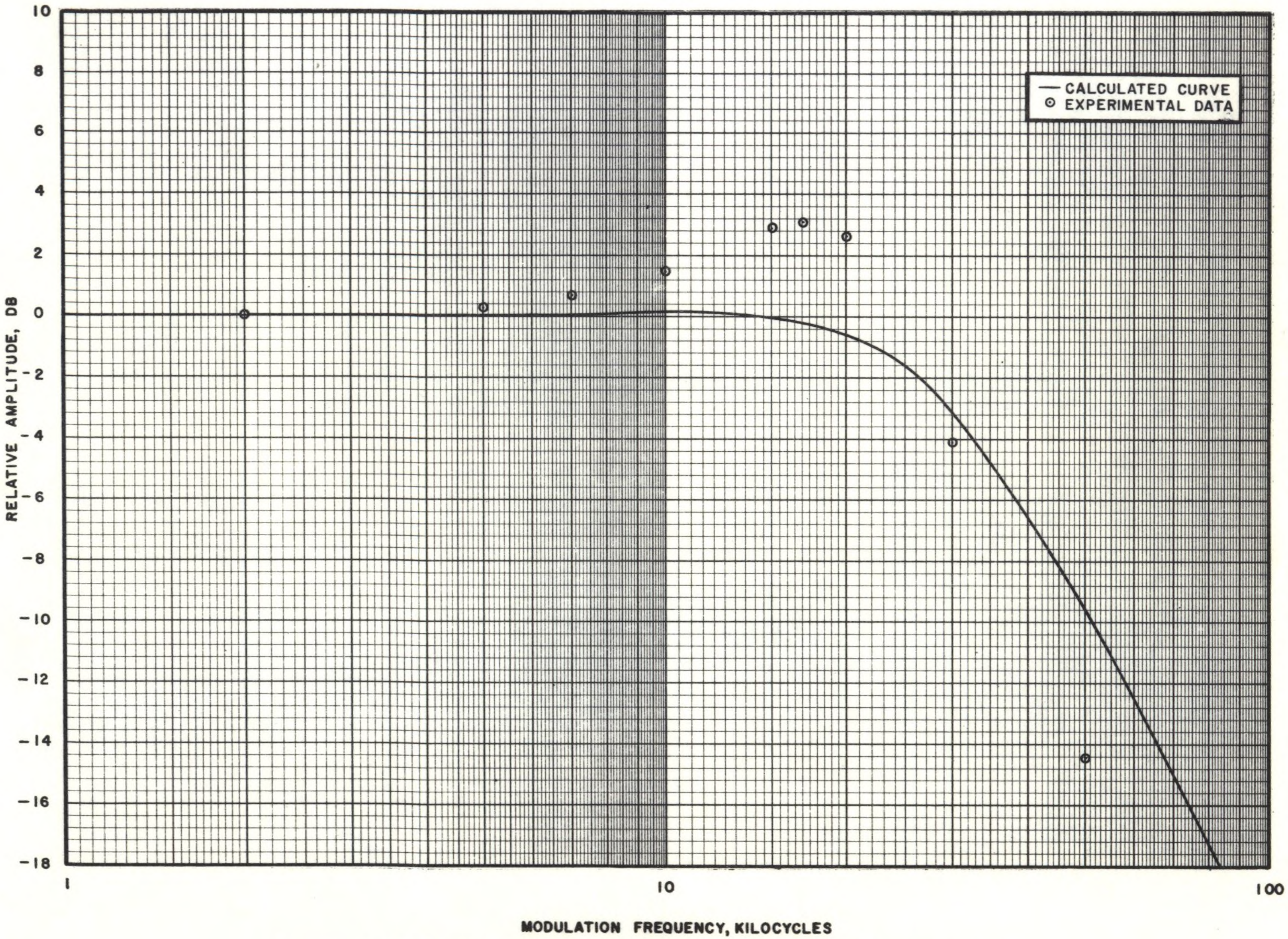

FIGURE 10 LOOP TRANSFER FUNCTION FOR SECOND ORDER LOOP NO. 1

bandwidth. This results in design values of:

$$\alpha = 2\pi \times 7{,}500$$

$$\beta = 2\pi \times 7{,}500$$

$$\gamma = 2\pi \times 45{,}000$$

$$K_1K_2 = 3.5$$

These values were again substituted into equations 37, 35, 39, 47, and 29 to give respectively noise bandwidth, signal-to-noise improvement, phase deviation reduction factor, input-to-discriminator function, and loop transfer function. This information is presented in tables 1, 2, and 3, and figures 11 and 12.

The design of the two previous loops resulted in a loop gain of only 3.5. This does not reduce the deviation in the i-f to unity, as was originally thought necessary, although it does give an equivalent transfer function. However, to complete the study it seems desirable to experimentally try loops with higher gains. To accomplish this the values of β, γ, and K_1K_2 were scaled up from the values used in second-order loop-1 designed in this section to give a reasonably flat transfer function although wider than before. The value of α was held the same as before. This results in design values of:

$$\alpha = 2\pi \times 7{,}500$$

$$\beta = 2\pi \times 28{,}300$$

$$\gamma = 2\pi \times 100{,}000$$

$$K_1K_2 = 5.35$$

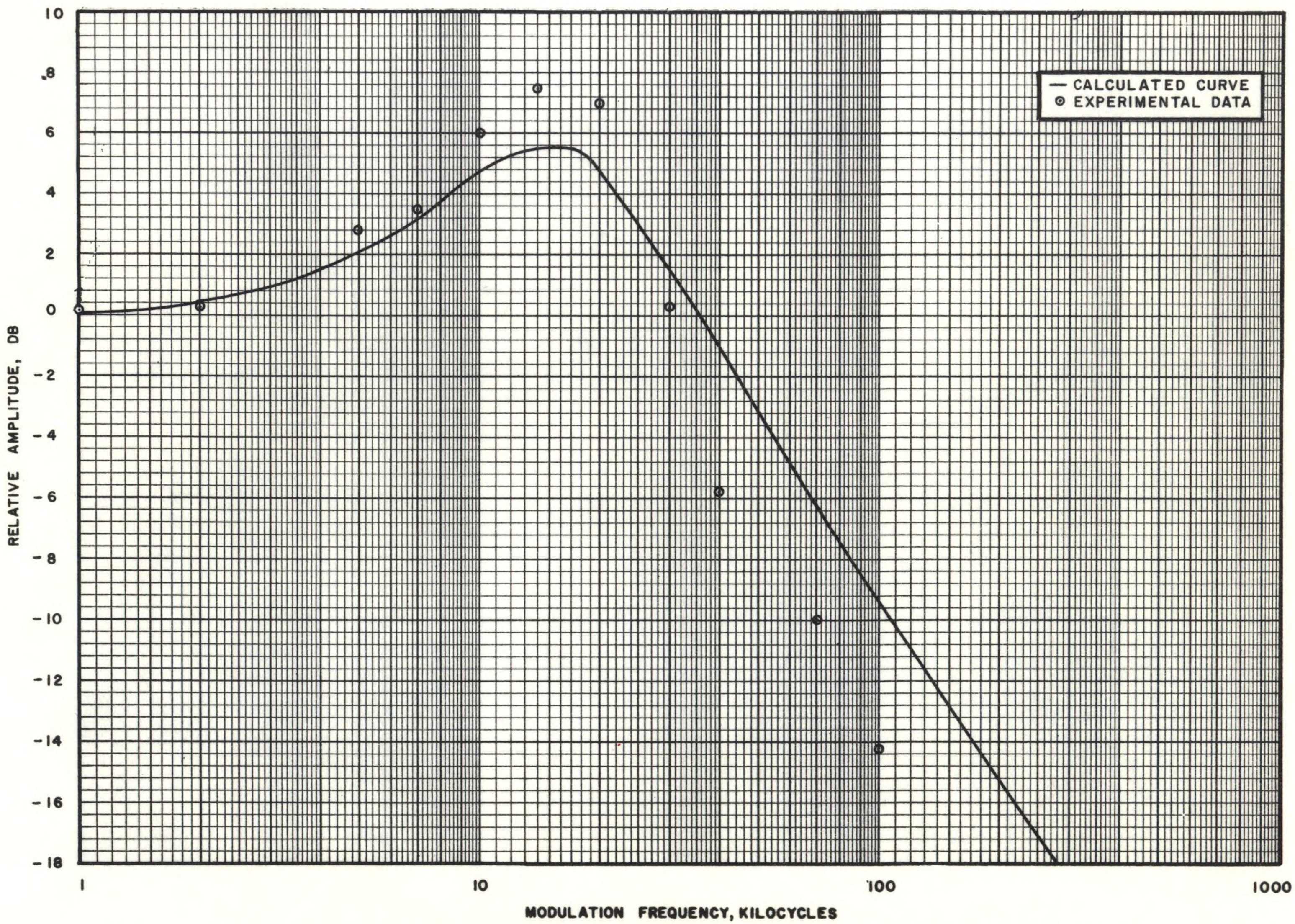

FIGURE 11 INPUT TO DISCRIMINATOR TRANSFER FUNCTION FOR SECOND ORDER LOOP NO. 2

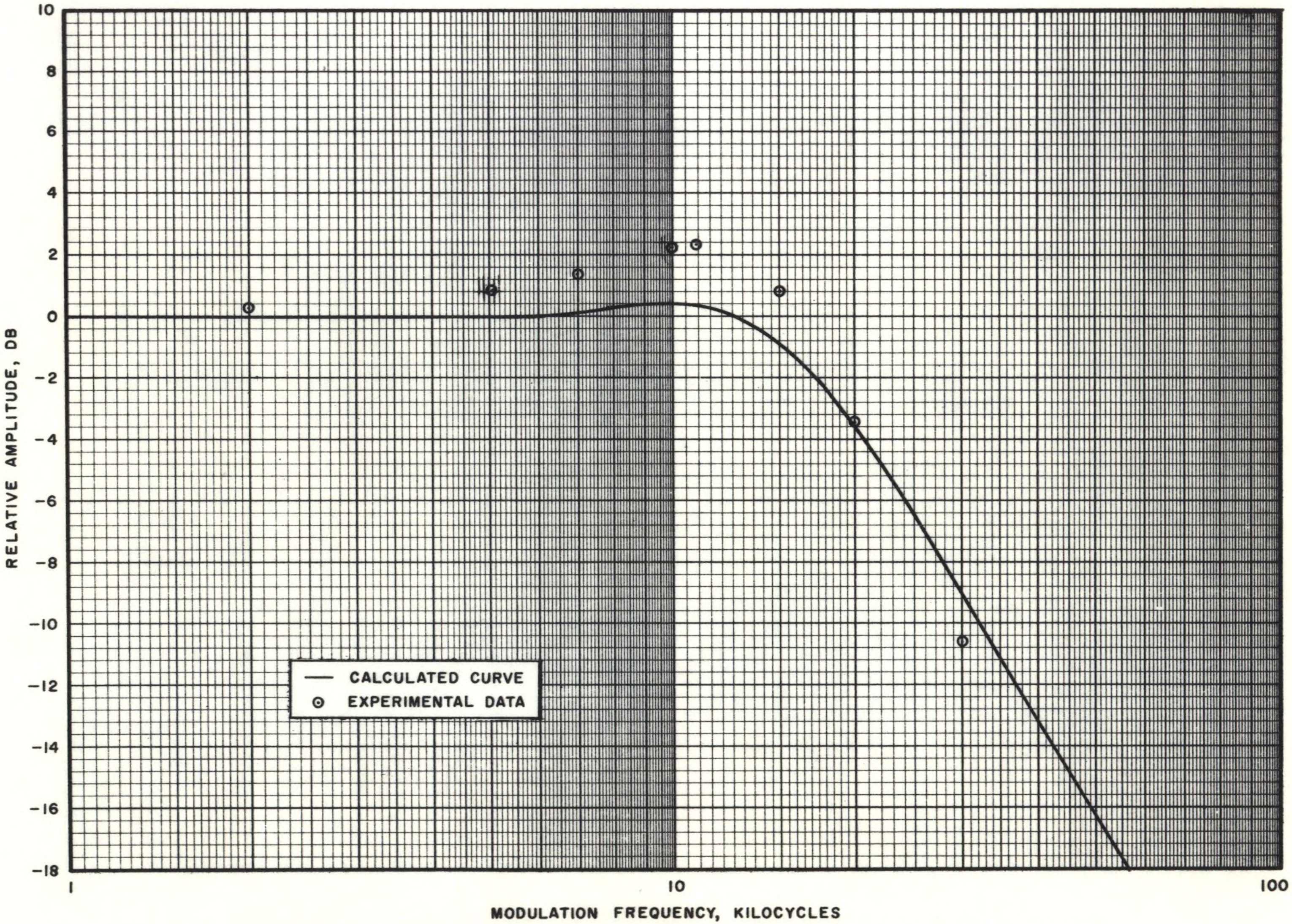

FIGURE 12 LOOP TRANSFER FUNCTION FOR SECOND-ORDER LOOP NO. 2

These values were again substituted into the design equations with the results shown in tables 1, 2, and 3, and figures 13 and 14.

The final second-order loop was designed to reduce the deviation to approximately unity or less in the narrow-band i-f and to minimize the loop noise bandwidth. While fulfilling the requirement of providing a transfer function from input-to-discriminator of at least $\pm$ 45 kc, it does not provide a flat transfer function. However, it does provide an interesting comparison and is closer to the original thinking at the start of the study. In fact, this loop was actually designed and tested before the three previous cases, but is presented in this order as being a more logical development. The value of α was chosen to be the same as the previous designs. The value of β was reduced to $2\pi \times 7.5$ kc as in second-order loop-2. A loop gain was chosen which reduced the index to approximately unity in the i-f, and γ was determined from equation 42. A summary of the resulting values is:

$$\alpha = 2\pi \times 7{,}500$$

$$\beta = 2\pi \times 7{,}500$$

$$\gamma = 2\pi \times 45{,}000$$

$$K_1K_2 = 6.5$$

These values were substituted into the design equations with the results shown in tables 1, 2, and 3, and figures 15 and 16.

For all four second-order loops designed, the i-f filter was constant with a 3-db bandwidth of 15 kc. This is the same as the first-

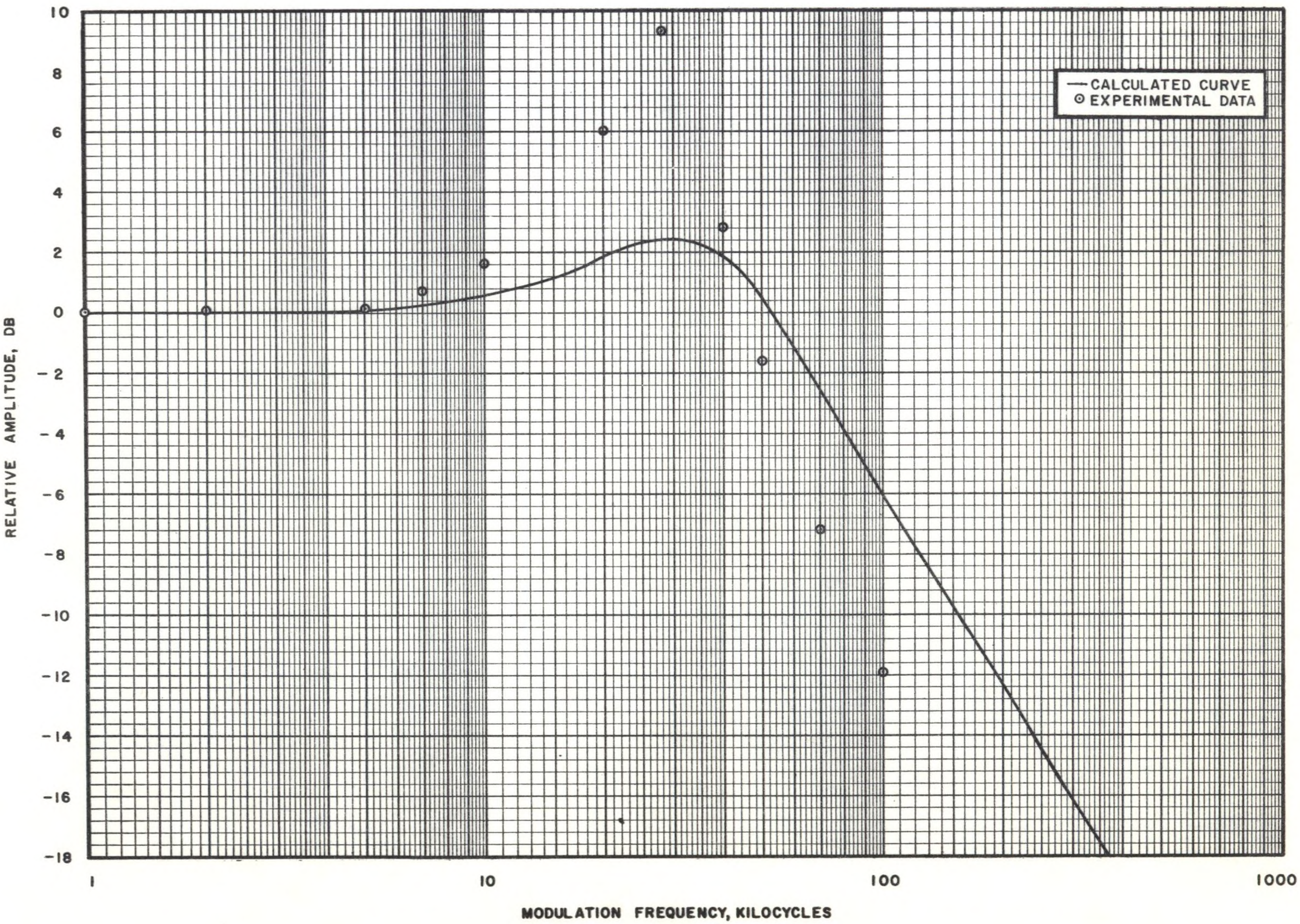

FIGURE 13 INPUT TO DISCRIMINATOR TRANSFER FUNCTION FOR SECOND ORDER LOOP NO. 3

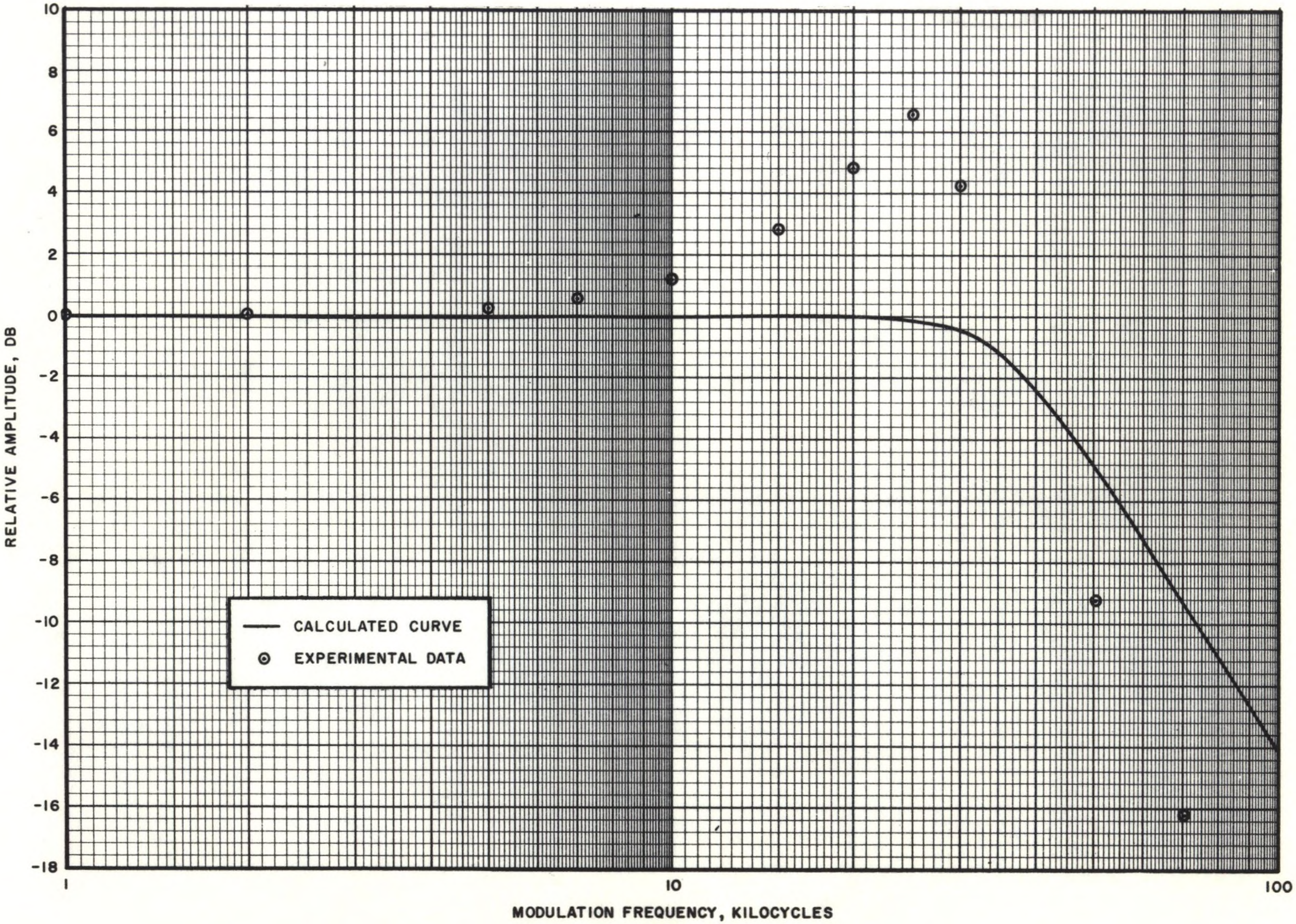

FIGURE 14 LOOP TRANSFER FUNCTION FOR SECOND ORDER LOOP NO. 3

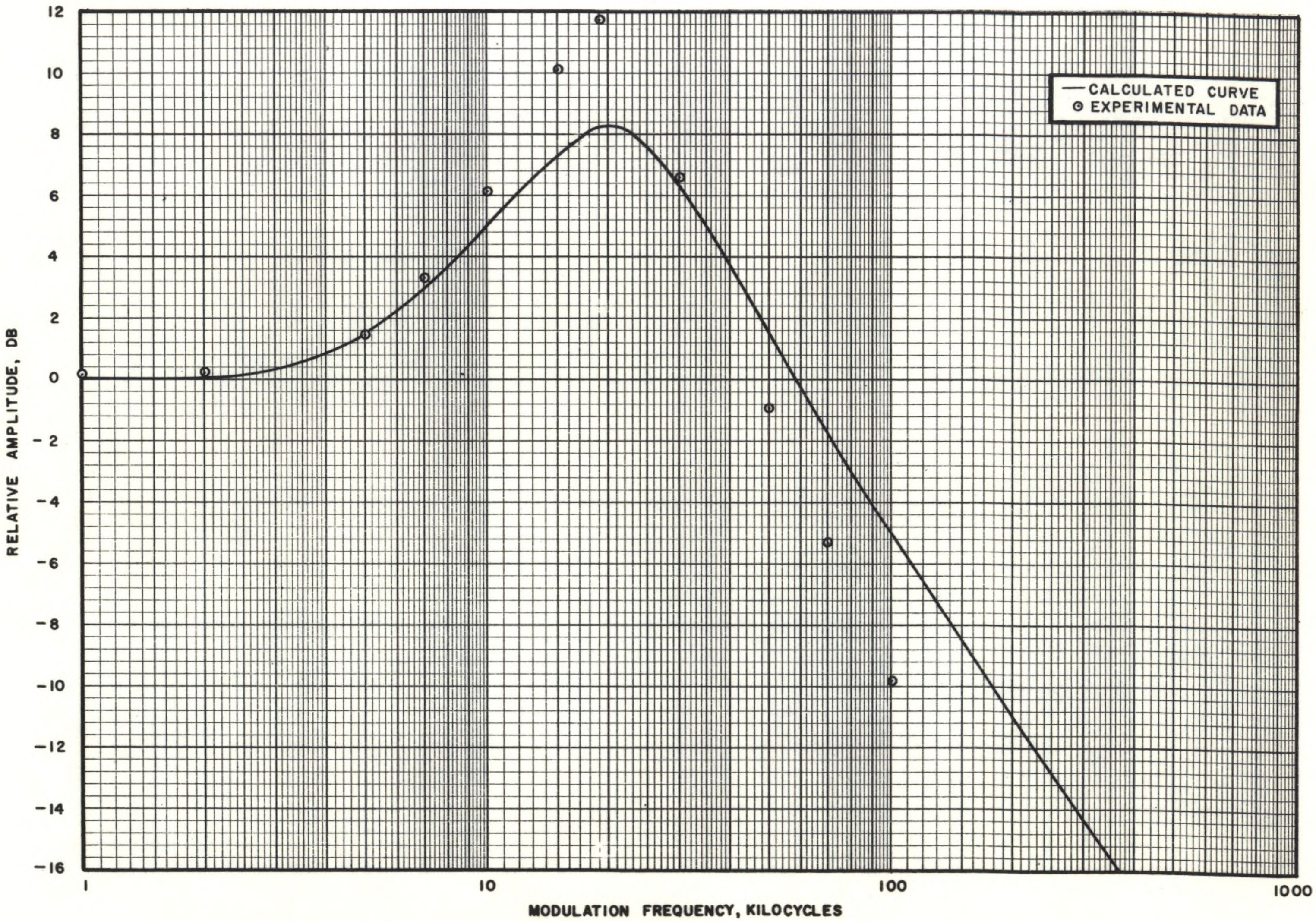

FIGURE 15 INPUT TO DISCRIMINATOR TRANSFER FUNCTION FOR SECOND ORDER LOOP NO. 4

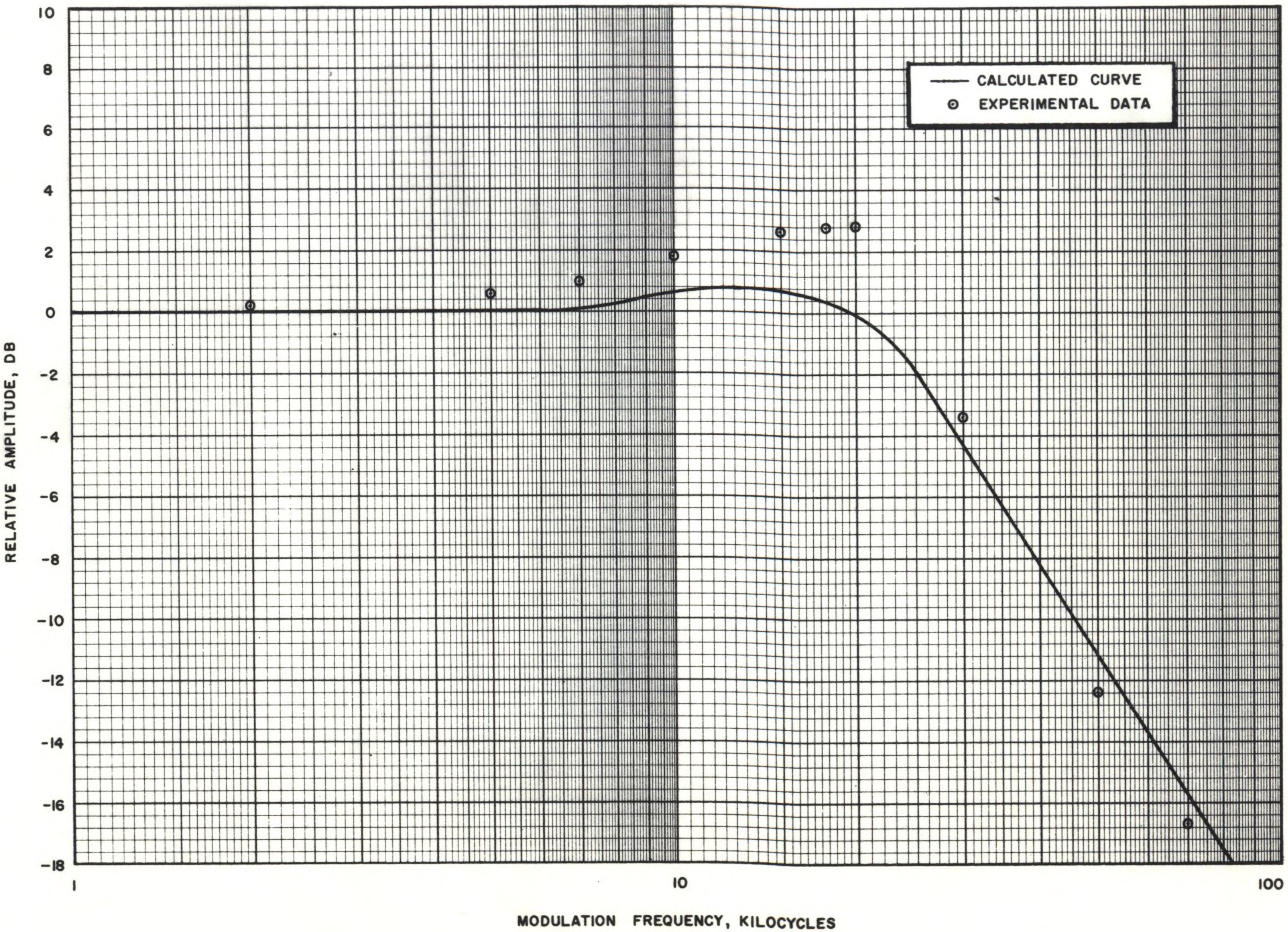

FIGURE 16 LOOP TRANSFER FUNCTION FOR SECOND ORDER LOOP NO. 4

order loop design. Thus, in all cases the discriminator threshold improvement over open-loop should be the same and be the ratio of the filter noise bandwidths. As calculated in Chapter IV-B this improvement is 6.27 db. The difference in the closed-loop designs is in loop noise bandwidth and transfer functions.

CHAPTER V

CIRCUIT DESIGN

A block diagram of the equipment used for the experimental portion of the study is shown in figure 17. The schematics of the equipment designed and built during the study are shown in Appendix C along with pertinent data taken on the equipment. Appendix D is a list of test equipment used during the laboratory work.

A 60-mc voltage-controlled oscillator was built for a signal source. This can be frequency-modulated with a test oscillator or other audio program material. A high-gain 60-mc i-f amplifier was used as a constant noise source. The output noise voltage was monitored by a Boonton r-f meter and adjusted to a fixed level by varying the amplifier agc voltage.

Both the signal and noise were attenuated to a low level. Variations in input signal-to-noise ratio were obtained by the variable attenuator in the noise generator lead while the signal was held constant. This simplified the circuit design by reducing the required dynamic range of the receiver amplifiers and limiter, since in most cases the signal is the larger of the two voltages.

The receiver consisted of a low-gain 60-mc amplifier followed

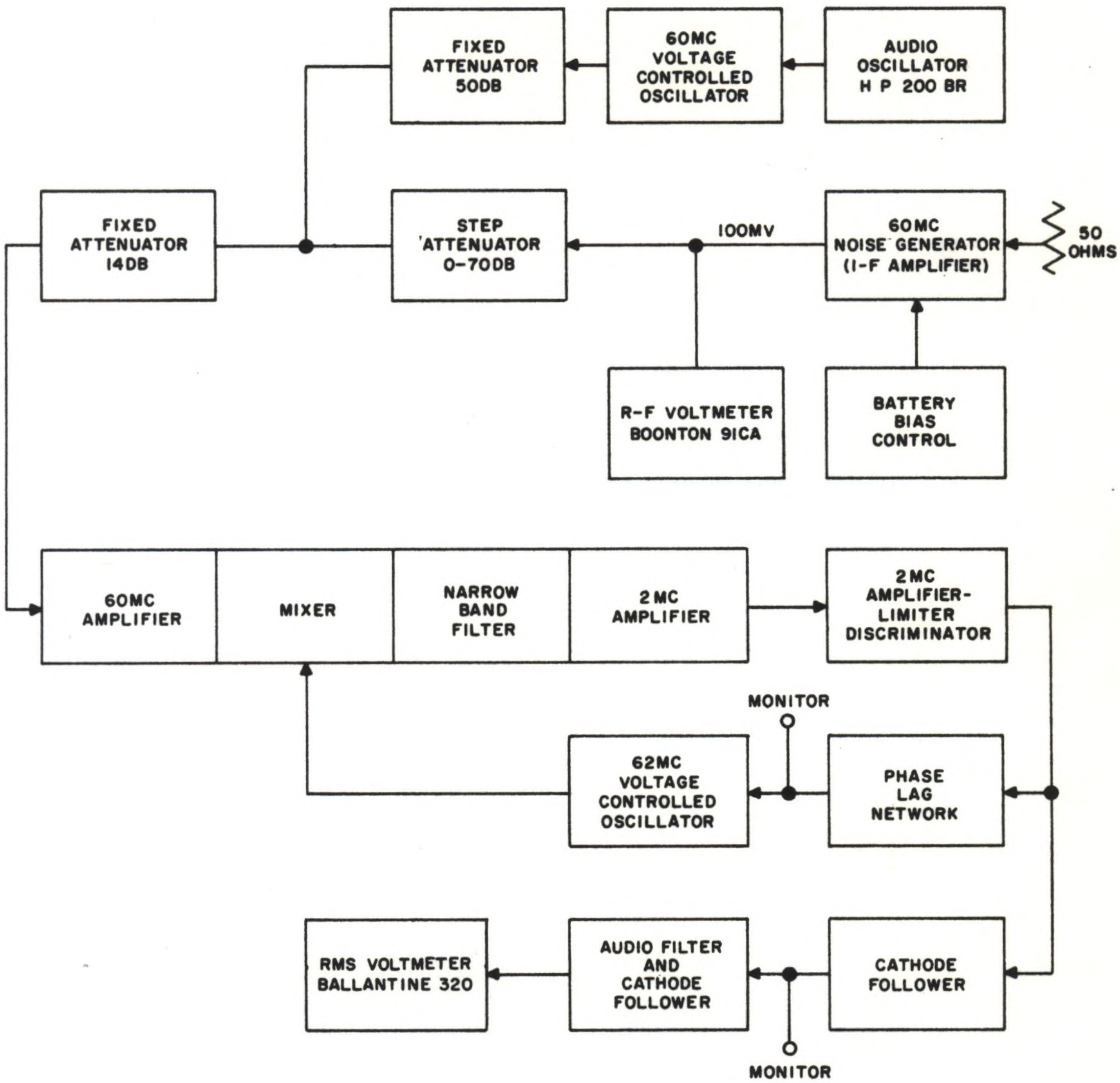

FIGURE 17. BLOCK DIAGRAM OF EXPERIMENTAL EQUIPMENT

by a mixer with a 2-mc output frequency. The plate circuit of the mixer was a narrow-band plug-in filter, which was a 90-kc double-tuned circuit for open-loop measurements and 15-kc single-tuned circuit for closed-loop measurements. This was followed by a 2-mc amplifier.

The second receiver chassis contained a second 2-mc amplifier, a one-stage limiter and a broad-band discriminator. A gain control was included following the limiter to make possible the adjustment of loop gain for closed-loop detection.

A 62-mc VCO was used as the local oscillator signal and was modulated by the discriminator output. The additional filtering required for the second-order loop was placed before the VCO. The VCO had the capability of being changed to crystal control for open-loop tests. However, it was found to be sufficiently stable with grounded input that it was not used as a crystal oscillator for the measurements.

To prevent loading, a cathode follower was used for obtaining the signal from the discriminator. This was followed by the 5-kc audio filter and a second cathode follower to provide a low impedance output. A Ballantine True RMS Voltmeter was used to make signal and noise measurements on the output. The meter was chosen because of its ability to read rms voltage regardless of wave shape.

All of the circuits in the feedback loop, with the exception of the narrow-band filter, were designed to be broadband so that phase shift across them would not be significant in the range of frequencies of interest. This was assumed in all of the calculations. In practice the amplifier circuits were broad-band with little phase shift below 150 kc. The discriminator, however, was not as wide as could be desired and did have some effect upon the results. The open-loop transfer function showing the actual bandwidth is presented in figure C-13 of the appendix.

The phase lag network used in the second-order loops is shown in figure C-8 along with the values of components used. The output impedance of the discriminator was approximately 20,000 ohms and was included in the filter design.

CHAPTER VI

EXPERIMENTAL RESULTS

A. Input-to-Discriminator Transfer Function

In Chapter IV the closed-loop designs were based upon the criterion that the input-to-out transfer function be at least as wide as the open-loop detector transfer function. Since the transfer function for both open- and closed-loop detectors include the discriminator function, $j\omega$, it became more practical to compare the transfer function from input-to-discriminator. This was done in Chapter IV and curves plotted in figures 7, 8, 9, 11, 13, and 15.

To measure this transfer function directly would require the input modulation index, $\Delta f/f$, to be constant over the frequency range, i.e., the peak deviation to increase with frequency, and would require the measurement of modulation index at the discriminator input. In practice it was more convenient to maintain the input deviation constant, and measure the deviation into (voltage out of) the discriminator. By this method the measured values were maintained at a more uniform level above circuit noise. The measurement point used was after the first cathode follower and before the audio filter. A Ballantine True RMS Voltmeter was used to measure the signal amplitude.

The data was taken in this manner for open-loop and the five closed-loop cases. It was normalized and is presented on the same curves with the calculated data.

A comparison of measured and calculated data indicates reasonably good correlation. However, in each closed-loop case the measured data peaks higher and then falls off more rapidly than calculated. It is felt that this is caused by the loop circuits, primarily the discriminator, not being sufficiently wide so as to add negligible phase shift as assumed for the calculations.

B. Closed-Loop Transfer Function

The closed-loop transfer function is taken from the signal input to the local oscillator output, and is an indication of loop noise bandwidth. This was calculated in Chapter IV for the five closed-loop circuits and presented in figures 8, 10, 12, 14, and 16. It will be noted that for the first-order loop the closed-loop transfer function and the input-to-discriminator transfer function are identical.

Measurement of this function directly would require maintaining the input modulation index constant as the modulation frequency is varied and measuring the modulation index on the 62-mc VCO output. A more practical technique that was used is to keep the input deviation constant and effectively measure the VCO deviation by measuring the voltage into the VCO. This voltage was measured by use of a high impedance oscilloscope probe which had negligible loading effect upon the circuit.

A comparison of measured and calculated data in figures 8, 10, 12, 14, and 16 indicates good correlation. As with the input-to-discriminator functions, however, the peaks are higher and the rolloff more rapid for the measured values. This again is attributed to the fact that the discriminator is not sufficiently wideband to be negligible.

C. Signal-to-Noise Improvement

The signal-to-noise ratio in the output of the open-loop discriminator detection circuit has been given by equation 11. The method used to verify this was to measure the carrier power at the output of the mixer chassis and then measure the noise power with the carrier removed. By knowing the noise bandwidth of the open-loop filter to be 100 kc (Chapter IV-A) the noise spectral density at the input can be calculated. The following data was taken with the noise attenuator setting at 40 db.

Carrier voltage out of mixer chassis = 238 mv

Noise voltage out of mixer chassis = 35 mv

$$\Phi_N = \left(\frac{N}{S}\right)^2 \frac{1}{2B_N} = \left(\frac{35}{238}\right)^2 \frac{1}{100\text{kc}} = 2.16 \times 10^{-7} \frac{(\text{radians})^2}{\text{cps}}$$

From equation 11 the S/N ratio in the output can now be calculated. For a peak deviation of 30 kc, a modulation frequency of 5 kc, an i-f filter 90 kc wide, and an audio filter with a 5-kc 3-db point, equation 11 gives:

$$(S/N)^2_{out} = 8.44 \times 10^3, \quad \text{or } 39.25 \text{ db}$$

The signal-to-noise ratio in the output was measured by first measuring signal plus noise at the cathode follower output with the true rms meter. The deviation was removed from the signal and a measurement of output noise made. For the conditions given above, these measurements were:

$$S + N = 720 \text{ mv}$$

$$N = 7.2 \text{ mv}$$

$$(S/N)^2 = 10^4 \text{ or } 40 \text{ db}$$

This differs from the calculated value by only 0.75 db. This difference can be attributed to the manner in which noise was measured. As discussed in several articles on f-m[4], measurement of noise with the carrier present but deviation removed is an approximation and in error by 1-2 db, depending upon the modulation index.

Equations 23 and 35 give the output S/N ratio for the closed-loop cases. As calculated in Chapter IV the closed-loop detector gives an improvement factor which is approximately equal to the open-loop detector improvement factor. To verify the calculations the S/N ratio at the output was measured with the loop closed. The loop was then opened, the 90-kc filter substituted for the 15-kc filter, and the S/N measured for the open-loop case. This was done for all five closed-loop configurations at two modulation frequencies for each configuration. The difference between open- and closed-loop measurements is given in table 4. The calculated values for the same conditions were presented previously in table 2. A comparison shows very good agreement in most cases. Only for loops 2 and 3 does the difference between measured and calculated values exceed 1 db, and never does it exceed 2 db. This indicates that the closed-loop output S/N ratio is predictable with the derived equations and is approximately the same as open-loop detection.

D. Threshold Improvement Measurements

The five closed-loop detection circuits were designed to be approximately equivalent to the open-loop detection circuit in quality so that a direct comparison of the detection thresholds could be made. To determine the threshold point, data was taken and a curve plotted showing measured output S/N ratio as a function of input S/N. A description of the procedure used in obtaining

	MODULATION FREQUENCY	
	1 kc	5 kc
First-Order Loop	-0.5 db	-0.36 db
Second-Order Loop-1	-1.0 db	-0.26 db
Second-Order Loop-2	-3.8 db	-1.54 db
Second-Order Loop-3	-2.54 db	-1.8 db
Second-Order Loop-4	-4.49 db	-2.59 db

Table 4. Closed-Loop S/N Improvement Referenced to Open-Loop Results

these curves, figures 18 through 22, is as follows: A specific closed-loop configuration was implemented using the narrow-band 15-kc filter, and a phase lag network in the feedback loop for the second-order loops. The input noise was varied by means of the step attenuators indicated in figure 17. For each attenuator setting the output signal-to-noise ratio was determined by first measuring the output signal-plus-noise with a modulation frequency of 5 kc and peak deviation of 30 kc. The output noise

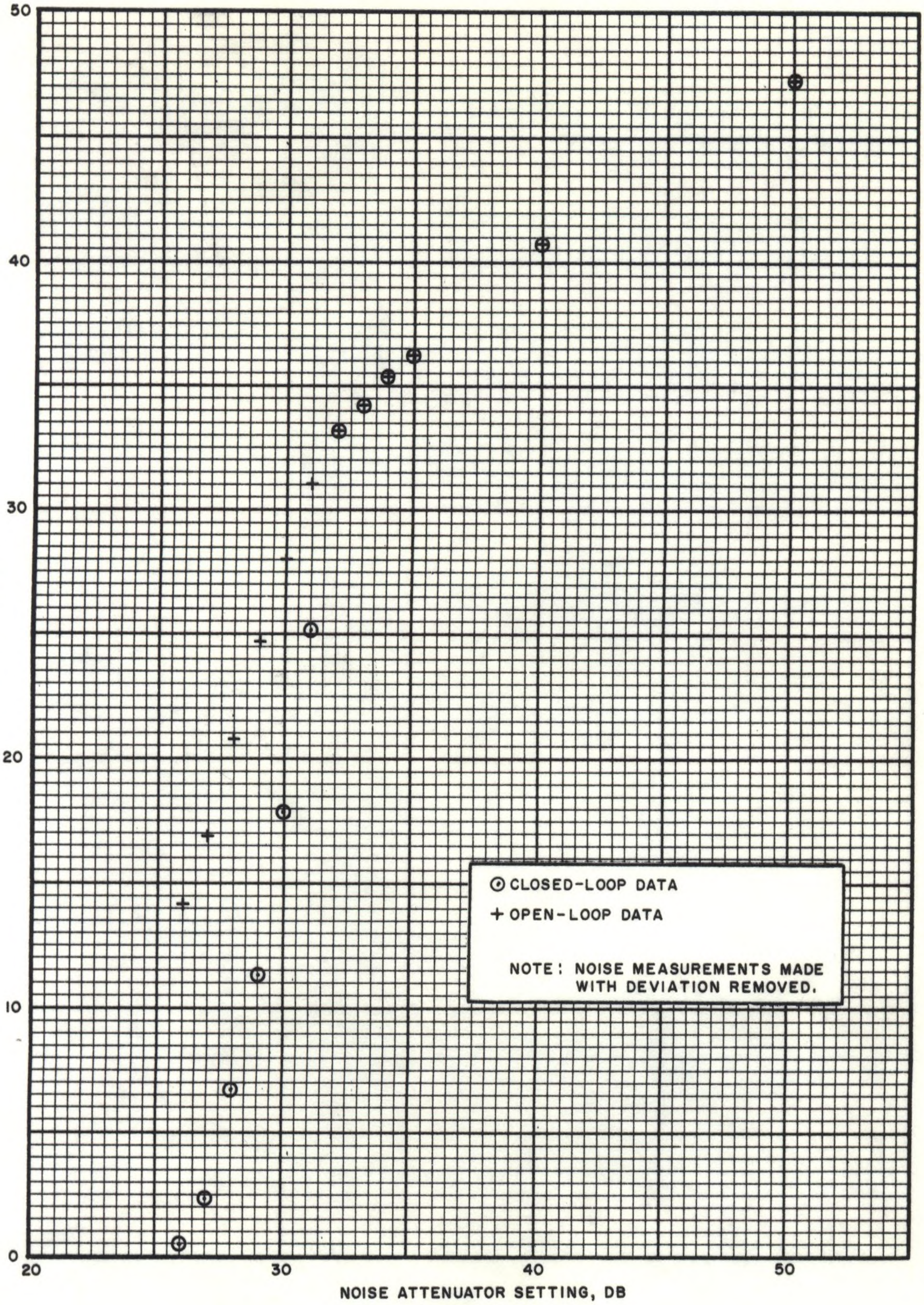

FIGURE 18 OUTPUT S/N CURVE, FIRST-ORDER LOOP AND OPEN-LOOP

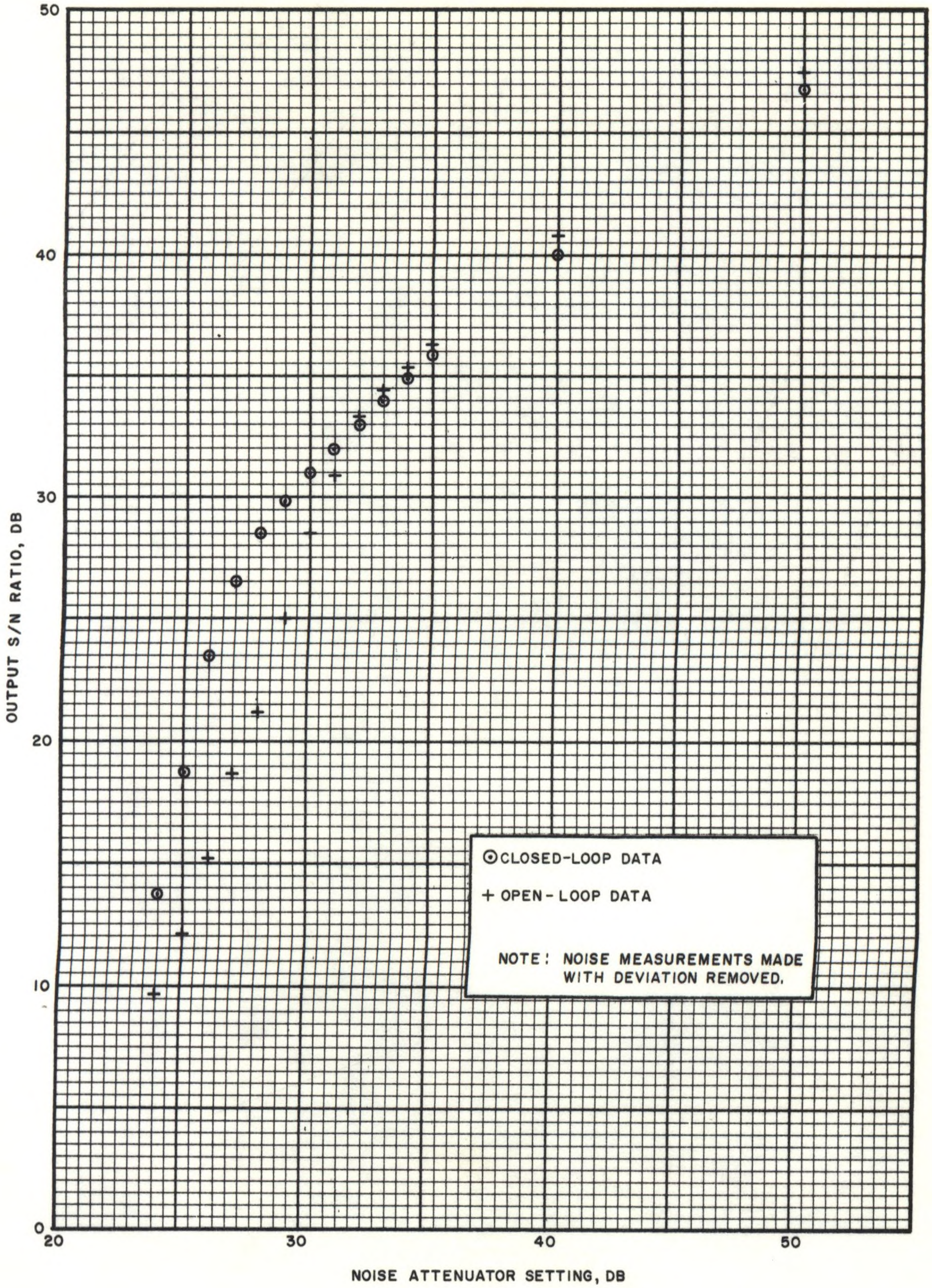

FIGURE 19 OUTPUT S/N CURVE,
SECOND ORDER LOOP NO. 1 AND OPEN-LOOP

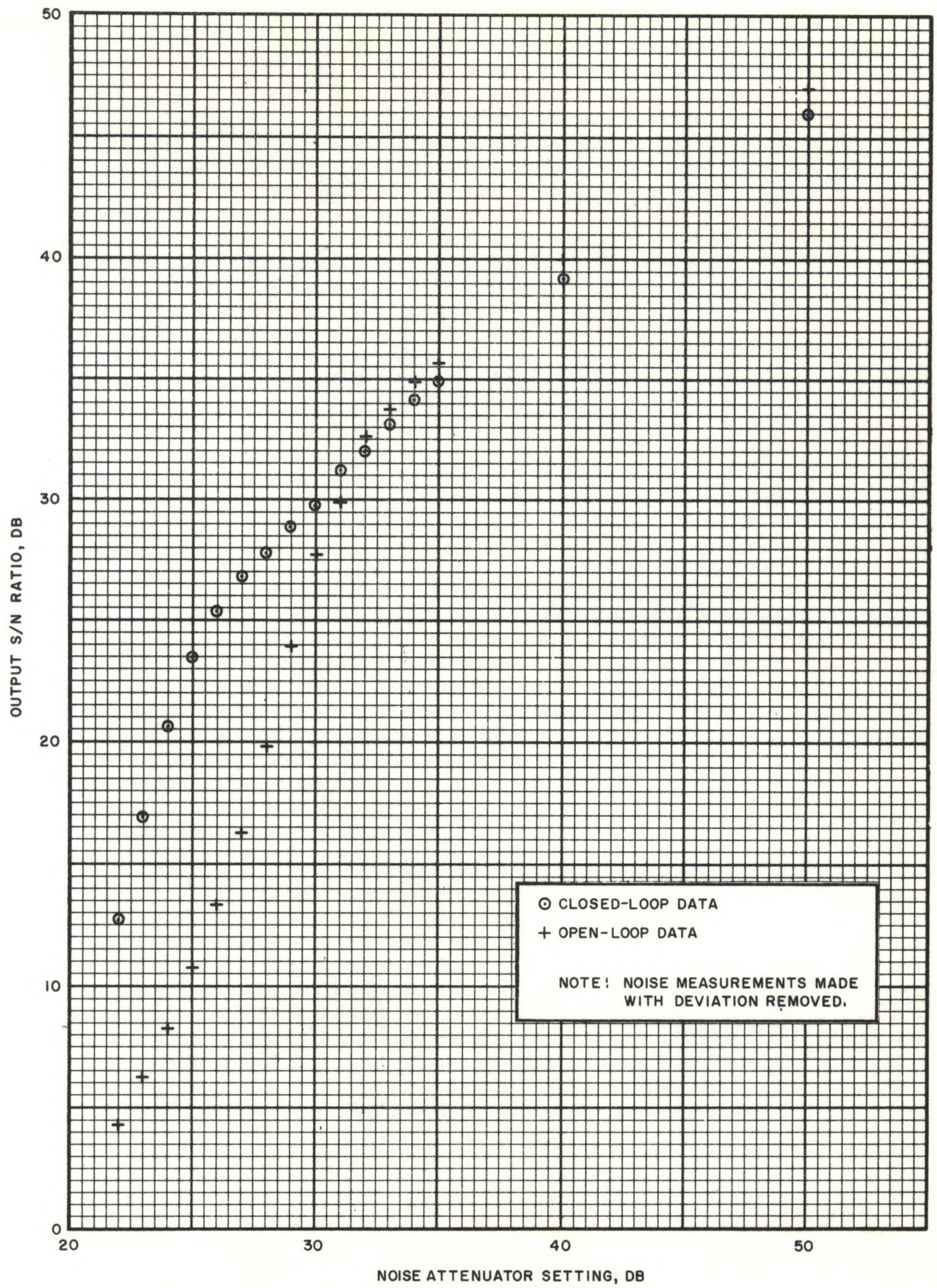

FIGURE 20 OUTPUT S/N CURVE,
SECOND ORDER LOOP NO. 2 AND OPEN-LOOP

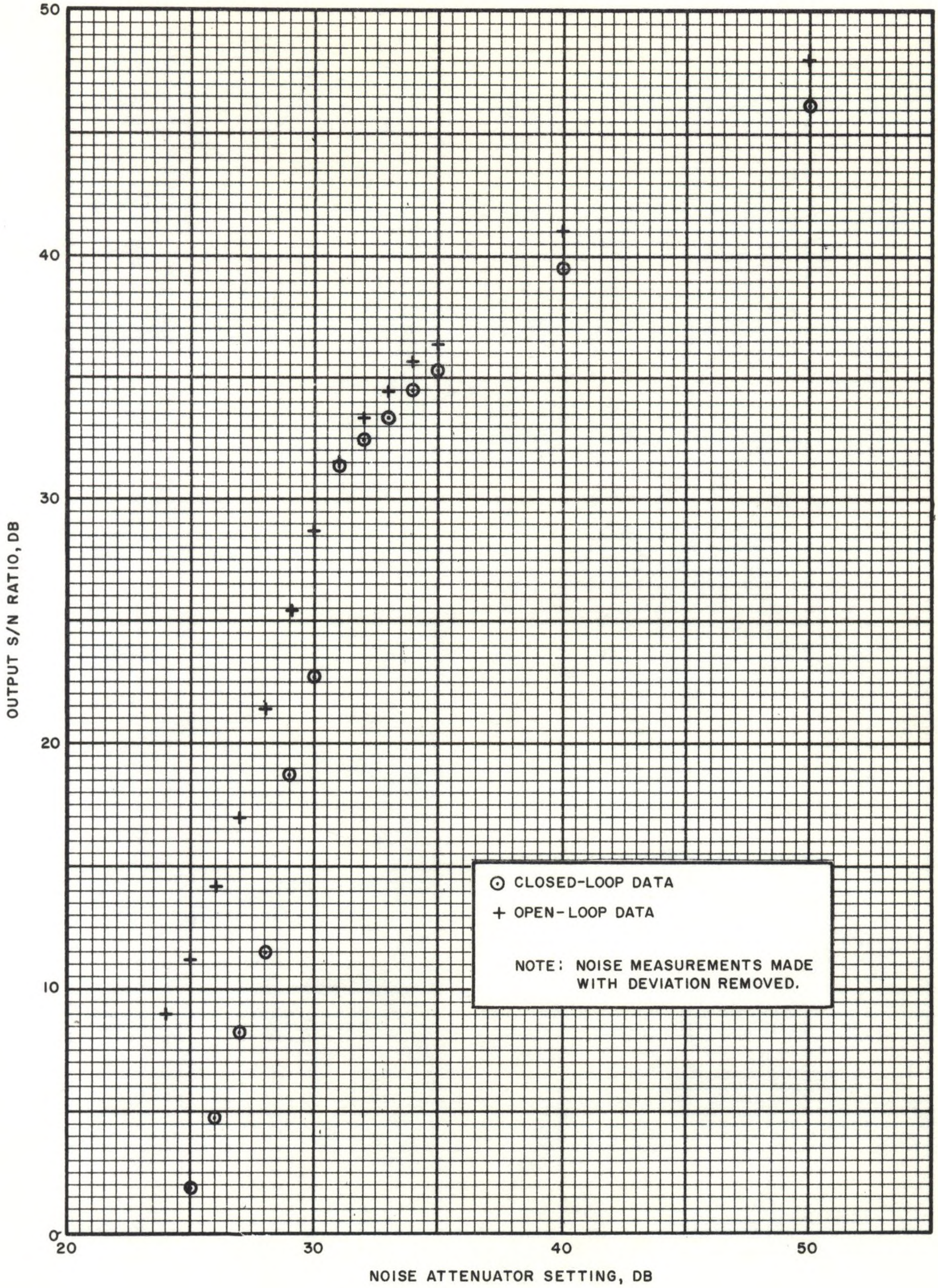

FIGURE 21 OUTPUT S/N CURVE, SECOND-ORDER LOOP NO. 3 AND OPEN-LOOP

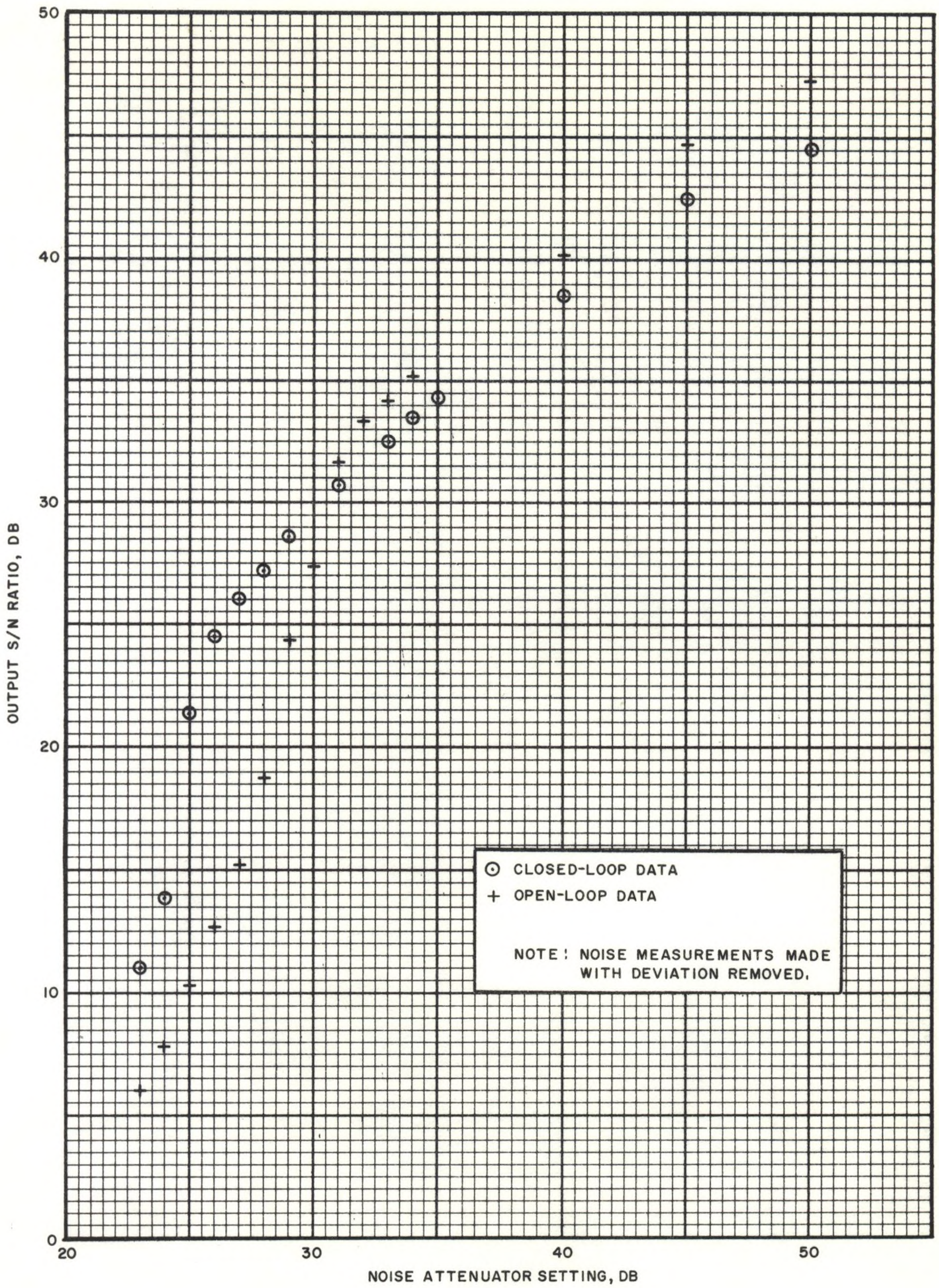

FIGURE 22 OUTPUT S/N CURVE,
SECOND ORDER LOOP NO. 4 AND OPEN-LOOP

was measured by removing the modulation. Since the signal and noise are uncorrelated, the output signal power can be determined from the measurements by knowing the signal and noise add in an rms manner. The output S/N obtained is plotted in the figures as a function of the noise attenuator setting. After each set of closed-loop measurements the procedure was repeated with the loop open and the 90-kc filter replacing the 15-kc filter in the 2-mc amplifier. These open-loop measurements are plotted on the same curves.

An examination of the curves shows threshold improvement in three of the closed-loop cases, those in which the loop noise bandwidth is less than 70 kc. In two cases the indicated threshold improvement approaches the theoretical 6 db calculated in Chapter IV-B.

Although the measurements indicated improvement, the qualitative comparisons made by listening and observing the signal on the oscilloscope did not indicate threshold improvement for the closed-loop detectors. In the region of indicated threshold improvement, the closed-loop output signal contained large noise spikes which degraded the quality of the signal as heard by an observer, even though the noise spikes were present only a small portion of the time. However, when the modulation on the carrier was removed, the noise spikes disappeared and the audible background noise dropped by a very large amount. This is in contrast to the open-loop detector in which the background noise was almost identical in cases with and without modulation. Thus, this first set of measurements indicated improved noise suppression can be obtained with no modulation on the carrier if the loop bandwidth is sufficiently narrow.

In order to better compare the effects of loop bandwidth as determined by the phase lag filter independent of loop gain and the i-f narrow-band circuit, two additional loop configurations were tested. These had the same i-f filter and approximately the same loop gain as the second-order loop-4, but different loop bandwidths resulting from different phase lag filters. The loop constants and filter values are given in table 5 where the new designs are referred to as second-order loops 5 and 6.

Curves of output signal-to-noise ratio for the two new loops are shown in figure 23. The data was taken in the manner previously described. The narrower noise bandwidth configuration shows some improvement over the open-loop threshold of 32 db; again, the reason appears to be the fact that no modulation was present when the noise was measured.

The characteristics of the output signal can best be illustra-

	Second-Order Loop-5	Second-Order Loop-6
$\alpha/2\pi$	7.5 kc	7.5 kc
$\beta/2\pi$	15 kc	30 kc
$\gamma/2\pi$	64.4 kc	103 kc
K_1K_2	5.8	5.8
$2B_L$	87.3 kc	109.5 kc
R_o	20 kΩ	20 kΩ
R_a	162 kΩ	94 kΩ
R_2	39.2 kΩ	46.4 kΩ
C	100 μμfd	33 μμfd

Table 5. Additional Second-Order Loop Constants

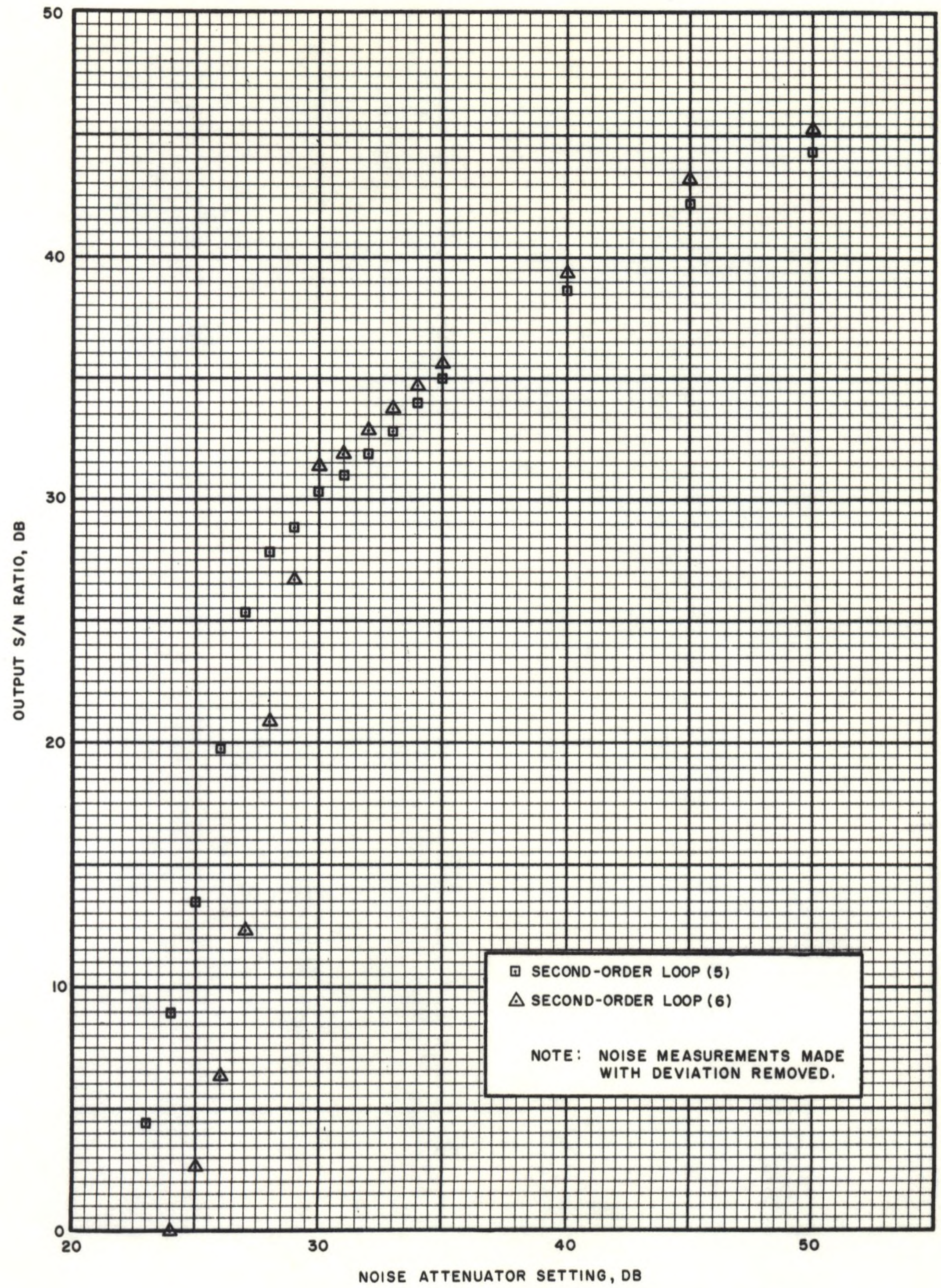

FIGURE 23 OUTPUT S/N CURVE, SECOND ORDER LOOPS NO. 5 AND NO. 6

ted in this report by the photographs in figures 24, 25, and 26. These photographs were taken of a single-sweep oscilloscope presentation of the output signal. The input deviation was 30 kc and modulation frequency 5 kc for all photographs. The four detection configurations were open-loop, and second-order loops 4, 5, and 6. The noise attenuator settings are 40 db (strong signal), 30 db (2 db below open-loop threshold), and 26 db (closed-loop threshold). The three sets of photographs are for identical conditions except for the oscilloscope settings. Oscilloscope sweep speeds were 1 ms/cm for figure 24 and 10 ms/cm for figures 25 and 26. The difference in figures 25 and 26 is caused by the oscilloscope gain setting, which is increased to show the fine detail in figure 25 but cuts off peak noise spikes. It is evident from these figures that the phase lag network is important in determining loop threshold.

To examine in a quantitative manner the effect of bandwidth on the zero-deviation threshold, table 6 is presented summarizing the results for the seven closed-loop configurations. The noise bandwidth given is the calculated value. The threshold was obtained from the break point of the curves in figure 18 through 23. The noise spectral density for each threshold can be calculated from the measured noise spectral density of 2.16×10^{-7} radians

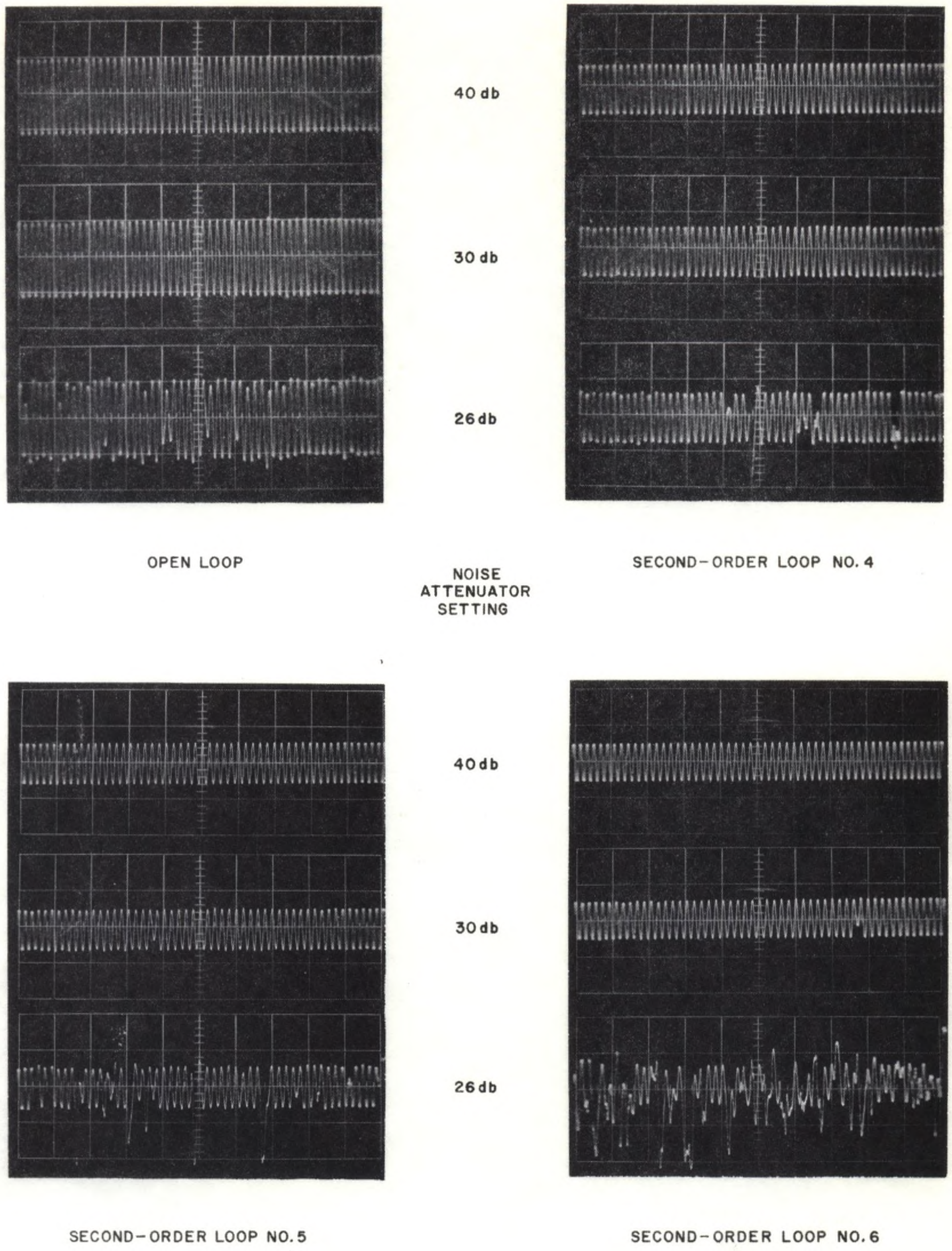

FIGURE 24 COMPARISON OF DETECTED SIGNALS WITH NOISE

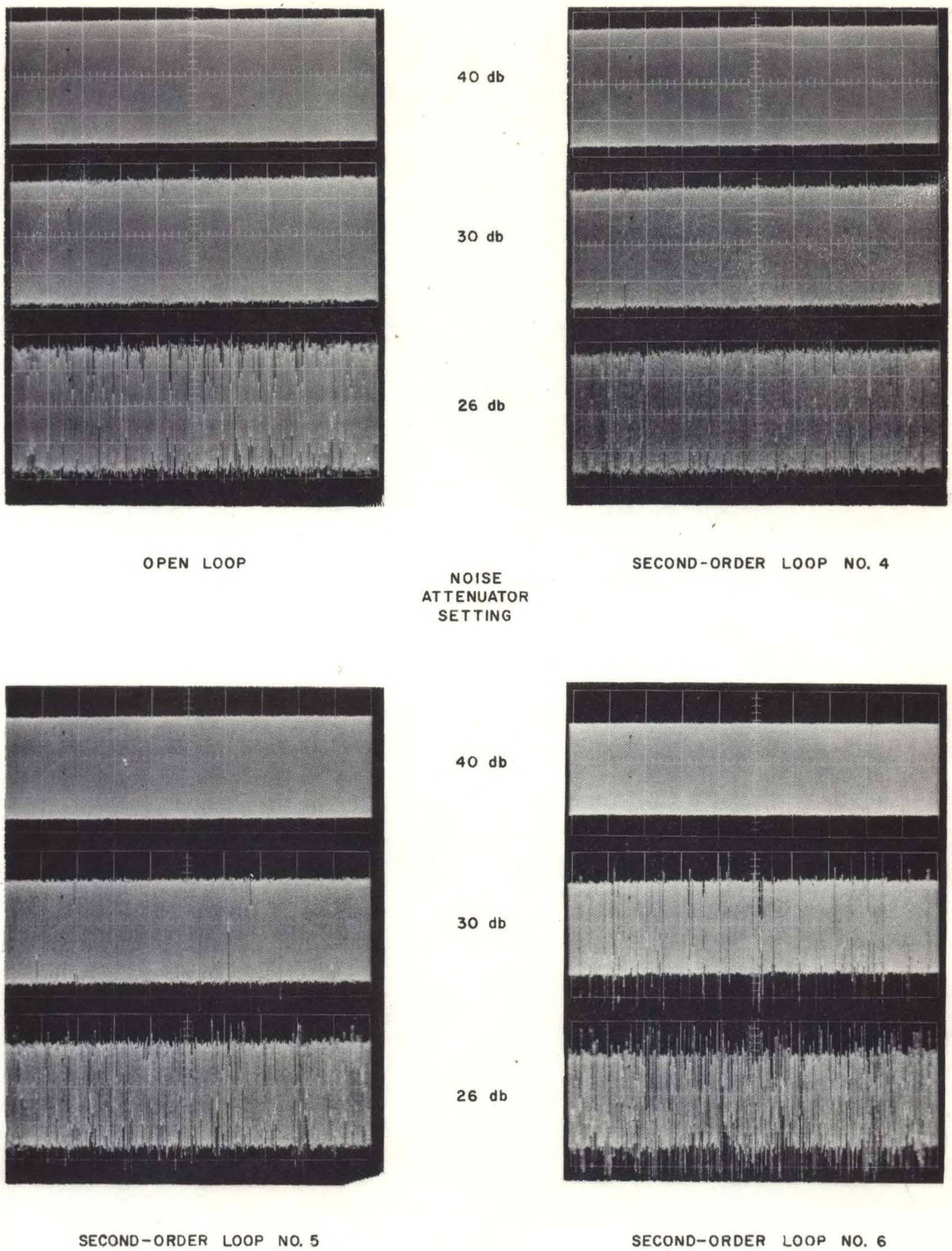

FIGURE 25 COMPARISON OF DETECTED SIGNALS WITH NOISE

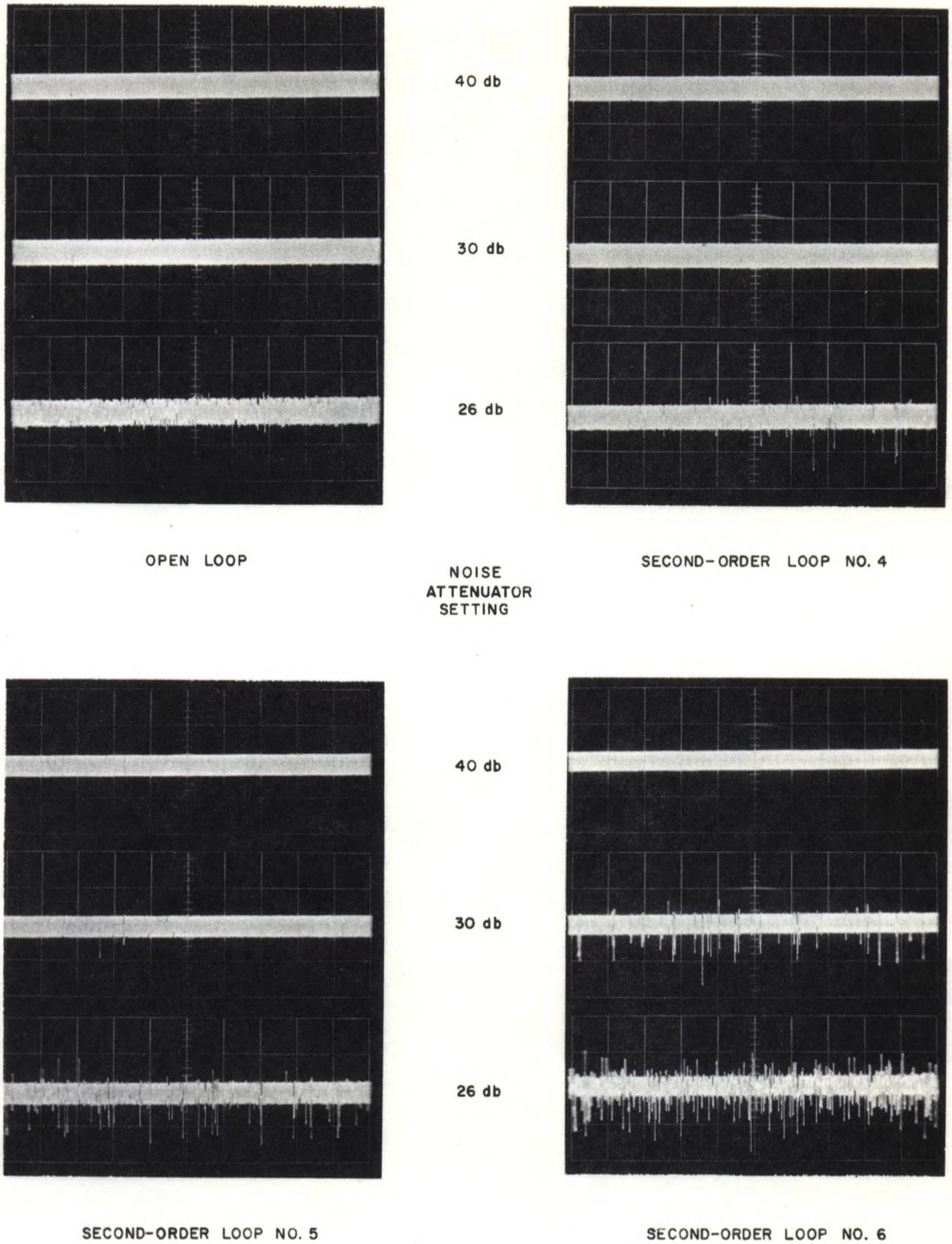

FIGURE 26 COMPARISON OF DETECTED SIGNALS WITH NOISE

Loop Configuration	$2B_N$ (Kilocycles)	Threshold (Attenua-tor Set-ting)	Φ_N(Threshold) (Radians^2/cps)	$\sigma_{\Delta f}$(Thresh-old) (Kilocycles)
First-Order Loop	141	32 db	3.43×10^{-6}	34.4
Second-Order Loop-1	68.75	28 db	1.36×10^{-6}	7.4
Second-Order Loop-2	46.1	26 db	0.857×10^{-6}	3.2
Second-Order Loop-3	102	31 db	2.73×10^{-6}	19
Second-Order Loop-4	69.3	26 db	0.85×10^{-6}	5.95
Second-Order Loop-5	87.3	28 db	1.36×10^{-6}	10.6
Second-Order Loop-6	109.5	30 db	2.16×10^{-6}	18.6

Table 6. Loop Threshold Characteristics for Unmodulated Carrier

squared per cps at a noise attenuator setting of 40 db. (Chapter VI-A) The rms frequency deviation of the local oscillator was calculated by use of equation 44. From the table it can be seen that for the two configurations which gave the expected 6-db threshold improvement with no modulation the rms local oscillator deviation at threshold was less than 6 kc. For higher deviations the threshold point is degraded. The process that causes loop threshold can be explained as follows. The local oscillator deviation caused by noise drives the signal out of the center of the 15-kc i-f filter. This reduces the signal level at the discriminator, while the noise level remains constant. When the signal level is reduced sufficiently the discriminator threshold is reached and the loop tends to loose-lock. The level at which this occurs depends upon the loop noise bandwidth. For example, the first configuration presented on table 6 shows a threshold when the attenuator setting is 32 db. The closed-loop discriminator threshold is approximately 6 db better than this value. The signal will be depressed 6 db when it is 12 kc off of the center frequency (see figure C-14). This is $0.35\sigma_{\Delta f}$, which indicates the signal is below the discriminator threshold 62% of the time. Repeating this process for the other configurations represented in table 6 indicates that loop threshold is reached when the S/N at the discriminator is below the discriminator threshold approximately 50% of the time.

The previous discussion has been concerned with the apparent threshold improvement, or more precisely, the threshold improvement with no modulation. In the previous measurements it became apparent indirectly that no threshold improvement was occurring for full deviation. In order to show this a different method of measuring output noise was used in which the modulation was not removed for the measurement. A 5-kc notch filter was built which has approximately 50 db of rejection at 5 kc. The output signal-plus-noise was measured as before, but the noise was measured by inserting the filter. It was realized that the filter would remove some noise so that an accurate S/N reading could not be obtained, but the threshold, or break point in the curve, should still be apparent. Figures 27 and 28 show the results of these measurements made on second-order loops 2 and 4. The threshold curve obtained by measuring noise with no modulation is repeated in the figures for comparison. The curves show what was apparent from the previous listening tests, that little or no threshold improvement occurred for 30-kc peak deviation. The flattening of the curve above 42 db S/N is due to the limited rejection of the signal by the notch filter. Above this point the noise measure-

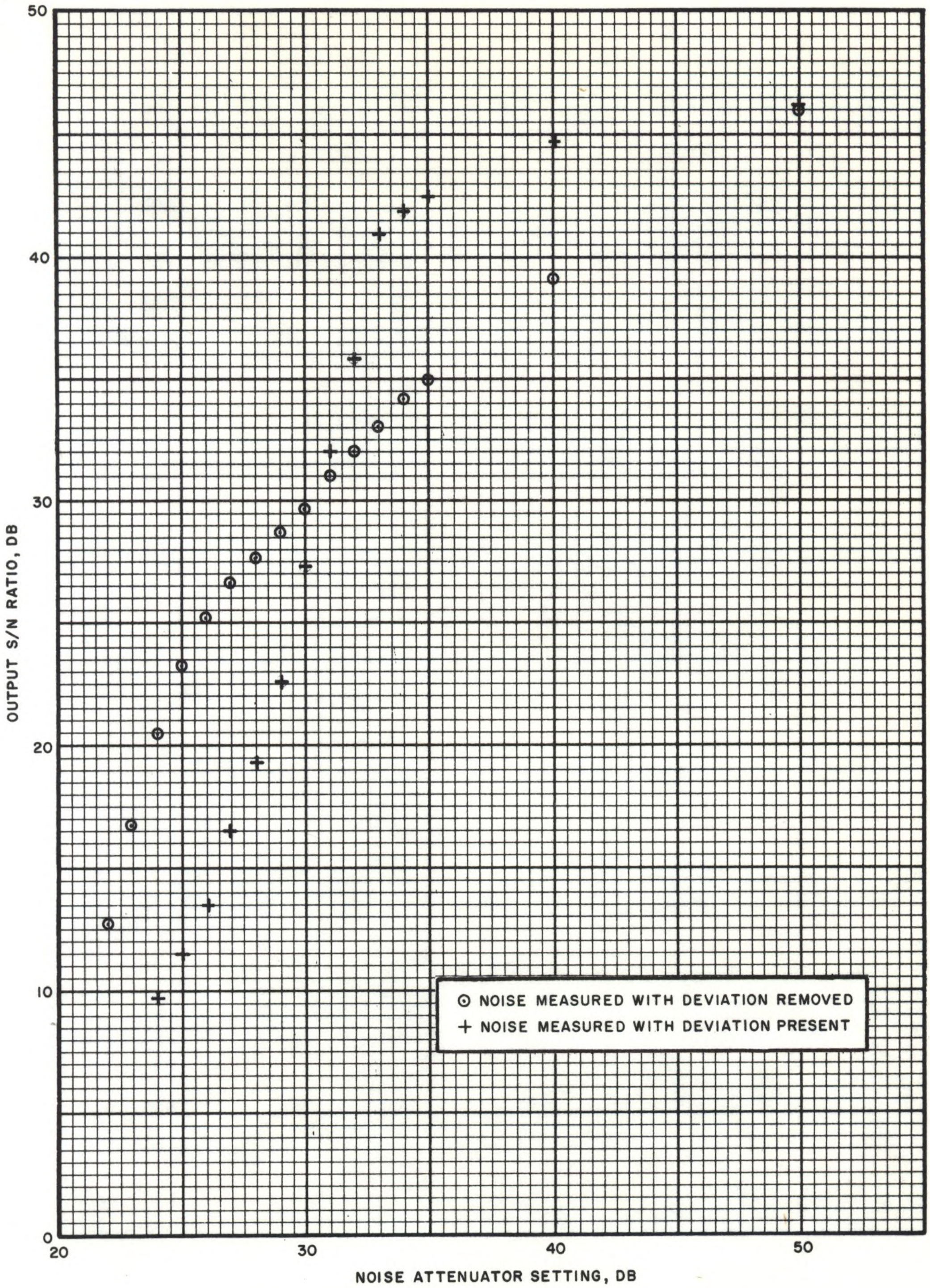

FIGURE 27 COMPARISON OF OUTPUT S/N CURVES FOR TWO MEASUREMENT TECHNIQUES, SECOND-ORDER LOOP NO. 2

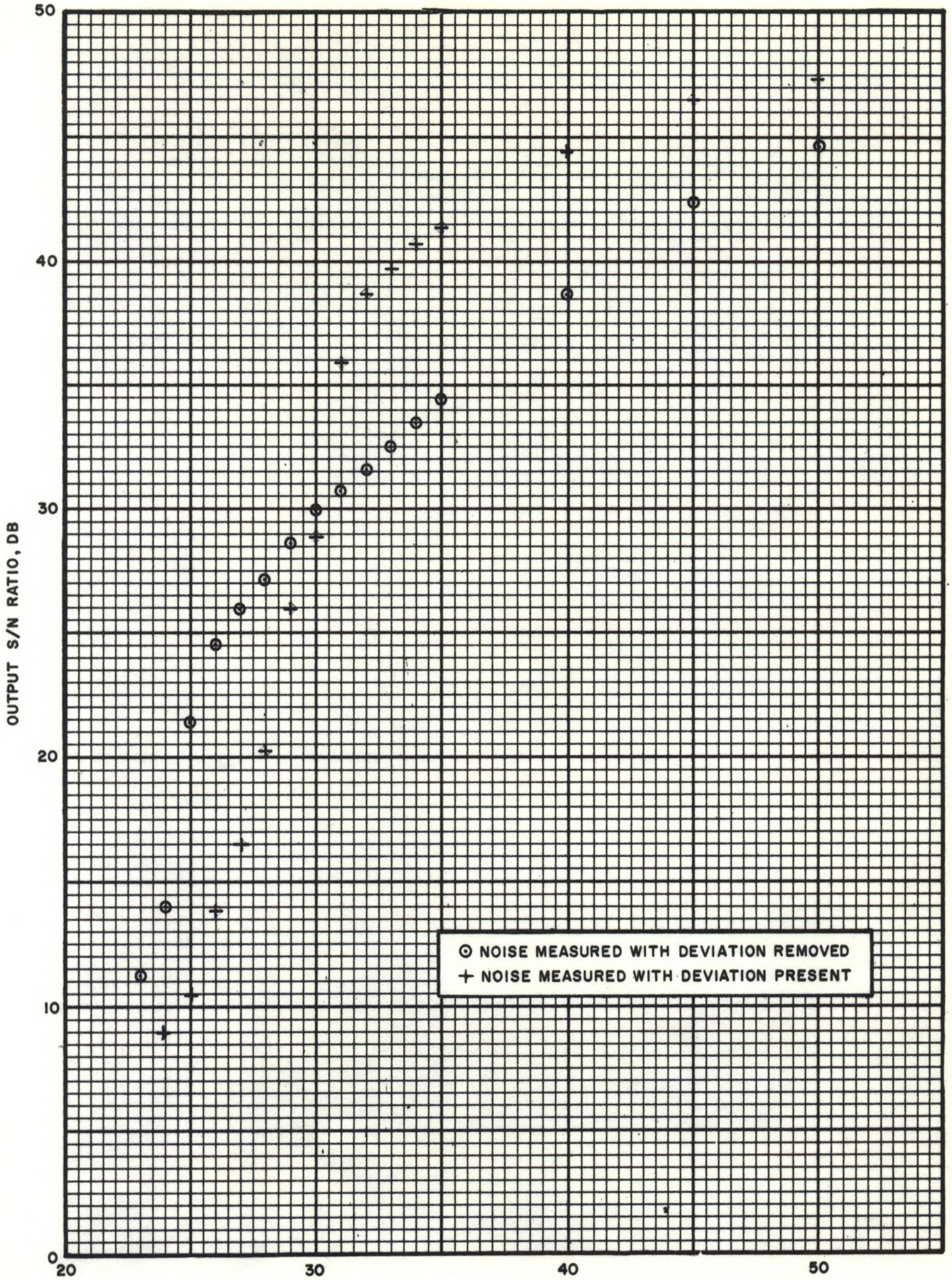

FIGURE 28 COMPARISON OF OUTPUT S/N CURVES FOR TWO MEASUREMENT TECHNIQUES, SECOND ORDER LOOP NO. 4

ment was of noise plus the leakage signal, which limited the maximum S/N measurable.

The data presented thus far shows the possibility of threshold improvement with no modulation and little threshold improvement with full 30-kc deviation. The next step was to measure threshold for peak deviations of 30 kc, 22.5 kc, 15 kc and 7.5 kc. This was done for second-order loop-2 and is presented in figures 29 through 32. The output noise measurement was made with modulation on the carrier by use of the 5-kc notch filter. The curves present a comparison of open-loop and closed-loop detection, with the same measurement procedures used for both curves. Summarizing the curves, they show:

No improvement with 30-kc peak deviation

2-db improvement with 22.5-kc peak deviation

4.5-db improvement with 15-kc peak deviation

5.5-db improvement with 7.5-kc peak deviation

From these measurements it appeared that a properly designed f-m detector using feedback would provide improved performance on signals with low average deviation such as voice, music or television.

To verify this, recordings of voice and music were used to modulate the 60-mc VCO to a level such that peak deviation did

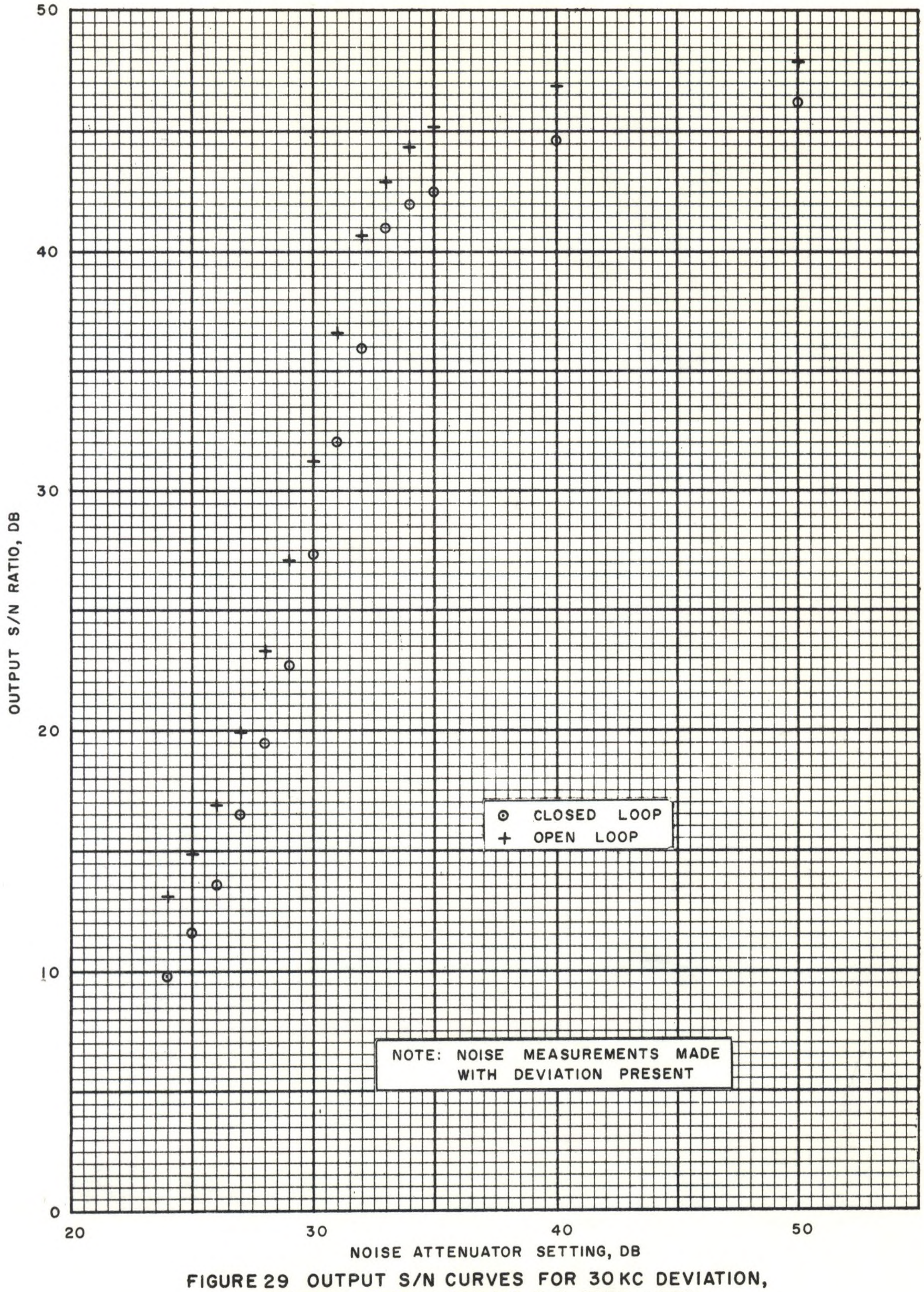

FIGURE 29 OUTPUT S/N CURVES FOR 30 KC DEVIATION, SECOND ORDER LOOP NO. 2 & OPEN-LOOP

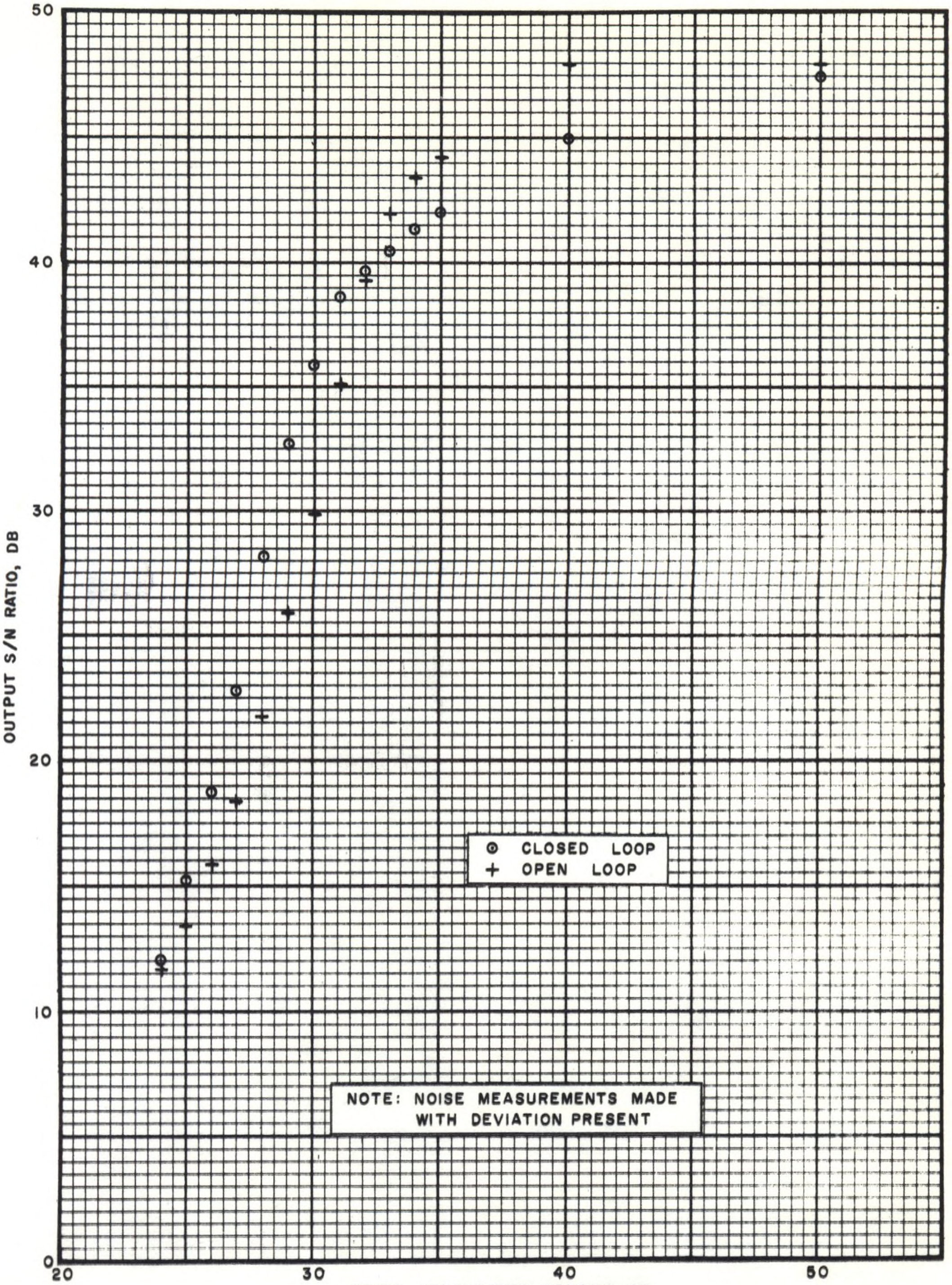

FIGURE 30 OUTPUT S/N CURVES FOR 22.5 KC DEVIATION, SECOND-ORDER LOOP NO. 2 AND OPEN-LOOP

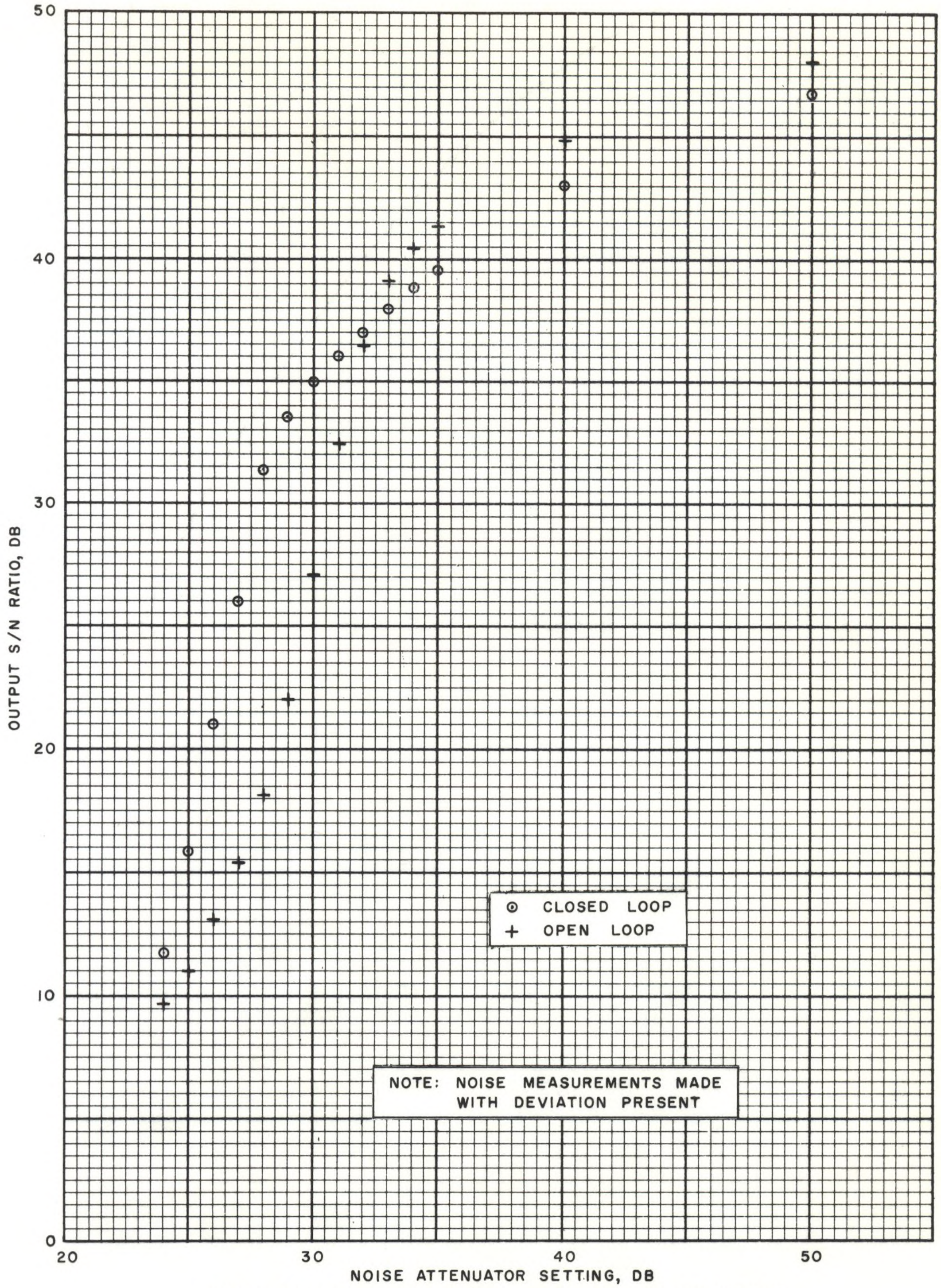

FIGURE 31 OUTPUT S/N CURVES FOR 15 KC DEVIATION, SECOND-ORDER LOOP NO. 2 AND OPEN-LOOP

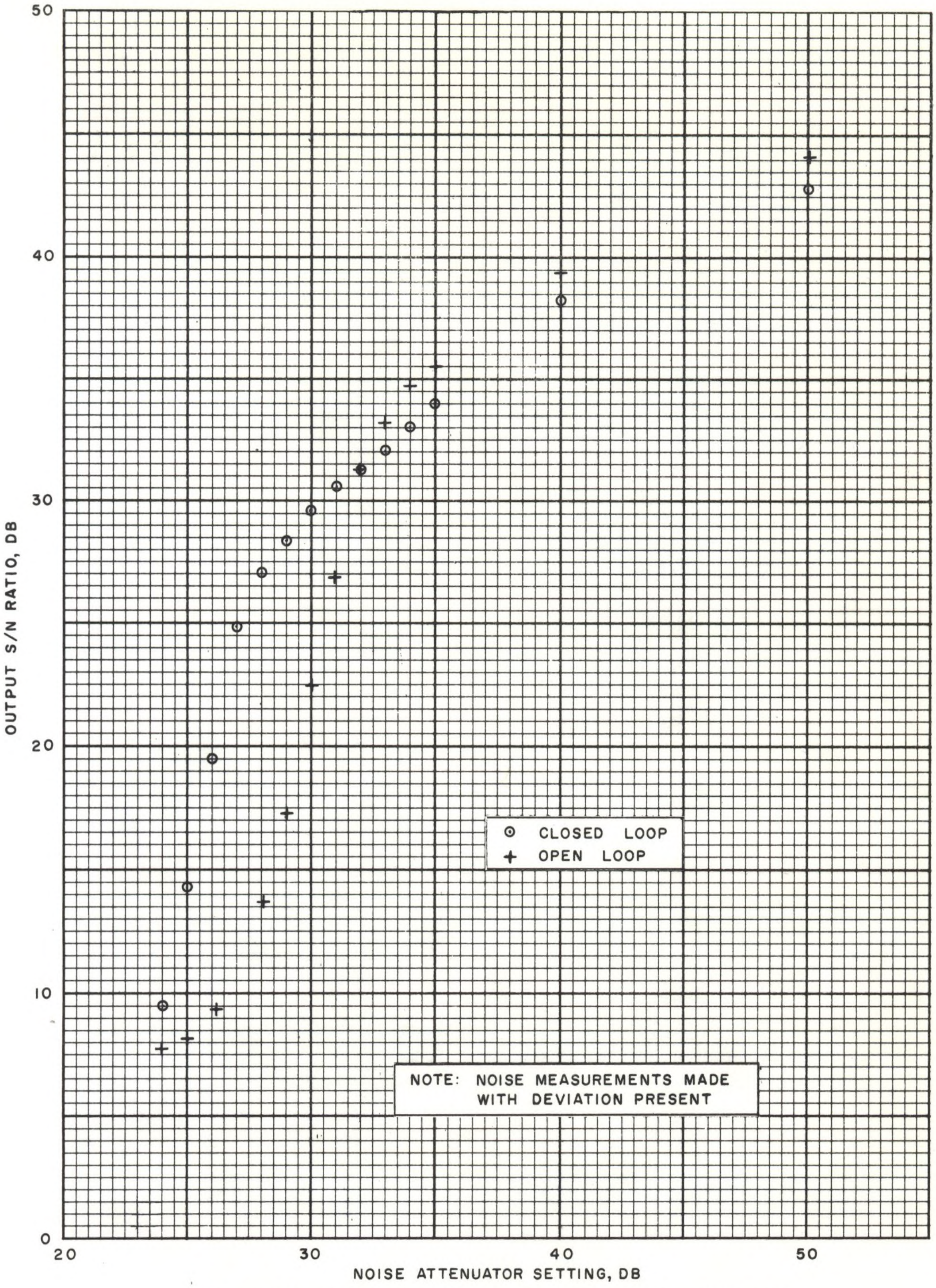

FIGURE 32 OUTPUT S/N CURVES FOR 7.5 KC DEVIATION, SECOND-ORDER LOOP NO. 2 AND OPEN-LOOP

not exceed 30 kc more than 10% of the time. The various loop detectors were tested with this input signal. Two showed a definite improvement in listening quality. These were second-order loops 2 and 4 with 2 the better of these two. With a noise attenuator setting of 26 db the quality of the open-loop detector output was very poor; the noise was highly objectionable. However, with second-order loop-2 the quality was good at a 26-db attenuator setting. There were "noise pops" present on peak deviations, however. Even at a level of 24-db noise attenuator setting the quality of detection was not exceedingly poor with this closed-loop detector. For strong signal levels there was no noticeable difference in quality of output signal between open-loop and closed-loop detection either in S/N or distortion characteristics.

E. Distortion Measurements

Harmonic distortion measurements were made at two modulation frequencies, 1 kc and 5 kc, using a Hewlett-Packard Model 330D Distortion Analyzer. The measurements were made with 30-kc deviation. The results of the tests on five closed-loop detectors are shown in table 7. Also included are measurements of the audio oscillator distortion measured directly, and the open-loop distortion. The results indicate an improvement in harmonic distortion for closed-loop detection over open-loop detection for 1 kc

Circuit Configuration	Modulation Frequency	
	1 kc	5 kc
Generator	0.2%	0.1%
Open-Loop	0.79%	0.45%
First-Order Loop	0.37%	0.33%
Second-Order Loop-1	0.6%	0.79%
Second-Order Loop-2	0.45%	1.1%
Second-Order Loop-3	0.37%	0.33%
Second-Order Loop-4	0.3%	0.6%

Table 7. Harmonic Distortion

and a degradation at 5 kc for 3 of the five closed-loop configurations. Generally, it appears that for the configurations tested the closed-loop detector adds little harmonic distortion over open-loop. For the cases where there was increased distortion, there are several possible causes. It could be caused inherently by the loop design which causes a peak in the input-to-discriminator transfer function. It could be caused by the fact that the discriminator was not sufficiently wide so as to add negligible phase shift, which resulted in a peak in the transfer function higher than the design level. A third source of distortion, especially in second-order loops 1 and 2, could be nonsymmetry in the i-f filter which, for large deviations, would not pass the upper and lower sideband components equally. Probably no one reason covers all of the cases. It is felt, however, that widening the discriminator and improving the symmetry of the i-f filter would appreciably improve the harmonic distortion.

Intermodulation distortion measurements were made in the following manner. The 60-mc VCO was modulated with equal amplitude signals at 4 kc and 5 kc of sufficient strength to produce a peak deviation of 30 kc with both signals present. At the detector output the 5-kc signal was removed by the notch filter. The remaining signal was applied to the Hewlett-Packard Distortion

Analyzer. The total 4-kc signal was measured by the analyzer. Then the internal notch filter of the analyzer was used to remove the 4-kc signal and measured the remaining distortion, primarily 1 kc as observed on the oscilloscope, as a percentage of the 4-kc signal. The results are presented in table 8. For each closed-loop measurement, the intermodulation distortion was also measured for the open-loop detector, and for the two audio generators directly. While the measurements present a relative distortion indication it is not felt that the absolute magnitudes are accurate because of the technique necessary for measurement. The 5-kc notch filter used reduced the 4-kc signal approximately six times as much as the 1-kc intermodulation. (See figure C-16) Thus, the measurement of relative amplitudes of the 4-kc signal and 1-kc intermodulation are high by this factor. Using a lower second frequency would improve the absolute accuracy, but it is felt that this would not be as severe a test since it appears that the greatest distortion occurs at the higher frequencies caused by the peaked transfer function characteristic.

The measurements show greater intermodulation distortion for the two loops with low (3.5) loop gains than for the loops with higher gains. From the measurements made it is not possible

Closed-Loop Circuit Configuration	Direct	Open-Loop	Closed-Loop
First-Order Loop	2.1%	2.3%	2.1%
Second-Order Loop-1	2.2%	2.25%	3.6%
Second-Order Loop-2	2.2%	2.25%	3.8%
Second-Order Loop-3	2.1%	2.3%	2.1%
Second-Order Loop-4	2.2%	2.8%	2.8%

Table 8. Intermodulation Distortion

to determine definitely the cause for the increased distortion in these cases. The input-to-discriminator transfer function peaks lower for these two cases but not significantly so. The fact that the modulation index is not reduced to approximately unity in the i-f because of the low-loop gain should not in itself cause distortion. However, this coupled with a somewhat unsymmetrical i-f filter could cause distortion. For larger deviations the upper and lower sideband structures are not passed as uniformly as with low deviations. Thus, it is felt that if the intermodulation distortion is objectionable, it could be improved by improving the symmetry of the i-f filter. In addition, widening the discriminator to reduce the large peaks in the transfer function should also help the intermodulation distortion.

CHAPTER VII

CONCLUSIONS

During the study program a means of applying linear analysis to f-m detectors, both open-loop and closed-loop, was developed. Using this analysis an open-loop detector and several closed-loop detectors were designed and their operational characteristics predicted. These were then constructed, tested, and the results compared to the predicted results. The study did not attempt to explore all possible configurations for feedback detectors. It is possible that other configurations, such as third-order loops, may offer some advantages. However, in accordance with the original purpose of the study, the following conclusions can be drawn regarding the use of feedback in the detection of frequency modulation.

1. The linear analysis developed and used during the study program satisfactorily described the operation of the detection circuitry above threshold, and appears capable of being used to accurately predict the operational characteristics of f-m detection circuitry designed to meet specific requirements. As in all analysis, to be valid the actual circuitry must conform to any assumptions made.
2. While the linear analysis only applies above threshold

it does provide a criterion for loop threshold determination based upon the threshold point of the discriminator used in the loop. As determined by measurements made during the study the loop threshold is dependent upon the amount of noise fed back to the local oscillator. This noise causes the local oscillator to deviate from its correct frequency resulting in the i-f signal not being centered in the pass-band thus reducing the signal amplitude. When this effect is sufficiently great to reduce the signal below the discriminator threshold approximately 50% of the time, the detected signal deteriorates rapidly producing the loop threshold effect.

3. A criterion was established and verified during the study to relate the quality of the detection system to the more familiar open-loop discriminator detector. By designing the shape and bandwidth of the closed-loop input-to-discriminator transfer function to approximate an equivalent open-loop transfer function which has a given quality, approximately equal quality can be obtained for both detectors.

4. An f-m detector can be designed using a feedback detection system to provide improved threshold characteristics over open-loop detectors for signals which have a low average

deviation. Such a circuit can provide approximately equivalent quality above threshold.

APPENDIX A

NOISE BANDWIDTH OF A DOUBLE-TUNED CIRCUIT

The transfer function of a double-tuned circuit with a damping factor of 0.707 is:

$$H(S) = \frac{D_o^2}{S^2 + \sqrt{2}\, D_o S + D_o^2}$$

where D_o is the 3-db point in radians per second.

The noise bandwidth is:

$$2B_N = \frac{1}{2\pi} \int_{-\infty}^{\infty} \left| H(S) \right|^2 dS$$

Evaluating by Newton, Gould and Kaiser:[13]

$$2B_N = \frac{D_o}{2\sqrt{2}} \quad \text{cps}$$

Expressing the bandwidth in terms of the 3-db bandwidth:

$$2B_N = \frac{\pi\,(2d_o)}{2\sqrt{2}} = 1.11\,(2d_o) \quad \text{cps}$$

where $2\pi d_o = D_o$.

APPENDIX B

NOISE BANDWIDTH OF A SINGLE-TUNED CIRCUIT

The transfer function of a single-tuned circuit is:

$$H(S) = \frac{\alpha}{S + \alpha}$$

The noise bandwidth is:

$$2B_N = \frac{1}{2\pi} \int_{-\infty}^{\infty} \left| H(S) \right|^2 dS$$

Evaluating by Newton, Gould and Kaiser:[13]

$$2B_N = \frac{\alpha}{2}$$

Expressing the bandwidth in terms of the 3-db bandwidth:

$$2B_N = \frac{\pi\,(2a)}{2} = 1.571\,(2a)$$

where $2\pi a = \alpha$.

APPENDIX C

CIRCUIT SCHEMATICS AND PERFORMANCE DATA

The schematics of all equipment built during the study are presented in figures C-1 through C-8.

Figures C-9 and C-10 show the modulation characteristics of the two VCO's. The direct output frequency, as measured by the Hewlett-Packard frequency counter, is plotted as a function of the d-c input voltage.

The 2-mc discriminator curve is shown in figure C-11. The curve was taken with a constant input level to the limiter-discriminator chassis of 300 millivolts. The d-c output voltage of the discriminator is plotted as a function of the input frequency deviation from 2 megacycles.

The 2-mc limiter characteristic is shown in figure C-12. A constant signal frequency of 2.0000 megacycles was used for the measurement. The output voltage was measured at the center-tap of the discriminator transformer secondary coil, and the input voltage at the input to the limiter-discriminator chassis.

The wideband open-loop response shown in figure C-13 was taken with the loop opened between the discriminator and 62-mc VCO. The 62-mc VCO was modulated by an audio oscillator to a constant peak deviation of approximately 5 kc. The discriminator output voltage was measured as a function of the input modulation frequency. For the measurement the narrow-band i-f filter was removed and replaced with a single-tuned circuit approximately 600 kc wide. An unmodulated input signal of constant amplitude and frequency at 60 megacycles was used for the mixer-chassis input.

The response of the 15-kc narrow-band and 90-kc wide-band filters are shown in figures C-14 and C-15. The curves were taken by measuring the voltage out of the mixer chassis for a variation of the mixer chassis input signal frequency.

The response curve of the 5-kc rejection filter is shown in figure C-16. The curve was taken by maintaining a constant voltage at the input terminals of the filter of approximately 1 volt. The output voltage was measured for a variation of input frequency. The meter used was a Ballantine True RMS Meter which was the only load on the filter.

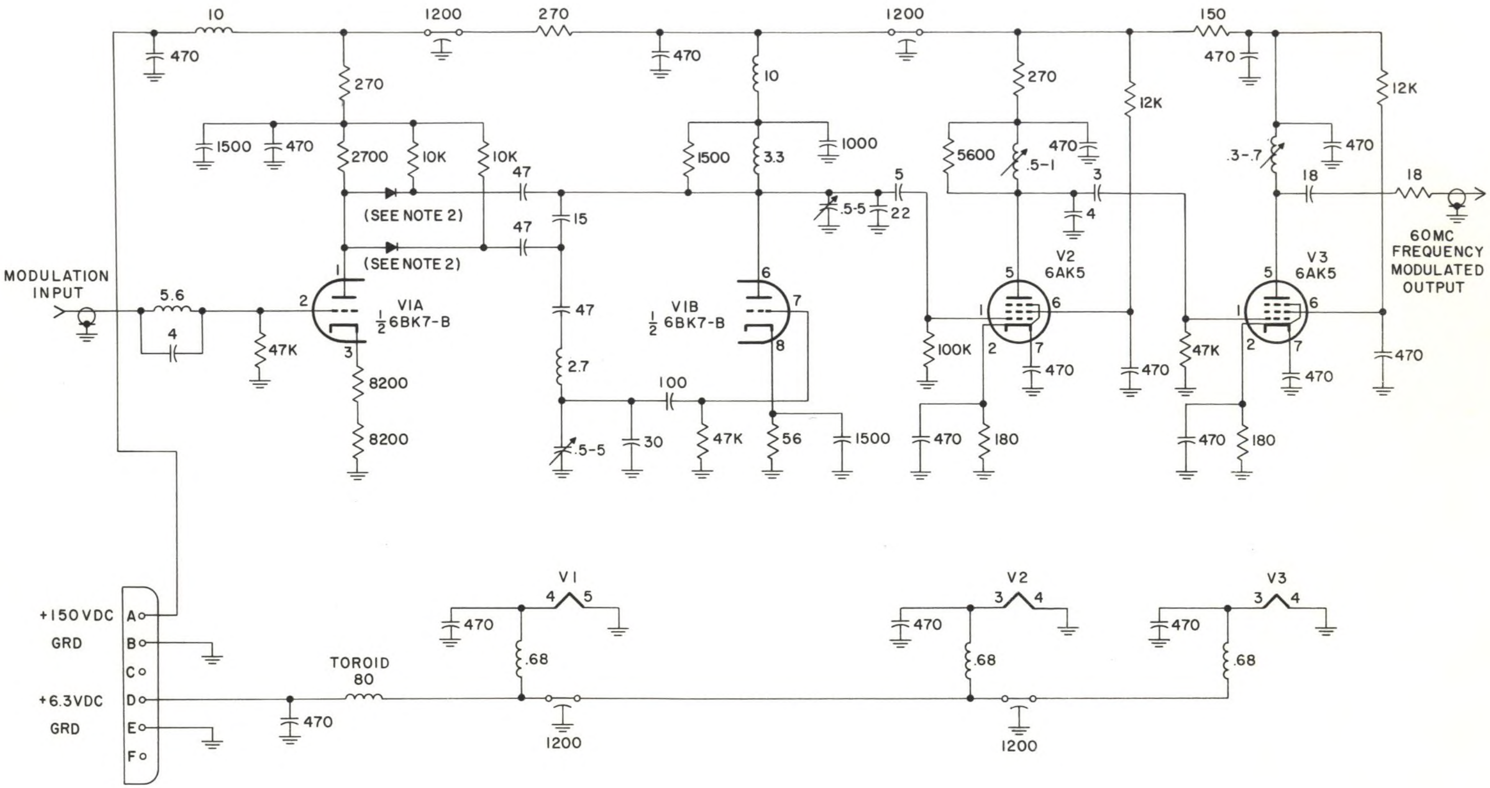

NOTES:

1. UNLESS OTHERWISE SPECIFIED, ALL RESISTANCE VALUES ARE IN OHMS ALL INDUCTANCE VALUES IN MICROHENRIES AND ALL CAPACITANCE VALUES IN MICROMICOFARADS.

2. SILICON CAPACITOR DIODE, TRANSITION SCI

FIGURE C-1 60MC VOLTAGE-CONTROLLED OSCILLATOR SCHEMATIC

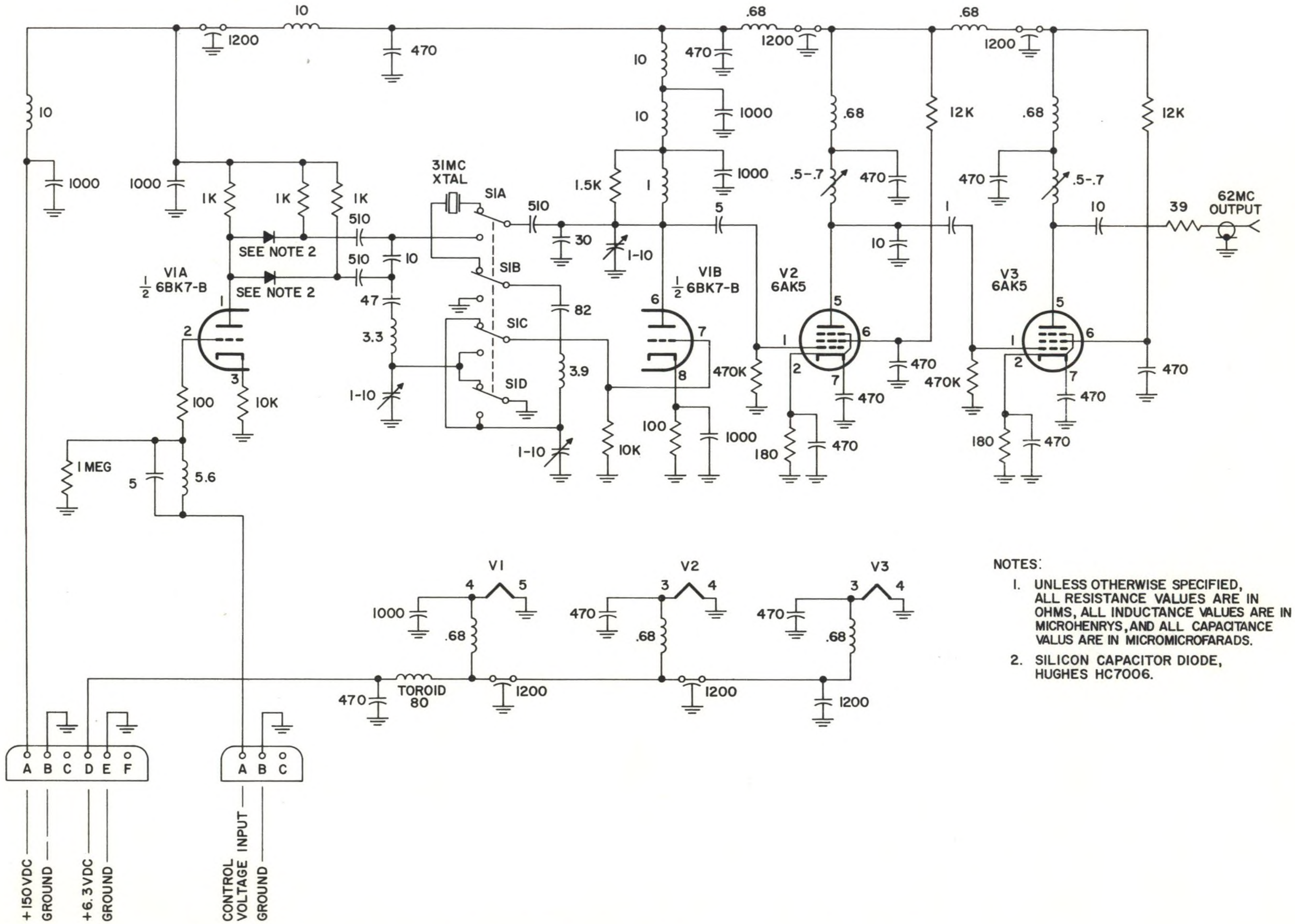

NOTES:

1. UNLESS OTHERWISE SPECIFIED, ALL RESISTANCE VALUES ARE IN OHMS, ALL INDUCTANCE VALUES ARE IN MICROHENRYS, AND ALL CAPACITANCE VALUS ARE IN MICROMICROFARADS.
2. SILICON CAPACITOR DIODE, HUGHES HC7006.

FIGURE C-2 62MC VOLTAGE-CONTROLLED OSCILLATOR SCHEMATIC

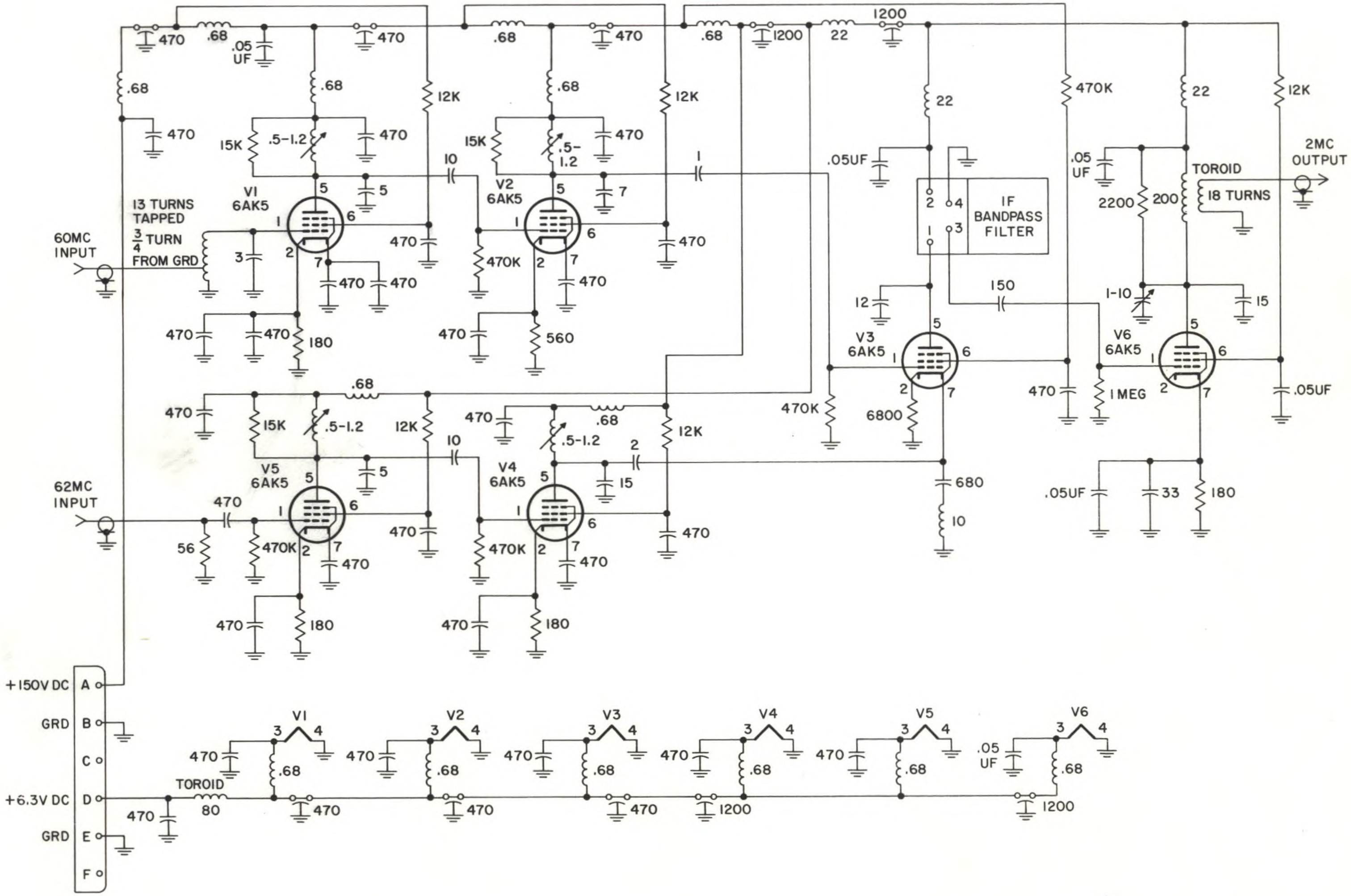

NOTE :

UNLESS OTHERWISE SPECIFIED, ALL RESISTANCE VALUES ARE IN OHMS, ALL INDUCTANCE VALUES ARE IN MICROHENRYS AND ALL CAPACITANCE VALUES ARE IN MICROMICROFARADS.

FIGURE C-3 60MC MIXER SCHEMATIC

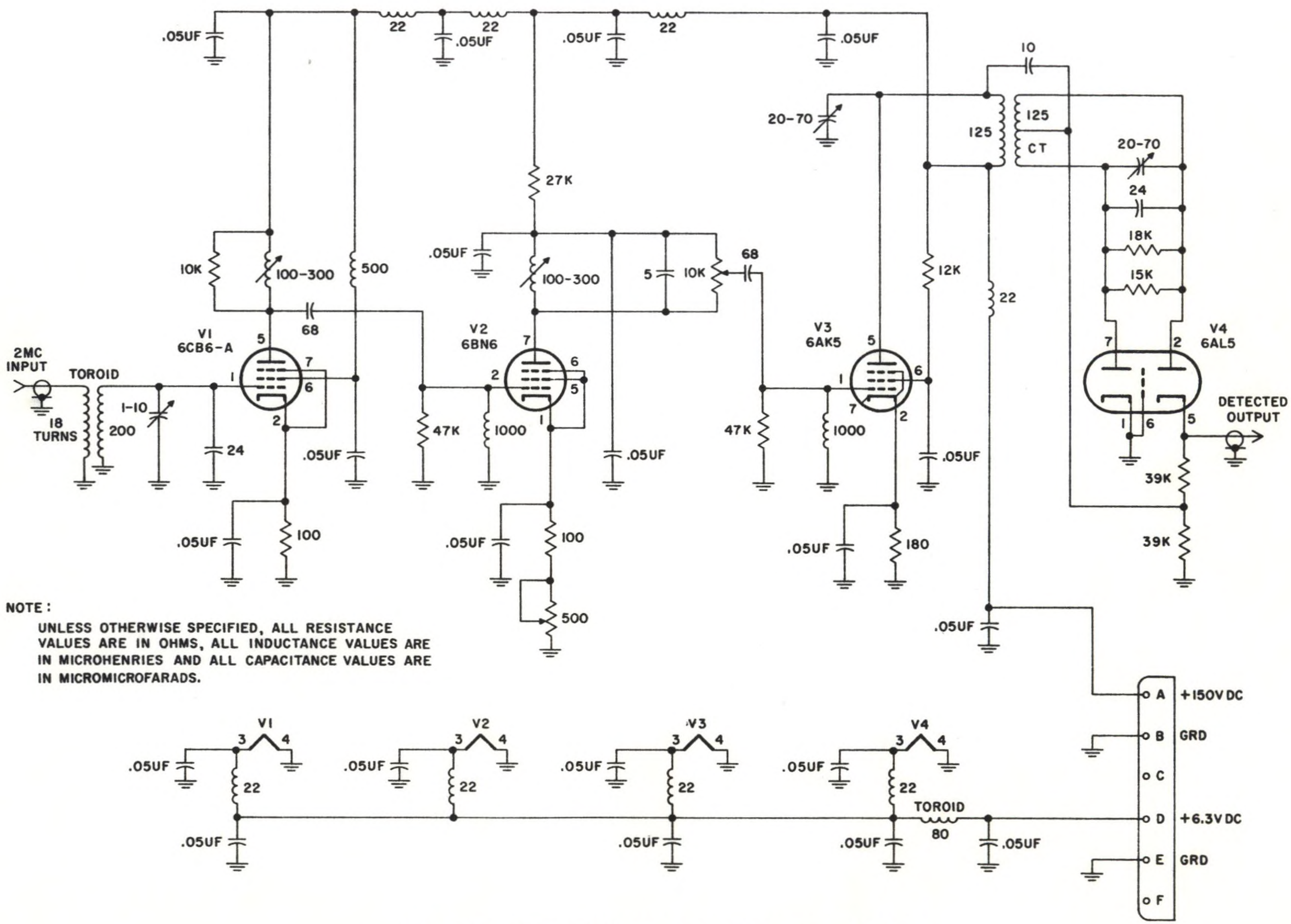

NOTE:

UNLESS OTHERWISE SPECIFIED, ALL RESISTANCE VALUES ARE IN OHMS, ALL INDUCTANCE VALUES ARE IN MICROHENRIES AND ALL CAPACITANCE VALUES ARE IN MICROMICROFARADS.

FIGURE C-4 2MC I-F, LIMITER, AND DISCRIMINATOR SCHEMATIC

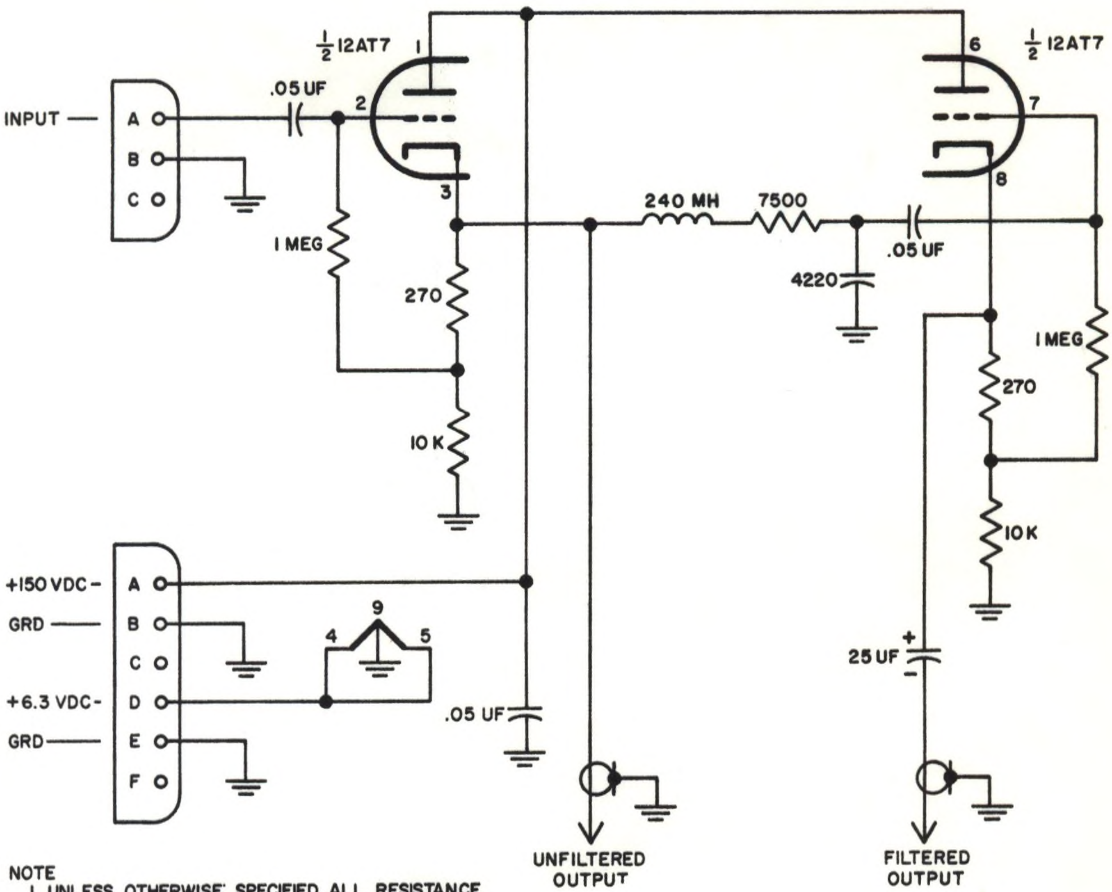

NOTE
1. UNLESS OTHERWISE SPECIFIED, ALL RESISTANCE VALUES ARE IN OHMS, ALL INDUCTANCE VALUES ARE IN MICROHENRYS, AND ALL CAPACITANCE VALUES ARE IN MICROMICROFARADS.

FIGURE C-5 5KC AUDIO FILTER AND CATHODE FOLLOWER SCHEMATIC

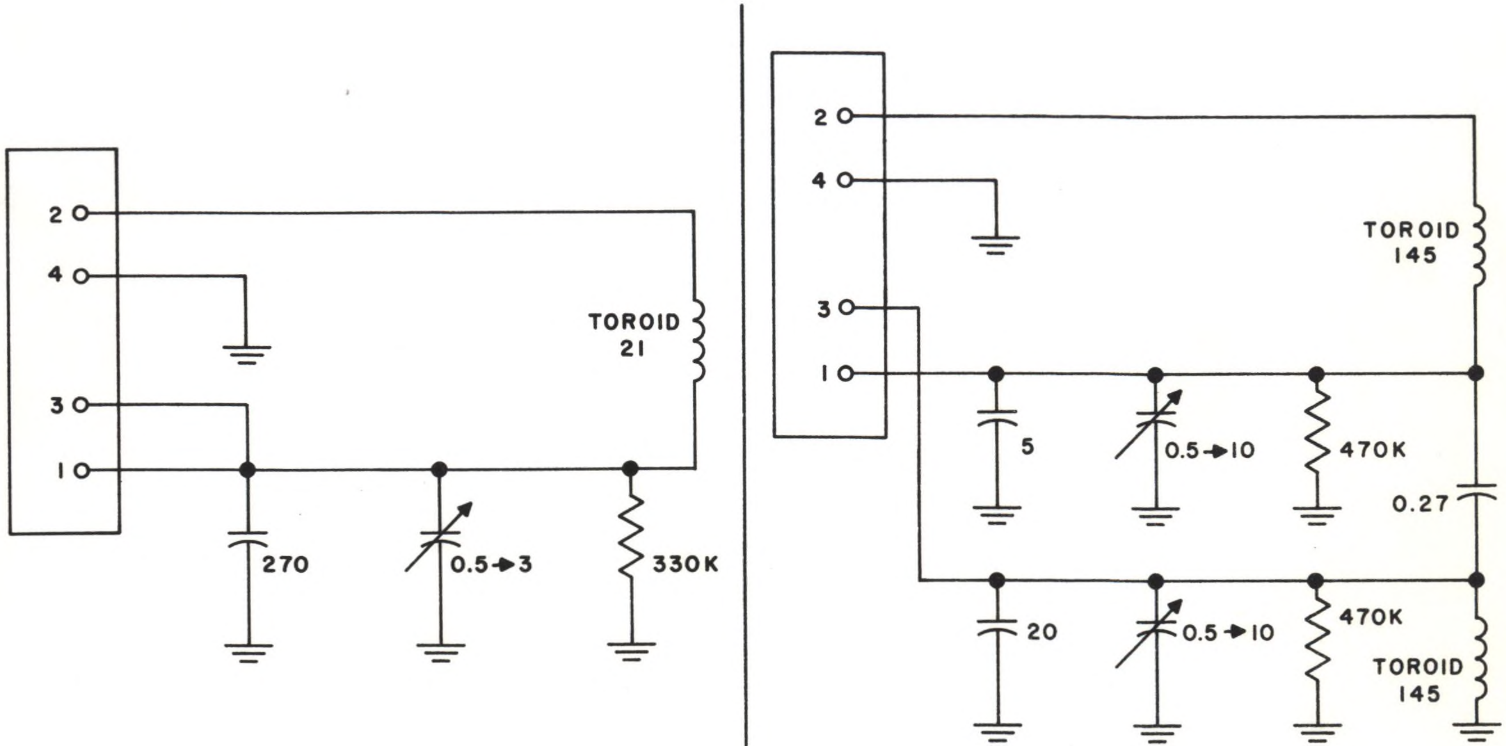

15KC BANDPASS FILTER
(SINGLE TUNED)

90KC BANDPASS FILTER
(DOUBLE TUNED)

NOTES:

ALL RESISTANCE VALUES ARE IN OHMS.

ALL CAPACITANCE VALUES ARE IN MICROMICROFARADS.

ALL INDUCTANCE VALUES ARE IN MICROHENRIES

FIGURE C-6 2-MC BANDPASS FILTER SCHEMATICS

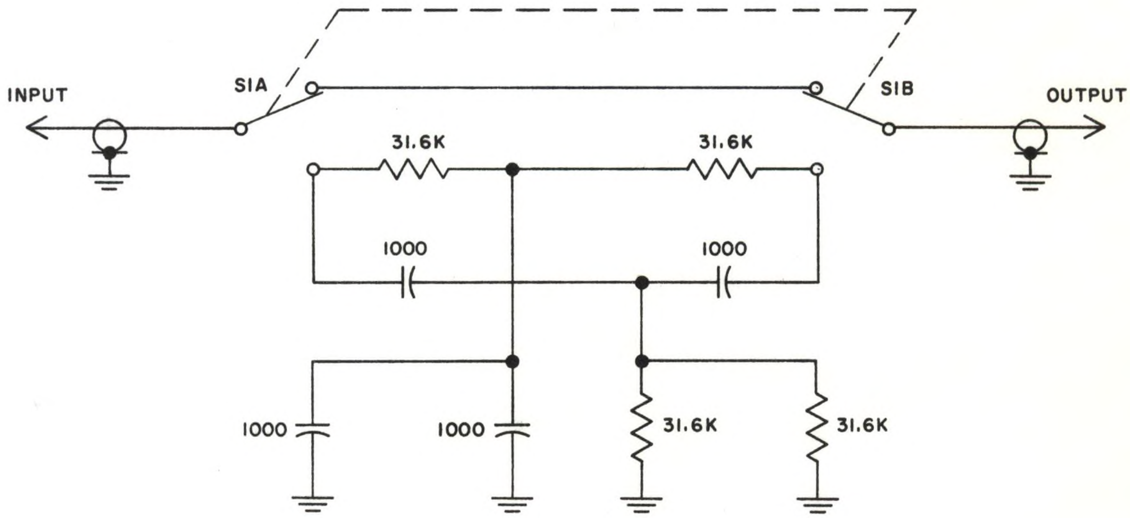

NOTE:
UNLESS OTHERWISE SPECIFIED, ALL
RESISTANCE VALUES ARE IN OHMS AND
ALL CAPACITANCE VALUES ARE IN MICROMICROFARADS.

FIGURE C-7 5 KC REJECTION FILTER SCHEMATIC

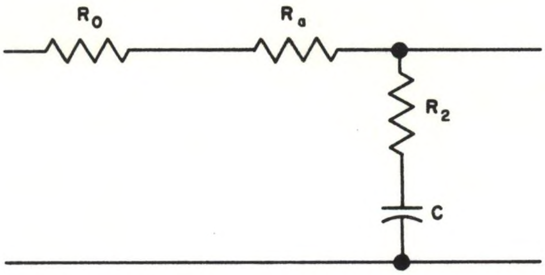

$$\frac{V_O}{V_{IN}} = \frac{R_2 C}{(R_1 + R_2)C} \left[\frac{S + \frac{1}{R_2 C}}{S + \frac{1}{(R_1 + R_2)\,C}} \right]$$

WHERE: $R_O + R_4 = R_1$

R_O = DISCRIMINATOR OUTPUT IMPEDANCE

β	γ	R_O	R_a	R_2	C
$2\pi \times$ 20KC	$2\pi \times$ 80KC	20K	106.8K	42.52K	47UUF
$2\pi \times$ 7.5KC	$2\pi \times$ 45KC	20K	156.7K	35.43K	100UUF
$2\pi \times$ 28.3KC	$2\pi \times$ 100KC	20K	101.9K	48.3K	33UUF

FIGURE C-8 PHASE LAG NETWORKS

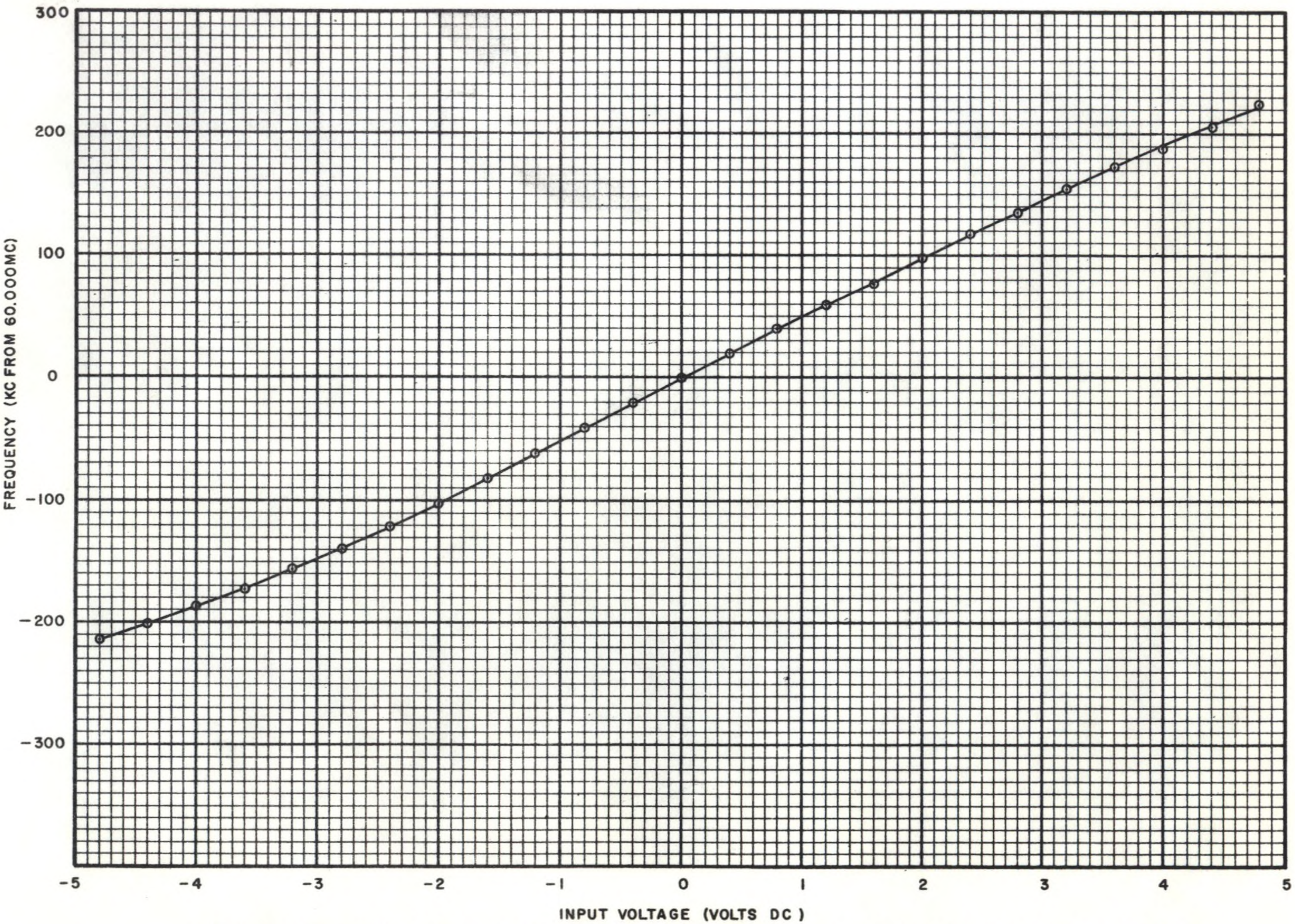

FIGURE C-9 60MC VOLTAGE CONTROLLED OSCILLATOR, OUTPUT FREQUENCY VS INPUT VOLTAGE

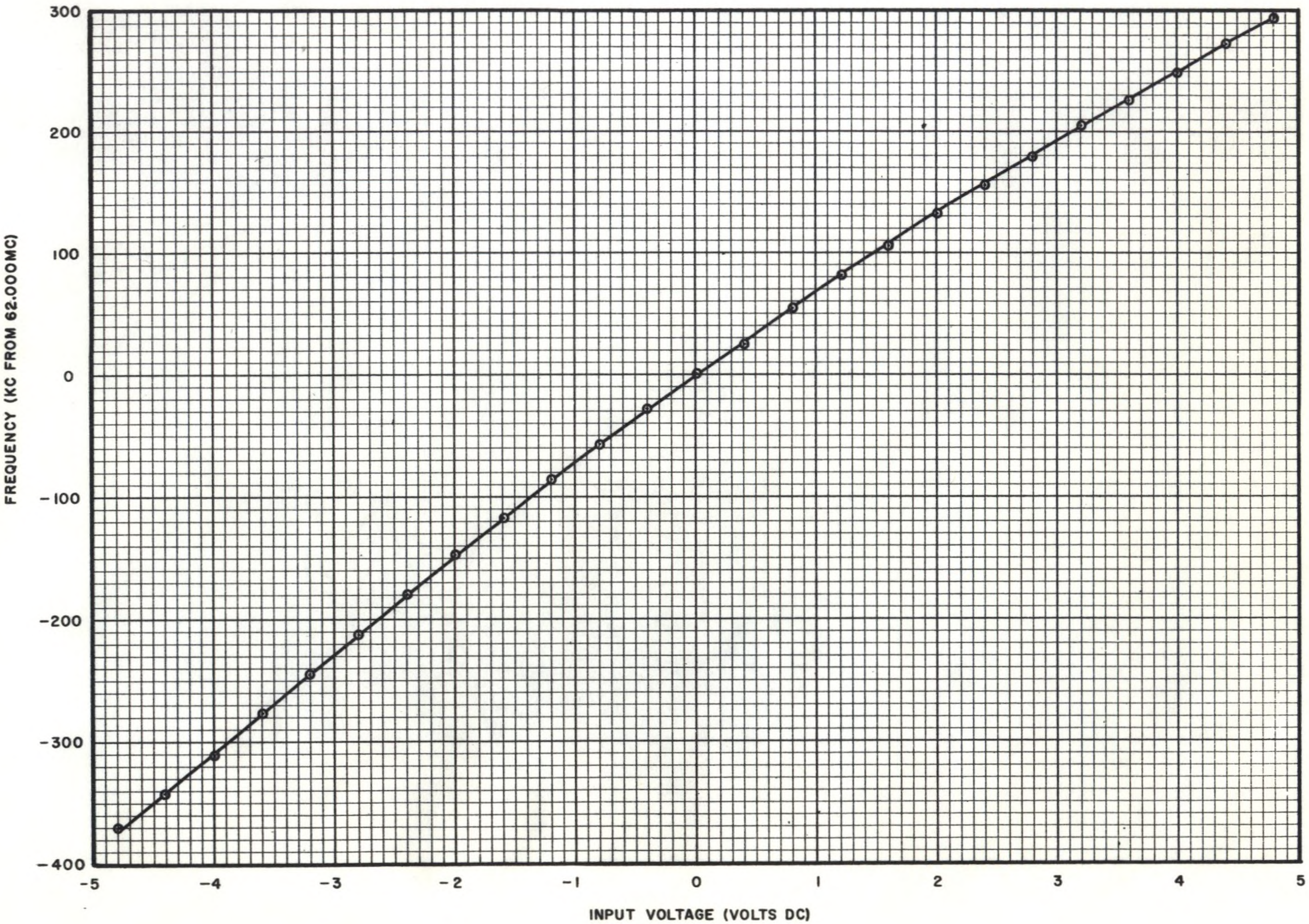

FIGURE C-10 62MC VOLTAGE CONTROLLED OSCILLATOR, OUTPUT FREQUENCY VS INPUT VOLTAGE

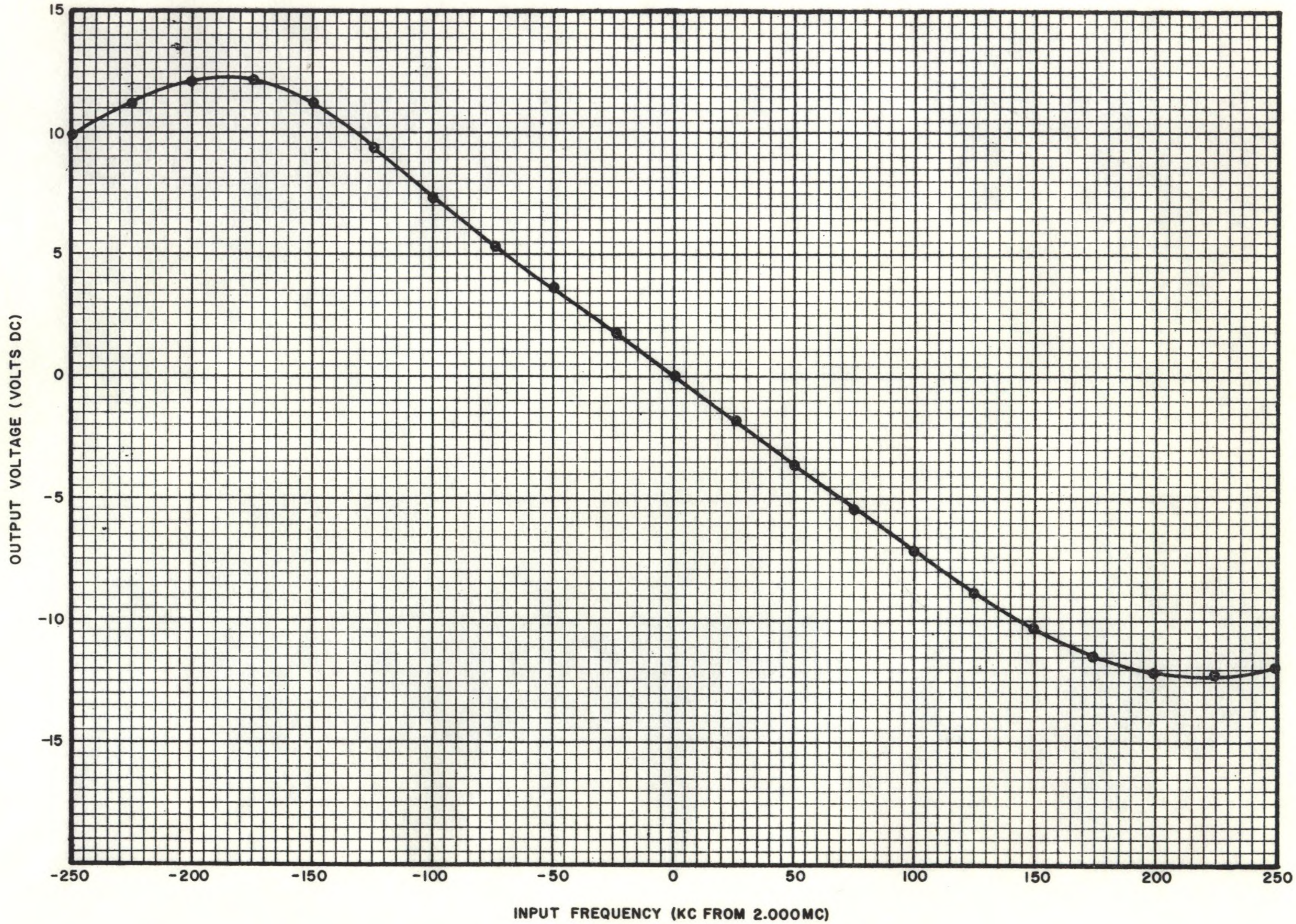

FIGURE C-II 2MC DISCRIMINATOR CURVE

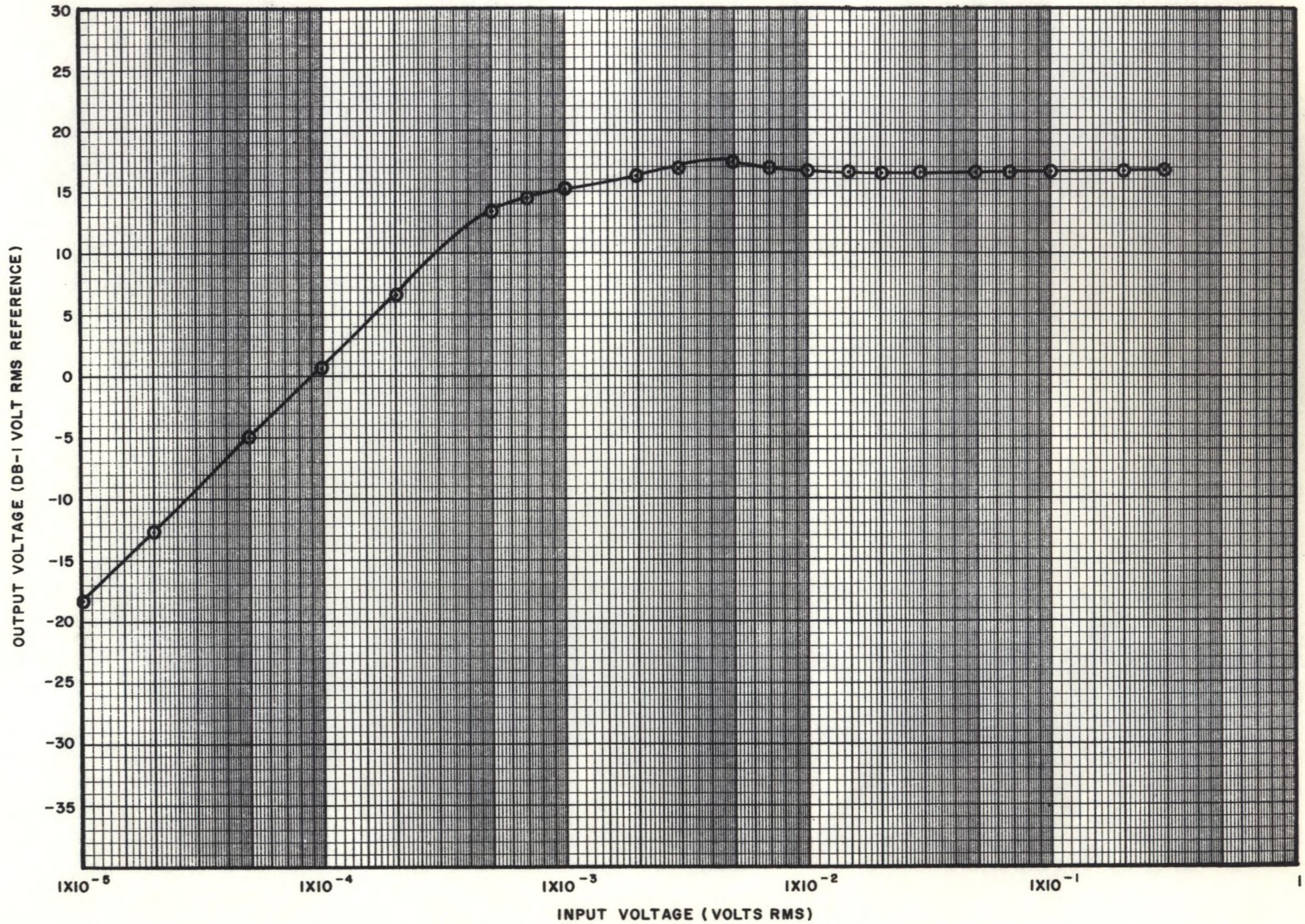

FIGURE C-12 2MC LIMITER CHARACTERISTIC

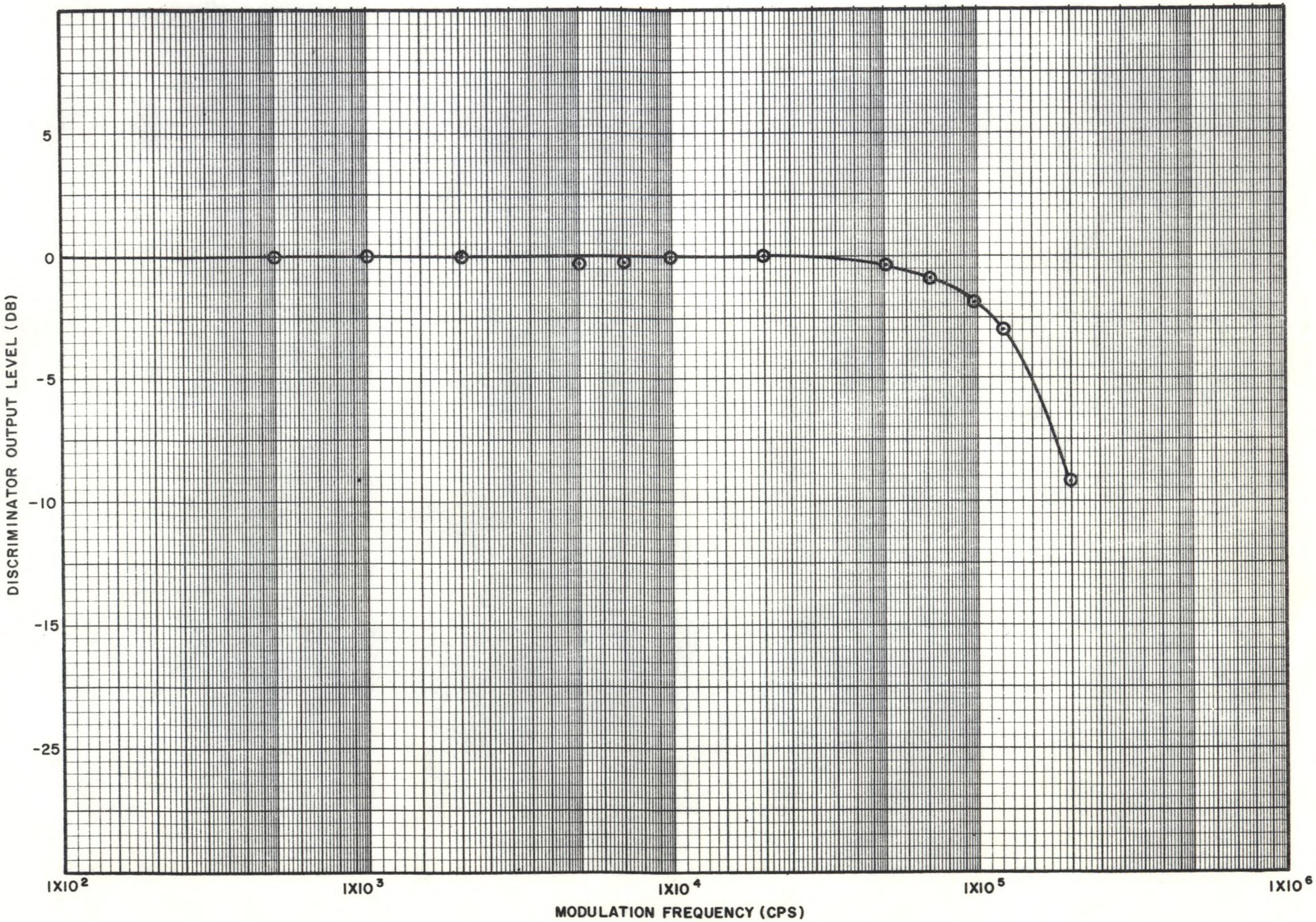

FIGURE C-13 WIDEBAND LOOP RESPONSE CURVE

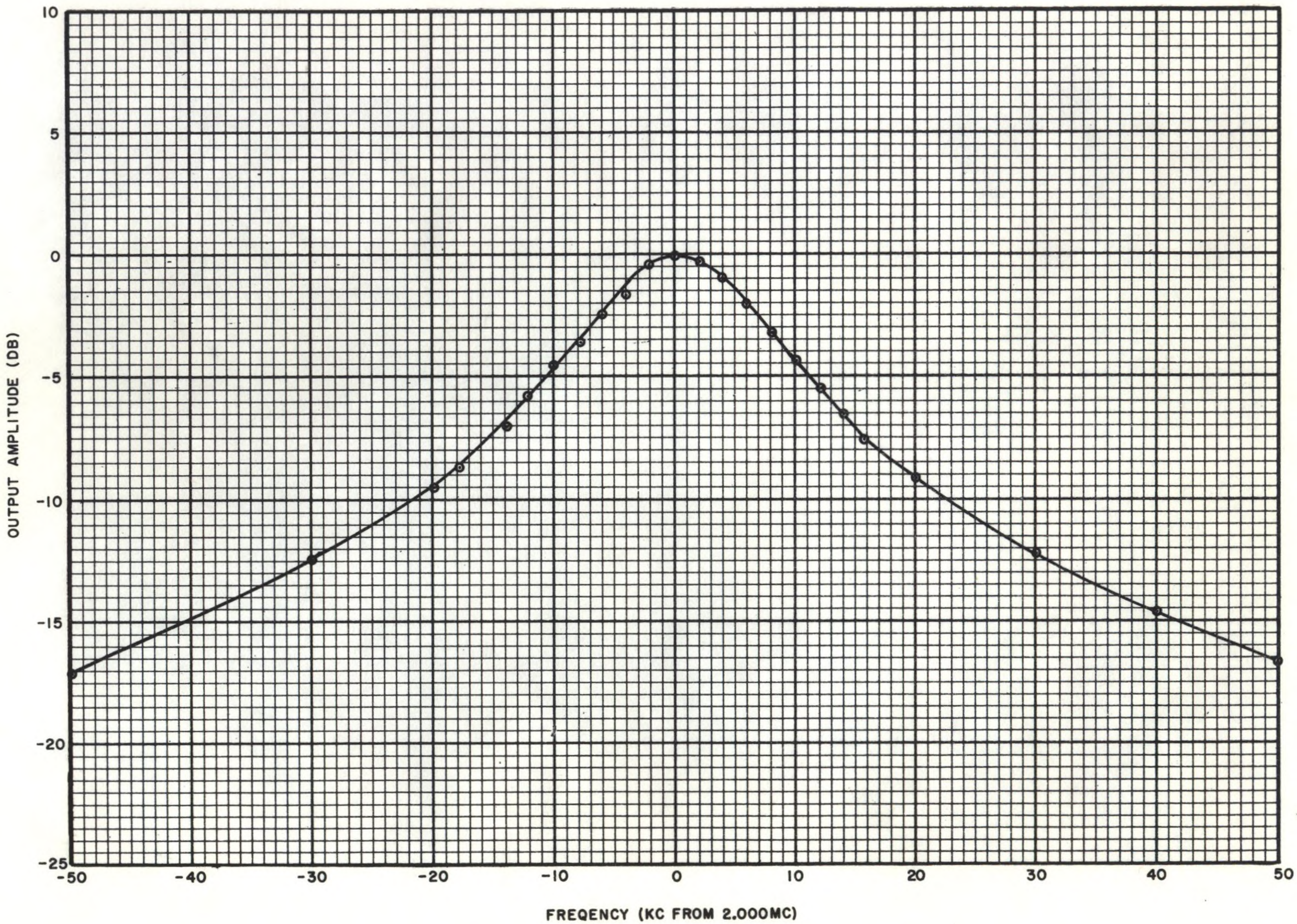

FIGURE C-14 NARROW BAND FILTER RESPONSE

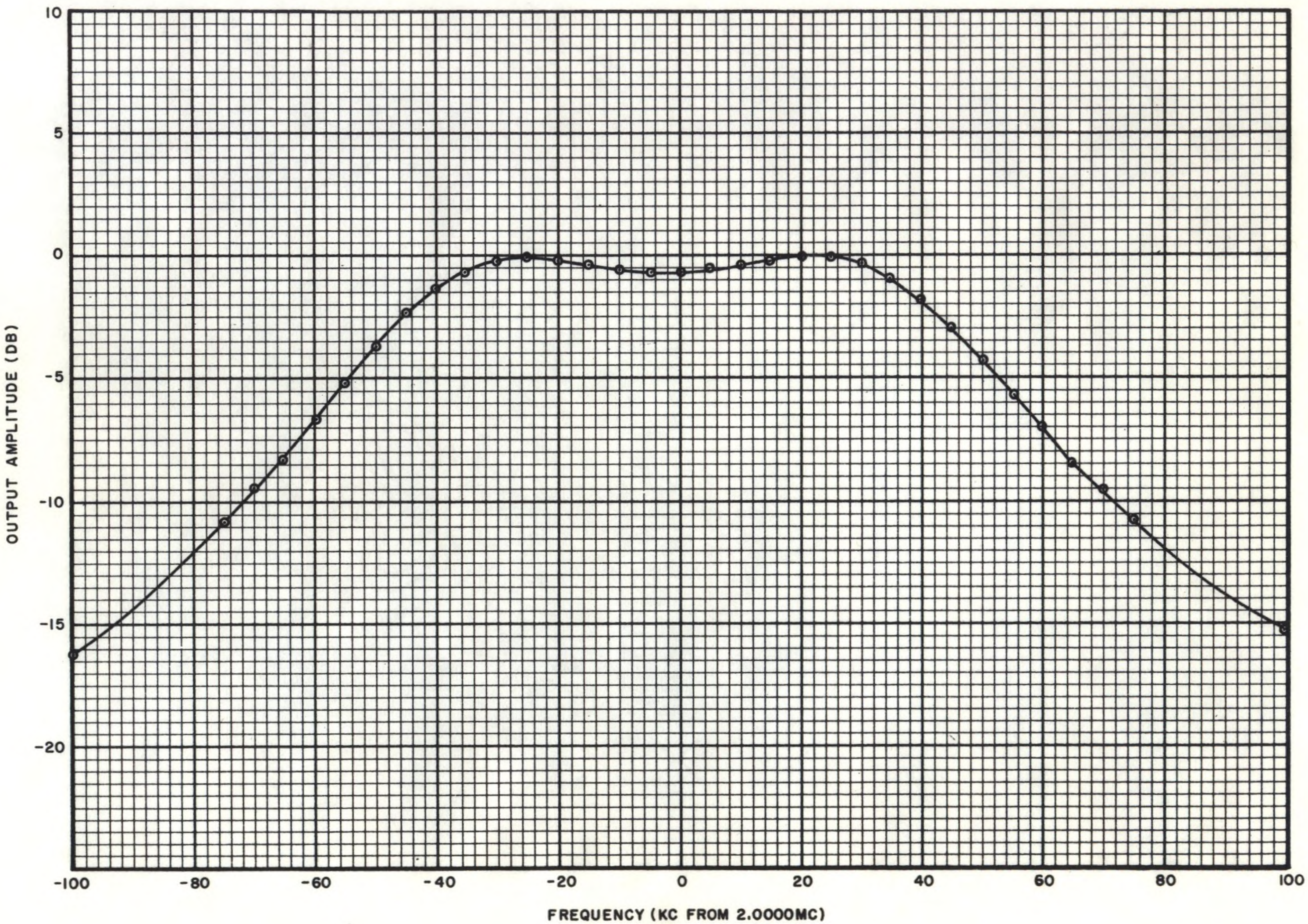

FIGURE C-15 WIDE BAND FILTER RESPONSE

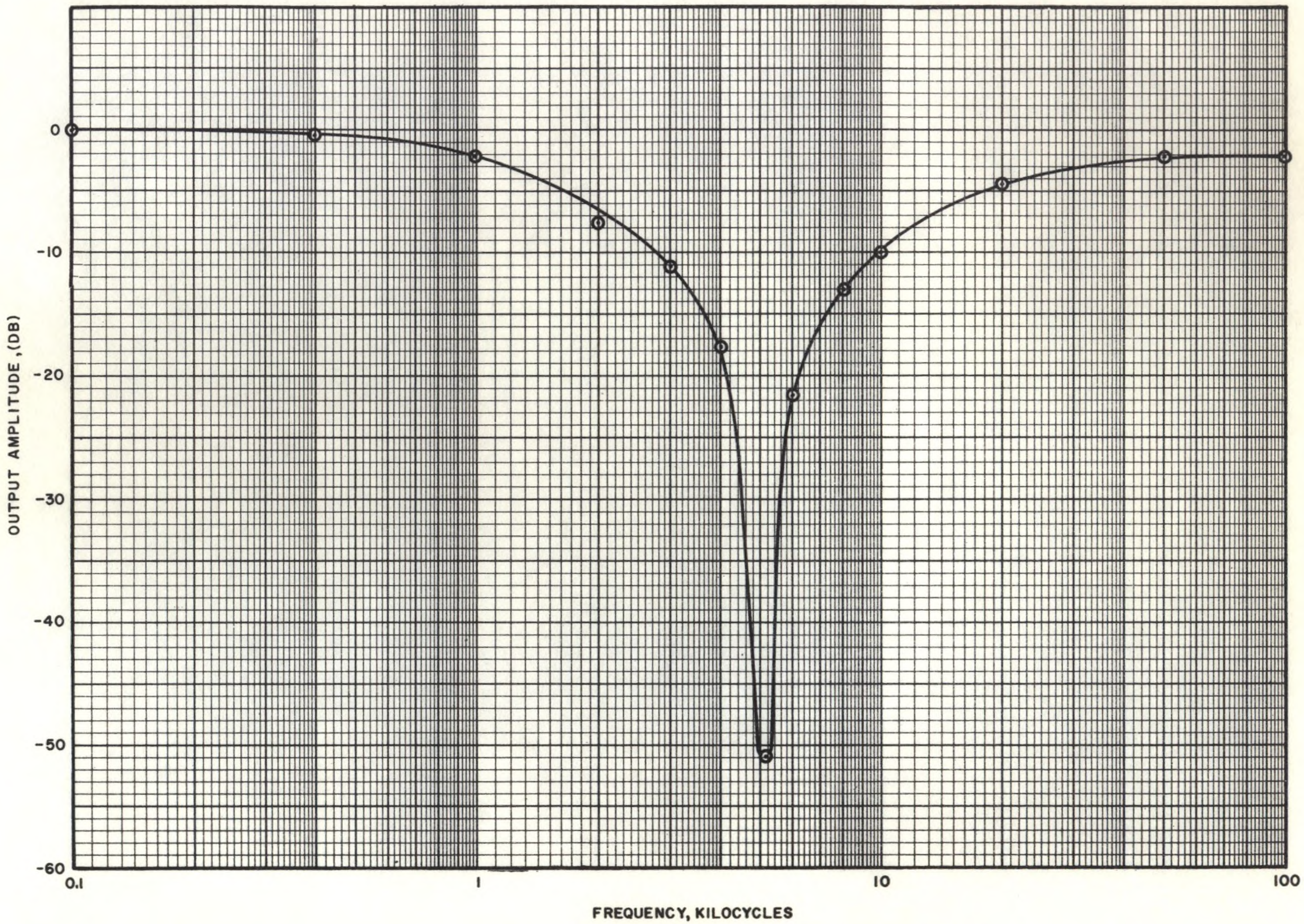

FIGURE C-16 5KC REJECTION FILTER RESPONSE CURVE

APPENDIX D

TEST EQUIPMENT LIST

1 - RF Voltmeter; Boonton Electronics Corp., Model 91CA

1 - True RMS Voltmeter; Ballantine Laboratories, Inc., Model 320

1 - Vacuum Tube Voltmeter; Hewlett-Packard, Model 400D

1 - Oscilloscope; Tektronix, Model 545 with Type 53/54K Plug-in Unit

1 - Frequency Counter; Hewlett-Packard, Model 524B with Frequency Converter Unit, Model 525A

1 - Audio Oscillator; Hewlett-Packard, Model 200BR

1 - Audio Oscillator; Heath, Model AG7

1 - Signal Generator; Measurements Corp., Model 82

3 - Push-Button Attenuators; Daven, Model RFB-552-50

1 - Push-Button Attenuator; Daven, Model RFB-550-50

3 - HV Power Supplies; Collins, Model 100

2 - Voltage Regulators; Collins, Model 200

1 - Voltage Regulator; Collins, Model 200A

1 - DC Power Supply; Electro, Model EFB

1 - Constant Voltage Transformer; Sola, Model 30808

1 - Constant Voltage Transformer; Raytheon, Model 6115

1 - Distortion Analyzer; Hewlett-Packard, Model 330D

1 - Vacuum Tube Voltmeter; Hewlett-Packard, Model 410B

BIBLIOGRAPHY

1. Chaffee, J.G., "The Application of Negative Feedback to Frequency Modulated Systems", Bell System Technical Journal, Volume 18, 1939

2. Carson, J.R., "Frequency-Modulation: Theory of the Feedback Receiving Circuit", Bell System Technical Journal, Volume 18, 1939

3. Morita, M. and Ito, S., "High Sensitivity Receiving System for Frequency Modulated Wave", IRE International Convention Record, Part 5, Communications Systems, Space Electronics and Telemetry, 1960

4. Felix, M.O. and Buxton, A.J., "The Performance of FM Scatter Systems Using Frequency Compression", Proceedings of the National Electronics Conference, 1958

5. L. Ya. Kantor, "Concerning the Noiseproof Feature of an FM Receiver with Frequency Feedback", Telecommunications, A Publication of the USSR Ministry of Communications, No. 10, 1959

6. Ruthroff, C.L. and Enloe, L.H. "Threshold Effects of the FM Demodulator with Feedback", Presented at URSI Conference in Washington, D.C. on 4 May, 1961, (To be published at a later date)

7. Gagliardi, R.M. and Miller, T., "Minimum Power Wideband Communication System for Space Vehicles", Proceedings of National Telemetry Conference, 22-24 May 1961, Chicago, Illinois

8. Davenport, W.B. and Root, W.L., "Random Signals and Noise", McGraw Hill Co., 1958

9. Davenport, W.B, "Signal-to-Noise Ratios in Band Pass Limiters", Journal of Applied Physics, Volume 24, pp 720-727, June 1953

10. Gilchriest, C.E., "Application of the Phase-Locked Loop to Telemetry and Remote Control", IRE Transactions on Telemetry and Remote Control, Volume TRC-4, June 1958

11. Stumpers, F.L.H.M., "Theory of FM Noise", Proceedings of the IRE, Volume 36, pp 1081, September 1948

12. Gardner, M.F., and Barnes, J.L., "Transients in Linear Systems", John Wiley and Sons, Inc., 1942

13. Newton, G.C., Gould, L.A., and Kaiser, J.F., "Analytical Design of Linear Feedback Controls", John Wiley and Sons, Inc., 1957